

Igor Koshelkov

Evaluation of mid-scale hydrogen distribution chains for compressed hydrogen

Master's thesis in Natural Gas Technology

Supervisor: Petter Neksa

Co-supervisor: Muhammad Zahid Saeed, Stian Trædal

June 2022

Igor Koshelkov

Evaluation of mid-scale hydrogen distribution chains for compressed hydrogen

Master's thesis in Natural Gas Technology

Supervisor: Petter Nekså

Co-supervisor: Muhammad Zahid Saeed, Stian Trædal

June 2022

Norwegian University of Science and Technology

Faculty of Engineering

Department of Energy and Process Engineering



Norwegian University of
Science and Technology

MASTER WORK

for

student

Igor Koshelkov

Spring 2022

Evaluation of mid-scale hydrogen distribution chains for compressed hydrogen
Vurdering av mellom-skala hydrogen distribusjonskjeder for komprimert hydrogen

Background and objective

There is an increasing concern related to climate change. This has led to the interest in using hydrogen as energy carrier and fuel for transportation, power production, industry and potentially other applications in order to avoid the end-use CO₂ emissions. Hydrogen is therefore expected to play a major role as energy carrier in a future low emission society.

Norway has vast amounts of energy resources in form of natural gas and electricity from hydro- and wind power. A valorization of these resources to produce hydrogen with a low CO₂ intensity may give great opportunities for Norway.

Utilization of hydrogen as fuel for energy demanding transport applications, such as maritime vessels, long-haul trucks and airplanes, are likely options. Fuel storage onboard could be in compressed or liquid form depending on the demands.

There are however several challenges related to the practical implementation of hydrogen as energy carrier. Most often the hydrogen is planned produced at a central location and distributed to filling stations or directly to the end user. Energy requirements, as well as cost for these chains are not fully investigated

The goal of the master work will be to build simulation models to study alternative distribution chains, from production to end use, with respect to energy requirements for compression or pumping, heating and or cooling, as well as looking into cost related aspects.

The following tasks are to be considered:

1. Define model distribution chains with typical capacities and component requirements for a mid-capacity demand, e.g. 3 tonnes H₂ per day. Relevant end user scenarios where final end use is fuel tanks with hydrogen in a compressed form should be defined. End storage/use could be fuel tanks for various transport vehicles, such as cars, trucks or maritime vessels.

2. Literature survey related to suitable components for these chains, with emphasis on the power demanding components, such as compressors, pumps and refrigeration/cooling systems, as well as commercially available storage tanks.
3. Develop simplified quasi-stationary and more sophisticated dynamic models for evaluation of the energy demands of the chains.
4. Perform a first optimization related to pressure levels, tank size requirement and component selection, given constraints on such as temperatures in tanks and filling times.
5. Perform case studies of the energy demand of the distribution chains for compressed hydrogen and compare it to a simplified chain using liquid hydrogen in the chain before end-use, as well as comparing it to power demand for production of hydrogen from electrolyzers.
6. Propose a plan for further work

-- “ --

The project work comprises 15 ECTS credits.

The work shall be edited as a scientific report, including a table of contents, a summary in Norwegian, conclusion, an index of literature etc. When writing the report, the candidate must emphasise a clearly arranged and well-written text. To facilitate the reading of the report, it is important that references for corresponding text, tables and figures are clearly stated both places.

By the evaluation of the work the following will be greatly emphasised: The results should be thoroughly treated, presented in clearly arranged tables and/or graphics and discussed in detail.

The candidate is responsible for keeping contact with the subject teacher and teaching supervisors.

Risk assessment of the candidate's work shall be carried out according to the department's procedures. The risk assessment must be documented and included as part of the final report. Events related to the candidate's work adversely affecting the health, safety or security, must be documented and included as part of the final report. If the documentation on risk assessment represents a large number of pages, the full version is to be submitted electronically to the supervisor and an excerpt is included in the report.

According to “Utfyllende regler til studieforskriften for teknologistudiet/sivilingeniørstudiet ved NTNU” § 20, the Department of Energy and Process Engineering reserves all rights to use the results and data for lectures, research and future publications.

Submission deadline: June 10th, 2022

- Work to be done in lab (Water power lab, Fluids engineering lab, Thermal engineering lab)
 Field work

Department for Energy and Process Engineering, *August 20, 2021*

Adjunct Prof. Petter Neksaå
Supervisor

Co-Supervisor(s):

Muhammad Zahid Saeed NTNU, Energy and Process Engineering
Stian Trædal SINTEF Energi AS

Preface

The presented work was written as the part of Natural Gas Technology master's programme at the Norwegian University of Science and Technology, NTNU. It is the continuation of the specialization project carried out in the autumn semester of 2021 and performed in collaboration with SINTEF Energi AS. Having background in the transportation and storage oil and gas, the topic piqued my interest in gaining knowledge in a relatively new field of hydrogen as an energy carrier. Furthermore, it was promising in gaining valuable experience working with a dynamic simulation software.

This work would not be possible without the teamwork of my supervisors. I am grateful to my principal supervisor, prof. Petter Neksa, and a co-supervisor, Stian Trædal, for their advice and feedback. I highly appreciate guidance and work from my co-supervisor, Muhammad Zahid Saeed, that helped me develop competence within Dymola software, an extensive part of the work. Special credits to Ingo Frohböse from TLK-Thermo GmbH for support with software models.

Summary

Hydrogen for industrial applications has been around for many years. However, it was not until a decade ago that it is started to enter a consumer market as an available sustainable alternative to fossil fuels. The reason behind using hydrogen is that it can potentially reduce emissions to zero, depending on how it is produced. Blue hydrogen is produced from methane reforming with CO₂ capture, and green - using energy from renewable energy sources. These types are of the primary interest in this case. In Norway, with its vast abundance of renewable energy sources, the implementation of hydrogen may give excellent opportunities to decarbonise the industrial sector and transportation. Having said that, its initially high price compared to other energy carriers calls for the study and development of efficient ways to store and distribute it, in addition to finding the best-case end-user scenarios.

The current project is the continuation of the specialization project, performed in the autumn semester, and makes an attempt to design the complete distribution system and examine its energetic demand. The distribution chain is a mid-scale one, with up to 3 tons per day production capacity, compressed hydrogen distribution system for heavy-duty transport as an end-user with 350 barg pressure rating. The results can be also representative for a similar distribution system for light passenger ferries. Hydrogen transportation is done by road transport in tube containers at 300 barg. Primarily compression and refrigeration work for transportation and storage operations is evaluated. It was decided to develop a dynamic model of the distribution chain, since it is important for the better understanding of many operations such as pressure vessel emptying and filling. For example, during compression into a vessel, compressor efficiency may change a lot depending on its performance curve. This is considered to give a better perspective on energetic performance of hydrogen distribution chain. Therefore, the main modelling is done in Dymola software, a modelling environment for dynamic simulations, with additional libraries for components and fluids provided by TLK-Thermo GmbH. A functional mock-up interface (FMI) approach is used to assemble and simulate the whole chain, consisting of separate Dymola models. Python language, as a connecting link for the whole simulation, is used with additional libraries.

The essential result of the modeling and simulation is combined specific energy demand for compression and refrigeration of hydrogen during transportation from a production site to an end-user. It makes 6.2 kWh/kgH₂ under our assumptions. Energy demand in different parts of the chain is presented as well as comparison of refrigeration versus compression. Intermediate and final results also provide ground for discussions on the chain design and modelling.

Sammendrag

Hydrogen for industrielle applikasjoner har eksistert i mange år. Det begynte å gå inn i et forbrukermarked som et tilgjengelig bærekraftig alternativ til fossilt brensel for cirka ti år siden. Årsaken til bruk av hydrogen er at det kan redusere utslippene til null, avhengig av hvordan det produseres. Blått hydrogen produseres fra metanreforming med CO₂ fangst, og grønt - ved bruk av energi fra fornybare energikilder. Disse typene er av hovedinteressen i denne saken. I Norge, med sin tilgjengelighet av fornybare energikilder, kan implementering av hydrogen gi utmerkede muligheter til å avkarbonisere industrisektoren og transport. Når det er sagt, krever den i utgangspunktet høye prisen sammenlignet med andre energibærere studier og utvikling av effektive måter å lagre og distribuere den på, i tillegg til å finne de beste sluttbrukerscenarioene.

Det nåværende prosjektet gjør et forsøk på å designe og undersøke energisk etterspørsel etter et middels skala, opptil 3 tonn per dag, komprimert hydrogendistribusjonssystem for kjøretøyer som sluttbruker med 350 barg trykkklassifisering. Resultatene kan også være representative for et tilsvarende distribusjonssystem for passasjerferger. Hydrogen blir transportert med veitransport i rørcontainere på 300 barg. Primært komprimerings- og kjølearbeid for transport- og lagringsoperasjoner blir evaluert. Det ble besluttet å utvikle en dynamisk modell av distribusjonskjeden, siden den er viktig for bedre forståelse av mange operasjoner som trykkbeholdertømming og fylling. For eksempel, kompressoreffektiviteten kan endre seg mye avhengig av ytelseskurven under kompresjon inn i et fartøy. Dette anses å gi et bedre perspektiv på energiytelsen til distribusjonskjeden for hydrogen. Derfor gjøres hovedmodelleringen i Dymola-programvaren, et modelleringsmiljø for dynamiske simuleringer, med tilleggsbiblioteker for komponenter og væsker levert av TLK-Thermo GmbH. En functional mock-up interface (FMI) tilnærming brukes til å sette sammen og simulere hele kjeden, bestående av separate Dymola-modeller. Python programmeringsspråket, som er en forbindelseslenke for hele simuleringen, brukes med tilleggsbiblioteker.

Det vesentlige resultatet av modelleringen og simuleringen er kombinert spesifikt energibehov for kompresjon og nedkjøling av hydrogen under transport fra et produksjonssted til en sluttbruker. Den gir 6.2 kWh/kgH₂ under våre forutsetninger. Energibehov i ulike deler av kjeden presenteres samt sammenligning av kjøling versus kompresjon. Mellom- og sluttresultater gir også grunnlag for diskusjoner om kjededesign og modellering.

Table of Contents

Preface	i
Summary	ii
Sammendrag	iii
Nomenclature	v
Abbreviations	vi
List of Figures	vii
List of Tables	ix
1 Introduction	1
1.1 Background	1
1.2 Software	2
1.3 Objectives	2
1.4 Overview of the current state	2
2 Technology overview	5
2.1 Hydrogen compression	5
2.2 Gaseous hydrogen storage equipment	6
2.3 Hydrogen pre-cooling	8
3 Chain description	9
3.1 Layout	9
3.2 Compressed hydrogen refilling basics	11
4 Methods	13
4.1 Assumptions	13
4.2 FMI based workflow	13
4.3 Efficiency compressor	15
4.4 Thermal modeling of Type IV hydrogen cylinder	18
4.5 Compression after electrolyzer	20
4.6 Cascade storage model. The production site.	22
4.7 Trailer filling model	25
4.8 End-user refilling model	27
4.9 Cascade storage charging. End-user site	30
5 Results and discussion	33
5.1 Thermal simulations results of Type IV hydrogen cylinder	33
5.2 Chain simulation results	37
5.3 Chain simulation summary	48
5.4 Parametric studies	51
6 Conclusion and further work	54
6.1 Further work	56
Bibliography	57
Appendix	59

Nomenclature

\dot{V}	volumetric flowrate ($\frac{m^3}{s}$)
λ	overall volumetric efficiency
\dot{V}_t	theoretical volumetric flowrate ($\frac{m^3}{s}$)
η_v	volumetric efficiency due to clearance volume gas expansion
r_p	compressor pressure ratio
c	relative clearance volume
k	isentropic exponent
η_{is}	isentropic efficiency
p	pressure (<i>bar</i>)
h	specific enthalpy ($\frac{J}{kg}$)
V	volume (m^3)
\dot{m}	mass flowrate ($\frac{kg}{s}$)
f	compressor speed (<i>Hz</i>)
ρ	density ($\frac{kg}{m^3}$)
P	power (<i>W</i>)
A	geometric area (m^2)
d	geometric diameter (<i>m</i>)
L	geometric length (<i>m</i>)
W	work (<i>J</i>)
\dot{Q}	heat flow ($\frac{J}{s}$)
Q	heat (<i>J</i>)
T	temperature (<i>K</i>)
σ	tensile strength (<i>MPa</i>)
R_t	thermal resistance ($\frac{K}{W}$)
K	thermal conductivity ($\frac{W}{m \cdot K}$)
h_t	heat transfer coefficient ($\frac{W}{m^2 \cdot K}$)
c_t	specific heat capacity ($\frac{J}{kg \cdot K}$)

Subscripts

<i>suc</i>	compressor intake (suction)
<i>dis</i>	compressor discharge
<i>is</i>	isentropic
<i>tot</i>	total
<i>eff</i>	effective (actual)
<i>shaft</i>	compressor shaft
<i>w</i>	cylinder wall
<i>o</i>	outer (diameter)
<i>in</i>	inner (diameter)
<i>amb</i>	ambient

Abbreviations

FCEV	fuel cell electric vehicle
SAE	The Society of Automotive Engineers
DOE	The United States Department of Energy
ODE	ordinary differential equations
DAE	differential algebraic equations
HP	high pressure
MP	medium pressure
FMI	functional mock-up interface
FMU	functional mock-up unit
SOC	state of charge
PI	proportional-integral (controller)

List of Figures

1	Content included in SAE J2601	1
2	Components of a composite hydrogen storage tank	6
3	Hydrogen cylinder data summary	7
4	Compressed hydrogen road transport	7
5	Example of the buffer refilling system	9
6	Example of the cascade refilling system	9
7	Flow-sheet of the production site model	10
8	Flow-sheet of the end-user refilling site model	10
9	Target density for 300 bar cylinder	12
10	Data flow during simulation using FMUs and Python	14
11	Overview of the models used for simulation	15
12	Compressor efficiency for different pressure ratios at different speeds (solid line for R22 refrigerant and dashed line for R717)	16
13	Diagram explaining compressor efficiency in Dymola	17
14	Compressor performance curves	18
15	Dymola diagram view of the model for the cylinder filling	19
16	Dymola diagram view of the model for the cylinder emptying	20
17	Graphical view of the hydrogen compression after electrolyzer model in Dymola	21
18	Diagram of the cascade model	23
19	Cascade system charging algorithm	23
20	Graphical view of the cascade charging model in Dymola	24
21	Diagram of the trailer filling model	25
22	Trailer filling algorithm	26
23	Graphical view of trailer filling model in Dymola	27
24	Trailer filling simulation algorithm in Python	27
25	Diagram of the end-user filling model	28
26	Graphical view of end-user filling model in Dymola	28
27	End-user filling algorithm	29
28	End-user filling simulation algorithm in Python	30
29	Diagram of the end-user cascade charging model	30
30	End-user site cascade charging algorithm	31
31	Graphical view of end-user cascade charging in Dymola	32
32	Model validation	33
33	Temperature results with varying pressure ramp rate during filling	34
34	Pre-cooling influence on the final temperature without external heat exchange	35
35	Filled mass results with varying pre-cooling temperature	35
36	Temperature results for filling at 1 MPa/min and pre-cooling at -10 °C with varying ambient temperature	36
37	Temperature results with varying rate of vessel emptying	37
38	Pressure results of trailer filling simulation	38
39	Temperature results of the trailer filling simulation	39
40	Specific cooling work results of the trailer filling simulation	39
41	Pressure results of the cascade charging at the production site simulation	40
42	Temperature results of the cascade charging at the production site simulation	41
43	Pressure and temperature results for the intermediate storage filling simulation	42
44	Pressure results of the end-user refilling simulation for the first two vehicles	43
45	Pressure results of the end-user refilling simulation for the final filling operations	43
46	Temperature results of the end-user refilling simulation for the final filling operations	44
47	Pressure ratio of the compressor of the end-user refilling simulation	45

48	Combined specific energy consumption during each refilling operation	45
49	Pressure results of the cascade charging at the end-user site	46
50	Temperature results of the cascade charging at the end-user site	47
51	Combined specific work for hydrogen distribution throughout the chain	49
52	Maximum and minimum pressure levels at different parts of the chain	50
53	Screenshot from Excel-based version of HDRSAM with scenario parameters	51
54	Specific work depending on the total storage volume	52
55	Specific compression and cooling work at different ambient temperature	53

List of Tables

1	<i>Tube trailer and container specifications</i>	8
2	<i>Parameters for a vehicle onboard storage</i>	11
3	<i>General pressure, temperature constraints</i>	12
4	<i>Summary of the assumption for a compressor</i>	18
5	<i>Type IV cylinder data from Hexagon Purus</i>	19
6	<i>Type IV cylinder general assumptions for modeling of thermal effects</i>	19
7	<i>Initialization parameters for the compression after the electrolyzer model</i>	22
8	<i>Steel cylinder parameters</i>	22
9	<i>Initialization parameters of the cascade charging model at the production site</i>	24
10	<i>Assumptions for the two models in comparison</i>	33
11	<i>Cylinder emptying simulation parameters and results</i>	37
12	<i>End and initialization values for the cascade storage simulation</i>	40
13	<i>The summary of the cascade charging at the production site simulation results for compressor</i>	41
14	<i>End and initialization parameters for the intermediate storage</i>	41
15	<i>The summary of the intermediate storage simulation results for compressor</i>	42
16	<i>The summary of the end-user filling simulation results</i>	46
17	<i>End and initialization parameters for the cascade charging at the end-user site</i>	46
18	<i>Pressure and temperature results of the cascade charging at the end-user site</i>	47
19	<i>The summary of the cascade charging compressor results at the end-user site</i>	48
20	<i>Specific work results for hydrogen distribution throughout the chain</i>	48
21	<i>Parameters specified for HDRSAM calculation</i>	50
22	<i>Cascade volume data for parametric study</i>	52
23	<i>Specific work, end pressure, and COP data for different ambient temperature simulations</i>	52

1 Introduction

1.1 Background

Much research have been done on hydrogen as an energy carrier, from its production to storage and distribution. Hydrogen refilling stations for automotive vehicles have been operating for almost two decades but never received widespread adoption. This is not a surprise, as hydrogen infrastructure is related to many challenges. Hydrogen has the highest energy density by mass. On the other hand, its extremely low density under atmospheric pressure requires increasing of volumetric energy density. This can be done in several ways: material-based (chemically or physically bonded hydrogen with other materials) or physical-based (compression or liquefaction). All of this requires additional energy input, which brings cost up even more, in addition to the initial cost of hydrogen production. According to the International Energy Agency (IEA) report, hydrogen, obtained from methane steam reforming without carbon capture, is expected to become competitive with other fuels by the year 2030 [1]. However, much support still comes from governments. Considering that hydrogen is perceived as a promising future energy solution, more study on hydrogen applications is needed to acclaim commercial demand.

At the level of abstraction of this work, we find not so many standards or regulatory documents that can provide a process design basis. In general, hydrogen as a hazardous substance is covered by Norwegian regulatory documents [2] regarding its safe usage. However, they are essential on a more detailed design level. Therefore, the central document for the study is the Society of Automotive Engineers (SAE) J2601 Fueling Protocols which regulates gaseous hydrogen fueling of light-duty vehicles and is one of the few documents that set procedures for hydrogen usage as a fuel. At the latest release, it covers onboard storage capacity of 49.7 to 248.6 L (1.2 to 6.0 kg) for H35 (350 bar) category and from 49.7 to 248.6 L (2 to 10 kg) and greater than 248.6 L (more than 10 kg) for H70 (700 bar) category. There are also limitations on hydrogen delivery temperature during filling operations covered by the document. A summary of the content is presented in Figure 1.

Pressure Class Designation		H35			H70		
CHSS Capacity Range (Liters)		< 49.7	49.7 to 248.6	> 248.6	< 49.7	49.7 to 248.6	> 248.6
CHSS Capacity Range (kg)		< 1.19	1.19 to 5.97	> 5.97	< 2.0	2.0 to 10.0	> 10.0
CHSS Capacity Categories (nomenclature)		TBD	A, B, C	D	TBD	A, B, C	D
Maximum Flow Rate (g/s)		≤ 60	≤ 60	≤ 60	≤ 60	≤ 60	≤ 60
Fuel Delivery Temperature Category	T40	Not Included	Included	Not Included	Included		
	T30						
	T20						
	T10						
	Ambient						

Figure 1: Content included in SAE J2601

Source: [3]

SAE J2601 provides a solid basis for research related to light vehicle refuelling. In general, studies are focused on developing comprehensive models of hydrogen refilling systems for light transport to evaluate energetic performance and find the best solutions. In addition, several computer programmes were developed to help evaluate hydrogen filling station economy, for example, HDSAM (Hydrogen delivery scenario analysis model) and DOE H2A (The U.S. Department of Energy hydrogen analysis). HDSAM and heavy-duty refueling station analysis model (HDRSAM) include predefined scenarios for calculations and provide results based on a steady state operation.

This work aims to cover mid-scale hydrogen distribution chain dynamic operation as the whole. The primary objective is to develop software models and run simulations that can help to estimate energy requirements for the assumed hydrogen chain. However, by investigating the system's

dynamic behaviour, a better understanding of essential aspects of such a system's operation is also expected to be captured.

1.2 Software

The primary modelling is based on Modelica programming language, a non-proprietary equation-based language for modelling complex mechanical, electrical, and fluid systems. It was developed to simplify the modelling of dynamic systems, described by ordinary differential (ODE) and differential algebraic equations (DAE). Dymola environment by Dassault Systèmes is used together with TIL Suite, a component library, and TIL media, a library of fluid properties, both provided under the TLK-Thermo GmbH license. Dymola allows building models using graphical interface and components libraries and includes also proprietary solvers. However, since simulations are performed in Python, a separate package, Assimulo, is used which includes SUNDIALS solvers. SUNDIALS is a freely available package developed at Lawrence Livermore National Laboratory. "CVode", as a standard one, is used in the simulations.

As will be shown further in section 4.2, the model of the distribution chain is rather complex. Nevertheless, it can be simplified by using an FMI-based workflow approach. The main idea is to use Dymola for building models, "main construction blocks", of different parts of the chain, and then simulate them in a different software environment manually providing connection of the necessary data streams and automating the simulation process by writing scripts. Python language, together with Jupyter programming environment, is chosen for simulation with additional libraries. Further data analysis is performed using standard libraries, such as Numpy and Matplotlib. Additionally NIST REFPROP Python wrapper is used for intermediate thermodynamic calculations.

1.3 Objectives

As part of a long-term research effort aimed at energy investigation of mid-scale hydrogen distribution chains, this paper presents a compressed hydrogen scenario development and initial dynamic modelling for energy evaluation. The objectives for this study were to:

1. define a model of distribution chain with typical capacities and component requirements for a mid-capacity demand, e.g. 3 tonnes H₂ per day, with relevant end user scenarios where final end use is fuel tanks with hydrogen in a compressed form;
2. literature survey related to suitable components for these chains, such as compressors and pressure vessels;
3. develop simplified quasi-stationary and more sophisticated dynamic models for evaluation of the energy demands of the chains;
4. perform case studies related to energy demand of the distribution chains for compressed hydrogen;
5. propose a plan for further work.

1.4 Overview of the current state

Compressed and liquefied forms of hydrogen are the most widely used and commercially available forms of hydrogen transportation. Many studies investigate possibilities and areas of application for different types, including novel types on their experimental stage. Still, much work should be done to bring costs down to allow more widespread adoption of the energy carrier. For this matter, we can take a brief outline of the current technology.

Gaseous hydrogen transportation via pipelines is almost at the centre of practical matters nowadays as European energy providers are interested in using abundant natural gas infrastructure for hydrogen transportation purposes. Hydrogen export via existing natural gas trunk pipelines may be possible. This might be a way for the Norwegian economy since the domestic market does not widely use natural gas. Initial blends of hydrogen with natural gas with a further transition to pure hydrogen are being discussed. However, it is unlikely to happen in the near future because of the burden of safety and technical preparations. Many papers focus on finding the optimal solution for the materials for gaseous pipelines, as steel pipelines are subjected to hydrogen embrittlement under high pressures. Some thousands of commercial hydrogen pipelines are in operation today in the world (1600 km are present in the United States [4]). However, only a fraction is used for hydrogen delivery to refuelling stations [4]. C. Yang and J. Ogden [5] estimate costs for different means of transportation and show that pipelines become optimal only for high delivery rates, more than 8 tons per day, and distances, of 25 km and more. Their research provides a comprehensive estimation of the hydrogen distribution and operation cost of hydrogen refilling stations.

Hydrogen can be distributed via existing roads in gaseous or liquid form in trailers as an alternative to pipelines. The very process of hydrogen liquefaction is power demanding, and only three liquefaction facilities exist in Europe [2]. However, liquid hydrogen can be transported in large quantities with in smaller vessels. As estimated by Linde AG, the liquid form is preferable for long distances over 250 km or quantities more than 200 kg/day [6]. This, of course, will depend on the local parameters and should be evaluated by modelling for exact conditions.

Though scaling electrolysis facilities for hydrogen production is not deemed to bring down costs [2], the economic benefit of the central facility still exists. Hydrogen storage, due to its low volumetric energy density, has a large land footprint. It might be challenging to design on-site production, storage and distribution all together for each place of demand. Furthermore, at the early stages of hydrogen adoption, central production gives the flexibility of being accessible to different end-users.

A. Almansoori and N. Shah [7] point out that focus in hydrogen studies should lay on a thorough study of different distribution chains instead of particular components. Many up-to-date papers are available which use different techniques to model distribution systems. Still, they are mostly related to hydrogen refuelling stations for personal transport and are primarily done in uncertainty related to consumer demand. The area of automobiles is very competitive, and as of now, personal fuel cell electric vehicles (FCEV) have not made their way into the broad consumer market. This creates a dilemma of what should come first, demand for FCEV or facilities for their refuelling. On the other hand, heavy-duty FCEVs are considered to be more predictable in terms of demand and possibly mitigate the uncertainty of the market. However, less data is available in this area related to the design considerations and mostly limited to scarce pilot projects [4].

In the report of the International Energy Agency (IEA) [1], seven key recommendations are provided to scale-up hydrogen. One of them suggests more comprehensive research and development of hydrogen infrastructure. The more data is obtained for different areas of hydrogen usage, the more determinate decisions for investments can be made, directly related to the successful adoption of hydrogen in the near future. Still, research and development should be done in the areas that could really contribute to the society and economy without artificially over-inducing the adoption.

In the Norwegian Government's hydrogen strategy [2] the main contributors to the greenhouse gas emissions are discussed, and most promising areas are highlighted that can benefit from hydrogen usage. The transport sector is one of the largest sources of emissions. Thus focusing on means of transportation that can benefit from hydrogen can help reduce overall emissions significantly. In the long run, it should be planned with some degrees of flexibility included in the technology. This may accommodate the future expansion to lower scales at one end and add producers at another. Hydrogen production via electrolysis, as mentioned earlier, gives almost no gains when scaled up,

yet it can be done without significant investments [2].

As discussed in [8] software development and research focus on the medium to large time scale models of hydrogen supply chain, both technical and economical, while the focus of others falls on studying very specific parts of the chain. This leaves some blank spaces in the area of the distribution chain studies from production to an end-user with the effects of the system dynamics and its influence on the design and energy consumption.

2 Technology overview

This chapter provides overview of the existing technology for hydrogen distribution that might be relevant for the present work. It summarizes information from the previous specialization project as well as some new data.

2.1 Hydrogen compression

Several types of compressors are usually used for hydrogen compression [9]:

- positive displacement;
- centrifugal compressors; and
- non-mechanical compressors.

Dry piston compressors are type of the positive displacement compressors. Their construction is mostly the same as piston compressors for other gases, but sealing is usually much tighter as hydrogen molecules easily escape through microscopic pathways. To prevent hydrogen from contamination oil lubrication is not used. For most operations, especially for fuel cells, high purity hydrogen is needed. Another type in this category is ionic compressors. They operate similarly to piston compressors, only ionic liquid column instead of the piston is in contact with the gas. Ionic liquids do not contaminate compressed hydrogen, can be operated in a wide range of temperatures, and have almost no hydrogen solubility [10]. For example, Linde AG provides ionic compressor solutions for hydrogen filling stations for pressures from 25 MPa to 35 MPa [11]. Diaphragm compressors give oil-free hermetic compression of hydrogen employing an elastic membrane that performs reciprocating movements. They usually deliver hydrogen at high pressure with small volumetric flow rate and sometimes are used as the first stage in hybrid hydrogen compressors together with piston compressors. Other positive displacement compressors may include rotary compressors. Still, the problem for most types of positive displacement compressors is providing adequate sealing of working volume by manufacturing very tight tolerances.

Centrifugal compressors can give high volumetric flow rates with moderate pressures for pipeline hydrogen transport. However, in this case, blade tip velocities should be sufficiently higher than for natural gas to achieve optimal pressures for pipeline transport. This leads to the problem of manufacturing materials capable of operating under such conditions [9].

Non-mechanical compressors solve some challenges of their mechanical counterparts. *‘Fatigue associated with moving parts of mechanical compressors including cracking of diaphragms and failure of seals leads to failure in conventional compressors, which is exacerbated by the repeated starts and stops expected at fueling stations’*[12]. *‘Metal hydride compressors use metals that form hydrides via exothermic reactions and then release hydrogen at high pressures when heat is applied’* [9]. Electrochemical reactions can also be used to compress hydrogen. Under external voltage, hydrogen molecules dissociate to move through a proton exchange membrane (PEM) and recombine on the other side under high pressure. However, non-mechanical compressors are primarily in development and not used on commercial scales.

Piston and diaphragm types for the compressed distribution chain are compressors of choice. For most part, because of their commercial availability. Burkhardt Compression, a Swiss firm specialising in reciprocating compressors, present their view on gaseous hydrogen trailer filling and provide several key parameters for their compressors. Dry piston oil-free compressors for hydrogen range between 180 and 698 kW of rated power with corresponding mass flow rates from 95 to 550 $\frac{kg}{h}$. Their diaphragm compressor is rated at 89 kW with 44 $\frac{kg}{h}$ of mass flow (tested conditions: 30 bar suction pressure at 20 °C and 550 discharge). The operating pressure is claimed up to 550

bar.[13]

Compressors by Neumann & Esser Group, a German firm, provide solutions for high and low flow rates. The ‘TKH’, dry running hydraulic driven piston compressors, are reported to achieve pressures up to 3000 bar with low capacity. For high demand and pressures up to 250 bar, another dry running piston compressor is available with a possible installed power of more than 10 MW [14].

Mehrer compression GmbH, another German firm, produces diaphragm compressors for hydrogen compression at small scales. In collaboration with other firms, they provide examples of hydrogen filling stations for personal vehicles and buses. The reported volumetric capacity for the diaphragm compressor is between 15 to 500 $\frac{Nm^3}{h}$ depending on pressure [15].

2.2 Gaseous hydrogen storage equipment

Gaseous hydrogen gas can be stored and transported in standard cylinder tanks under pressure from 20 to 950 barg. To provide enough strength and durability, they are usually made of steel or aluminium compatible with hydrogen and other materials, such as polymers, carbon fibre, and composites. Depending on the complexity, they are denoted in roman numbers from I, simple metal tanks, to V, fully composite tanks [16]. The latter can withstand pressures higher than 700 bar [16]. Standard pressure levels are 350 and 700 bar for onboard hydrogen storage in light vehicles. Lower pressures can be used in heavy-duty vehicles where onboard space is less restricted. However, different materials and construction place additional restrictions on how hydrogen tanks can be used. During filling and discharge, materials are subjected to cyclic loads. The higher the pressure ratio during operations, the lower the number of cycles material can handle. Additionally, hydrogen temperature increases significantly during compression into storage vessels, and therefore materials should also provide thermal resistance. Otherwise, hydrogen cooling before it enters a vessel may be implemented.

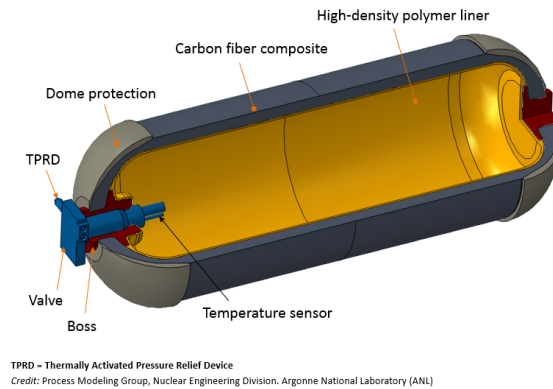


Figure 2: Components of a composite hydrogen storage tank

Source: <https://www.energy.gov/eere/fuelcells/physical-hydrogen-storage>

Gaseous hydrogen storage is well-proven technology and has been used for a long time. However, suppose there is a need to store large quantities of hydrogen. In that case, it becomes uneconomical due to enormous capital costs, high unit costs of energy for the compression of hydrogen, and poor weight characteristics. Gaseous storage takes around four times more space than liquid hydrogen storage [6]. All these create additional challenges in designing compressed hydrogen infrastructure. Different storage vessels types are used on road trailers and currently allow transportation of compressed hydrogen at pressure up to 500 bar [17].

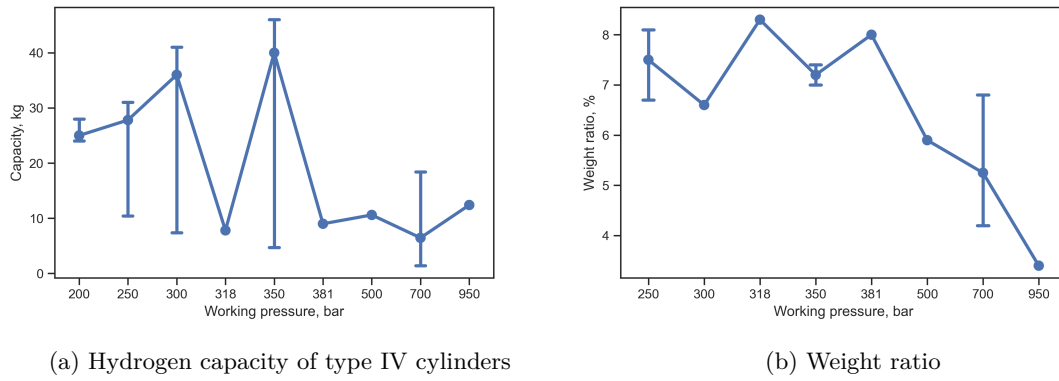


Figure 3: Hydrogen cylinder data summary

A typical type IV high pressure tank is shown in the figure 2. The figure 3a shows the summary of typical capacities for type IV cylinders produced by “UMOE Advanced Composites” and “Hexagon Purus” using openly available data. The graphic shows the median value for capacity at each pressure level and maximum and minimum available hydrogen capacities. Pressures of 250, 300, 350, and 700 bar have the largest variety of capacities, and these pressure levels are primarily used for the transportation and storage of hydrogen. Notably, 350 and 700 bar are the standard pressures for onboard tanks of FCEVs.

The figure 3b represents the weight ratio relation of the hydrogen weight to the weight of the cylinder. The data is only available for “Hexagon Purus” cylinders. It points to the fact that cylinders up to 500 bar have the best weight ratio. Thus, they are the most relevant pick for road transportation.



(a) Tube road semi-trailer by “Hexagon Purus”
Source: hexagonpurus.com



(b) Swappable container by “UMOE Composites”
Source: www.uac.no

Figure 4: Compressed hydrogen road transport

Other than more conventional steel trailers, current road transportation methods include tube trailers and swappable containers comprised of a number of type IV cylinders. In the figure 4a and 4b different forms of are presented. Some main parameters available from the manufacturers’ websites are summarized in the following table.

Table 1: *Tube trailer and container specifications*

Name	Operating pressure, bar	Hydraulic capacity, m^3	Nominal H_2 mass (15 °C)	Number of cylinders
X-STORE® 10 ft	300	8.4	178	24
X-STORE® 45 ft	300	45.15	958	129
X-STORE® 45 ft	318	45.15	1005	129
20' Hook MEGC standard	200	14.85	222	9
45' ISO high cube	300	42.35	895	22
45' ISO high cube	350	42.35	1016	22

2.3 Hydrogen pre-cooling

Depending on the design of hydrogen refuelling facilities and particular ambient conditions, pre-cooling of hydrogen stream before dispensing it to an end-user might be needed. More details on hydrogen refuelling are given further in the paper. However, a small overview of the hydrogen cooling process and refrigerators can be given.

According to the report by Amgad Elgowainy and Krishna Reddi from Argonne National Laboratory, refrigeration is a major contributor to the investment and running costs of hydrogen refuelling facilities [18]. Some of the reasons for that are low-temperature refrigeration, high instant cooling demand, and intermittency of operation. SAE J2601 protocol includes different hydrogen delivery temperature categories ranging from ambient without pre-cooling to -40 °C for T40 class stations. Other categories are T10, T20, and T30.

Analysing available manufacturer's data, specifically KUSTEC Corp., specialising in refrigeration equipment for hydrogen fueling stations, some general design choices may be outlined. Refrigerators can either provide active pre-cooling or passive. The passive system includes installed thermal mass, represented by an aluminium block, covering the main instant cooling load during hydrogen refueling. The chiller, in this case, operates almost continuously, charging up the thermal mass. This allows less powerful compressor drive but reduces the ability to provide many back-to-back vehicle refuelling operations. Active systems, on the other hand, work only on-demand basis. This requires high instant cooling power delivery. The later systems are also more expensive to install.

Refrigerators differ based on the hydrogen delivery temperature. Other than system design, it also affects the choice of a refrigerant. Products presented on the website include solutions with CO_2 as the only working fluid. Current research on using carbon dioxide as the refrigerant shows it to be an up-and-coming solution in many applications, especially low-temperature ones [19]. This is advantageous for T40 temperature class. CO_2 as a refrigerant has the highest safety ranking and the lowest impact on global warming (global warming potential equals 1), which is also essential to weigh when developing a sustainable distribution chain.

3 Chain description

3.1 Layout

Modern hydrogen refilling station designs can be broken down into two main categories: buffer and cascade systems. Storing hydrogen at pressure higher than vehicle tank allows quick refilling operations without need for a compressor with high throughput. The main difference between the two designs is the number of pressure levels. Examples of a buffer and a cascade system are shown in Figure 5 and 6.

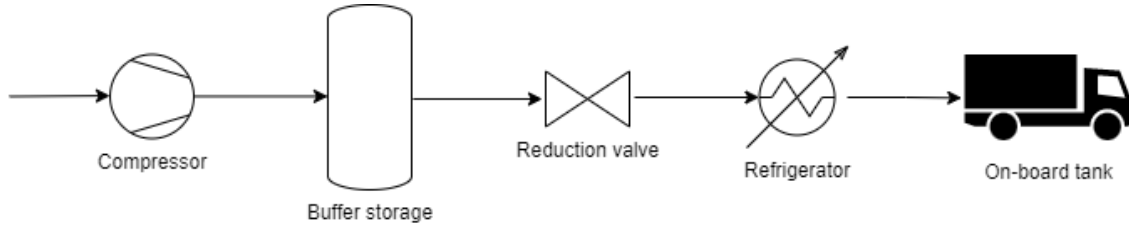


Figure 5: Example of the buffer refilling system

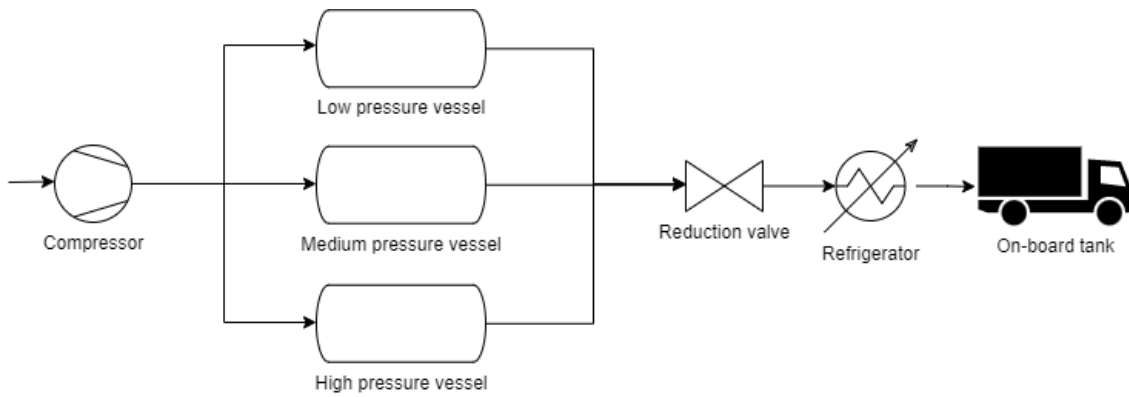


Figure 6: Example of the cascade refilling system

At least several studies exist that show the better energy performance of cascade storage systems at hydrogen refilling stations. For example, Lei Xiao et al. [20] presents a study on comparing energy efficiencies of the cascade and buffer storage systems. The results show better energy efficiency of the cascade system. Furthermore, typical layouts suggested in the review by National Renewable Energy Laboratory [17] include different configurations of cascade storage systems. Since the current work should typify the potential up-to-date compressed hydrogen distribution chain, the cascade layout for hydrogen storage is assumed as the main design principle. However, the modelling only of a two-level cascade system is considered. This is believed to give an optimum trade-off between model complexity and still be representative of an actual system.

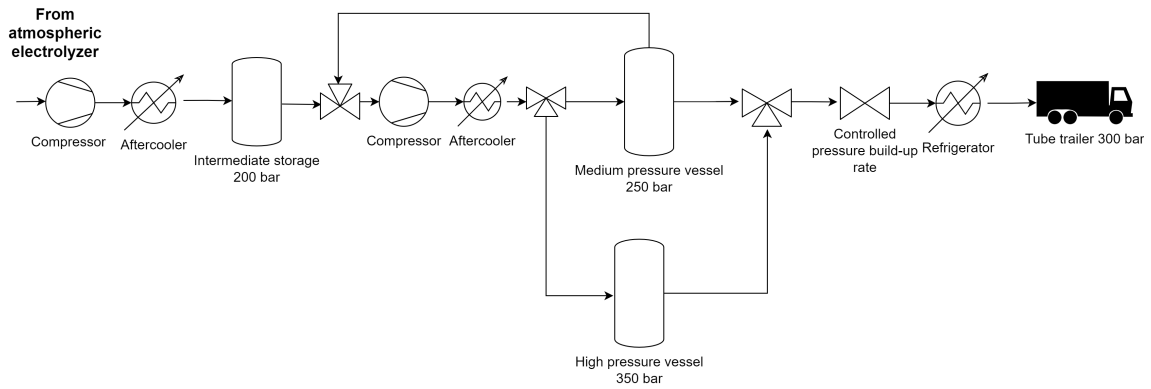


Figure 7: Flow-sheet of the production site model

The figure 7 shows the arrangement of the hydrogen production site. As of our knowledge, there are no universally proven designs. Thus, here the model mostly follows the idea of refilling station layout. Hydrogen is produced in the alkaline electrolyzer at atmospheric conditions. Then multistage compressor fills the intermediate storage volume, which is believed to be needed in the chain as long as the road transportation is not necessarily regular, and we opt for continuous hydrogen production. The volume should store at least daily amount of produced hydrogen. The medium (MP) and the high pressure (HP) vessels represent cascade storage and should be able to provide fast sequential refilling of the number of road trailers needed to distribute the daily production of approximately 3 tons. Thus, hydrogen is assumed to be dispensed in 3 road tube trailers with nominal capacity of 958 kg. Then compressed hydrogen is delivered to the end-user distribution site.

One more important detail is the usage of the same compressor to fill the MP tank from the intermediate storage and then the HP tank from the MP tank. This principle, for example, is shown in the presentation by “Mehrer Compression GmbH” [15]. This arrangement is believed to provide effective compressor re-use, reducing investment costs, of course, if a compressor can work in such broad range of suction pressure.

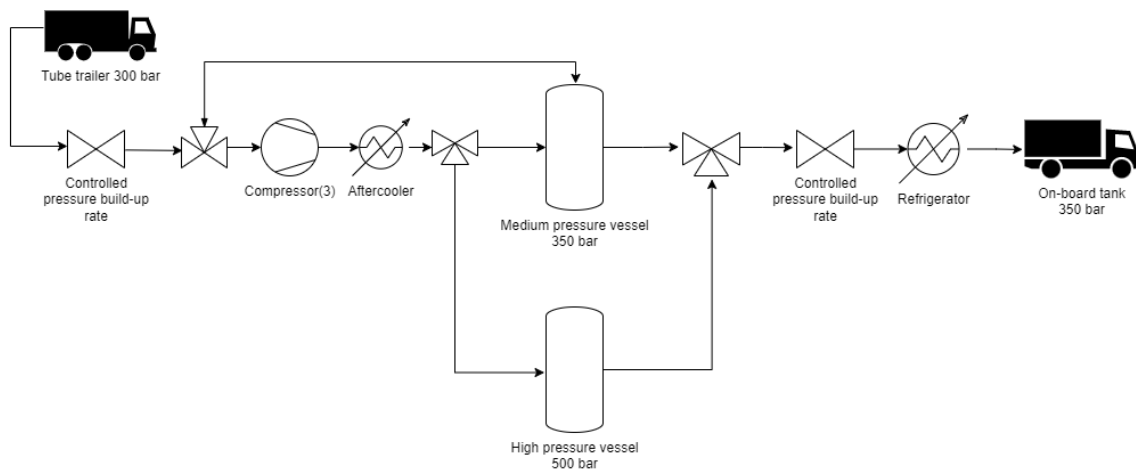


Figure 8: Flow-sheet of the end-user refilling site model

The end-user refilling site model is the modified production site model and is presented in the Figure 8. Here all the delivered hydrogen is assumed to be stored inside the cascade system, and the pressure levels are higher than at the production site. According to the protocol, the standard refilling pressure for road transport is 350 or 700 bar. As a reference, a heavy-duty vehicle is

considered with the working pressure of 350 bar. Other parameters are presented in Table 2. Data designated with an asterisk was collected from a manufacturer’s website [21]. Therefore, for the refilling operations with the cascade system, some considerable overpressure should be achieved for fast refilling. The second reason is that higher storage pressure will be needed compared to the production site. This is due to hydrogen volumetric density is very low, and refilling sites are usually very restricted in land use.

There are not many examples of hydrogen-operated maritime vessels. One operational unit of a light passenger ferry, “Sea Change”, is produced by “Switch Maritime”. Its specified compressed hydrogen capacity is 246 kg at 250 bar [22]. The modeling of such system would be very similar to the proposed heavy-duty vehicle refueling and trailer filling. Thus, we can assume that the model results could be also representative for light passenger ferries.

Table 2: *Parameters for a vehicle onboard storage*

Parameter	Value
Reference pressure*, bar	350.0
Reference temperature, C	15.0
Hydrogen capacity*, kg	38.0
Volume, m^3	1.6
Refilling time*, min	8-20

After each refilling operation, pressure in the high pressure (HP) storage is restored by compressing from the medium pressure (MP) storage. This allows dispensing maximum amount of hydrogen and complete end-user refilling.

3.2 Compressed hydrogen refilling basics

Unlike many other gases, hydrogen has a negative Joule-Thomson coefficient at temperatures and pressures found during the operations. Its inversion temperature is around 200 K or $-73\text{ }^\circ\text{C}$ at 20 bar. The end-user refilling and the trailer filling are done by throttling high-pressure hydrogen. With temperature rise during compression in the cylinder, this can lead to a temperature rise above operational inside the cylinder, thus, damaging polymer materials. During simulations, it is assumed that starting temperature at storage vessels, the tube trailer, and the onboard tank equals the ambient conditions.

When compressed rapidly into an empty volume, gas temperature rises significantly [23]. This may lead to underfilling of the volume, since pressure is higher at higher temperatures. To maximise refilled mass, a tank should be overpressurised during refilling operations to achieve target density or state of charge (SOC) at temperatures higher than reference. As an example, the following figure shows this relation for hydrogen obtained using NIST REFPROP. The red dot represents an operational reference point for the 300 bar cylinder at $15\text{ }^\circ\text{C}$ provided by a manufacturer. The blue line is 100% SOC and shows target pressure for different temperatures of the gas. The yellow line is limiting temperature of the cylinder.

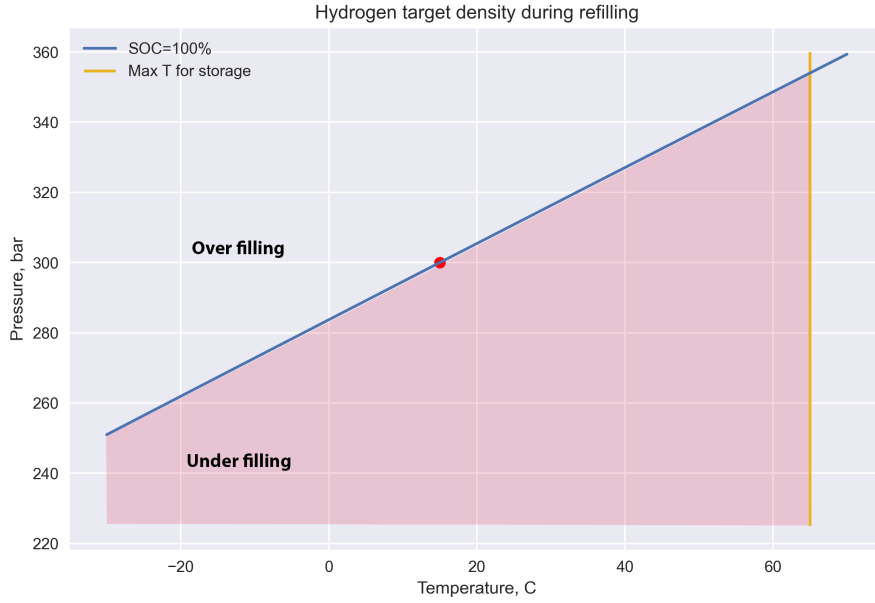


Figure 9: Target density for 300 bar cylinder

Operations that are modelled were assumed to be time-bounded. SAEJ 2601 fuelling protocol suggests time values for light-duty vehicle refilling operations under 3 min [3]. For the considered heavy-duty vehicles and maritime transport, time bounds most likely will not be so tight. However, they should be in the range of the current refilling time with conventional fuels. In this case, ambient cooling might not be enough to provide an acceptable temperature rise and desired refill time. For this matter, refrigeration of hydrogen is needed before dispensing it into the vessels. Pre-cooling below $-40\text{ }^{\circ}\text{C}$ is not allowed since it might brittle cylinder material.

Refilling thermodynamics directly influences hydrogen distribution network operations and energy efficiency of the system.

In practice, different refilling strategies exist in terms of flow rate control [3]. For modelling purposes, a constant pressure rise ramp rate is assumed for convenience. It allows to obtain the same refilling times independent of a tank volume.

The following table summarizes the distribution chain assumptions regarding compressed hydrogen storage.

Table 3: *General pressure, temperature constraints*

Section		Operational pressure (at $15\text{ }^{\circ}\text{C}$), bar		Operational temperature, $^{\circ}\text{C}$	
		Minimum	Maximum	Minimum	Maximum
Production site	Intermediate storage	20	200	-40	65
	MP storage		250		
	HP storage		350		
	Trailer	20	300	-40	65
Refilling site	MP storage	20	500	-40	65
	HP storage		350		
		Onboard tank	20(5)	350	-40

4 Methods

4.1 Assumptions

Before stepping into the actual modelling part, first, some requirements and restrictions for the model should be specified. Based on that, the overall complexity and the level of abstraction of the model would change.

1. The dynamic model should give the estimation of energy consumption, both compression and cooling, throughout a mid-scale hydrogen distribution chain. That includes capturing some of the system dynamic behaviour, for example, thermal effects.
2. Model should be representative of general operational conditions of the compressors, such as pressure ratio, suction pressure, and discharge pressure.
3. Give a hint at the expected storage volumes at chosen pressure levels and production capacity, not necessarily optimized.
4. The system layout is chosen to take the advantage of existing optimized designs. Thus, a cascade system is used for fast filling operations instead of a buffer system.

4.2 FMI based workflow

Functional mock-up interface (FMI) is a free standard that enables interaction of supported simulation environments (for example, Dymola) and functional mock-up unit (FMU), a special form of a computer model produced by a modelling software supporting the standard. This allows to develop models in different modelling environments and then run them together to study more complex models. However, at the moment, simulation interactions are mostly limited to data transfer into FMUs and then obtaining the result. This behaviour is very similar to functions in programming languages.

In the context of this work, the models are developed in Dymola, and further simulations and data manipulation are done using Jupyter notebook in Python language. To enable interaction and simulation of FMUs with Python, pyFMI 2.5 package is used together with Assimulo simulation package. There are two main reasons for using Dymola and Python together.

First, the modelling of the systems shown in the Figure 7 and Figure 8 involves complex control algorithms. Each model of the system part is shown in detail and discussed in the following sections. However, the general tendency is that modelling the whole system is more than twofold demanding as the modelling the two of its parts separately. Therefore, slicing the model into smaller pieces would be a more natural choice (of course, as long as it is possible), thus, improving model computational performance and stability. Smaller models are also more general and can be used in other simulations and studies.

Secondly, the nature of the considered hydrogen distribution chain model is dynamic with discrete operations. While Dymola models perfectly cover the dynamic part, the discrete part, i.e. refilling operations of vehicles and trailers is easier to model by writing Python code. For example, Python allows running a "while" loop to simulate and find the number of heavy-duty vehicles that can be refilled by repeating the same simulation. This significantly simplifies the modelling work. Another example is the existence of transient periods in the chain for which the dynamics is not very important, and they can be modelled by writing a proper script.

And most important is the fact that such approach allows automation of simulation. Writing a script gives possibility to run as many simulations as needed with varying parameters, and then analyze and manipulate data in the preferred manner.

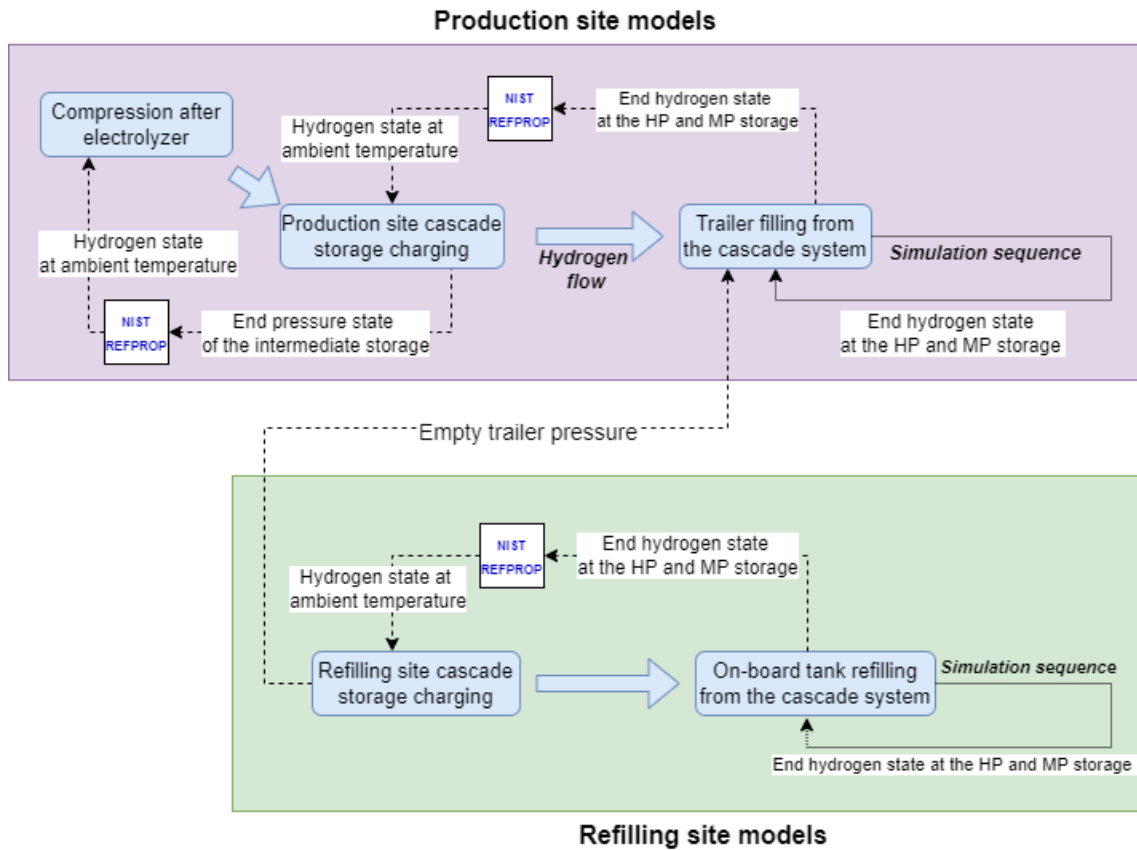


Figure 10: Data flow during simulation using FMUs and Python

In the figure 10, separate models are presented in blue. The blue arrows show physical hydrogen stream. More detailed flow-sheet of each of the models is presented in Figure 11. Dashed lines in Figure 10 represent data streams. Results obtained from one model are transferred as initial conditions to the other model. Additionally, intermediate calculations can be included. In this work, NIST REFPROP is used to obtain new hydrogen states assuming isochoric temperature change to the ambient conditions inside storage tanks between some operations.

Some models are simulated in a sequence, such as filling of the trailers at the production site and end-user vehicles at the refilling site. After each filling operation, end hydrogen state at each of the storage vessels is passed to the next simulation. The sequence continues until specified conditions are reached.

The complete model is simulated assuming stable operating conditions. This means that initial operations to fill the storage at the production site are not considered.

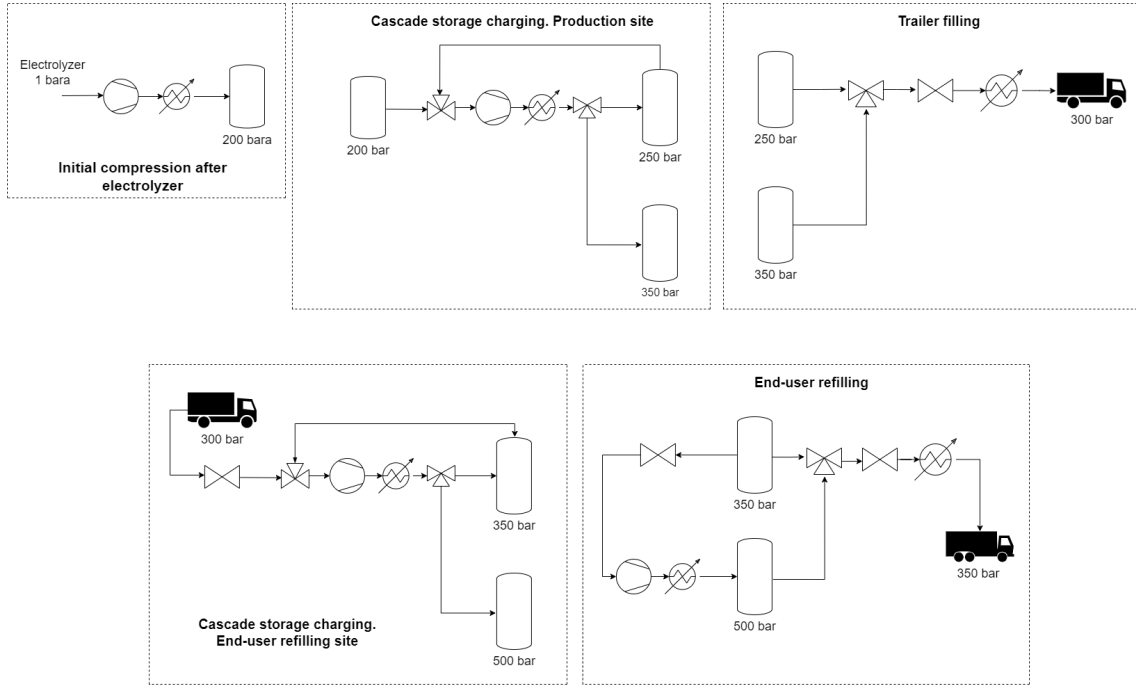


Figure 11: Overview of the models used for simulation

4.3 Efficiency compressor

Isentropic efficiency is the relation of work done by an ideal machine that follows isentropic cycle and actual power consumption that can be presented by the following relation:

$$\eta_{is} = \frac{W_{is}}{W_{tot}} . \quad (1)$$

The example of a real diagram is shown in Figure 12. As can be seen, the overall efficiency reaches its maximum at some pressure ratio of compressor operating range. For low-pressure ratio values, it decreases sharply, tending towards zero as the ratio approaches 1. At pressure ratios higher than optimal, a tendency for a decline in efficiency can also be seen, though not as steep.

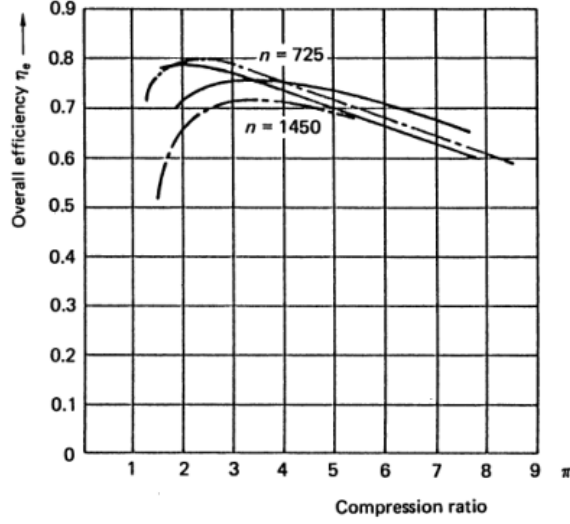


Figure 12: Compressor efficiency for different pressure ratios at different speeds (solid line for R22 refrigerant and dashed line for R717)

Source: [24]

In this work, we try to make valid assumptions regarding the efficiency of compressors that can be used. The report from the National Renewable Energy Laboratory (NREL) of the U.S. Department of Energy points out that at the time of the publishing, there were not enough actual data on real-world hydrogen compressor applications [17]. Estimated values in the report range from 50% to 80% for pessimistic and optimistic cases, with 65% as a base case [17]. We want to be closer to the lower bound and continue with 55% maximum isentropic efficiency for all compressors.

Another important characteristic for a positive displacement compressor is its volumetric efficiency. Actual volumetric flow through a positive displacement compressor can be presented as

$$\dot{V} = \lambda \dot{V}_t \quad (2)$$

where \dot{V}_t - theoretical volumetric flow resulting from piston movement, λ - overall volumetric efficiency.

The overall volumetric efficiency includes different sub-losses that result in decreased volumetric flow. This may include gas heating from the cylinder walls on suction that leads to its expansion, pressure loss over suction valves, clearance volumetric efficiency - the expansion of gas left in clearance volume, and leakages through valves and piston [24]. Overall volumetric efficiency is difficult to model without actual performance data. However, clearance volume volumetric efficiency can be taken into account. The following relation is used to calculate clearance volumetric efficiency [24] which is implemented further to plot a curve:

$$\eta_v = 1 - \left(r_p^{1/k} - 1 \right) c \quad (3)$$

where c - relative clearance volume, k - isentropic exponent.

Table efficiency compressor model by TLK Thermo is used in the model. Its main principle sums down into several equations. The first one is to find the outlet state of compressed gas. As seen from Figure 13, P_{VLE} represents power needed for actual compression of gas. The value is higher as compared to isentropic power consumption P_{isen} . Additional losses, such as mechanical friction, are included in effective isentropic efficiency and define compressor power demand at the shaft,

P_{shaft} . The following equation describes isentropic efficiency in the model:

$$\eta_{is} = \frac{h_{is\ discharge} - h_{suc}}{h_{discharge} - h_{suc}}, \quad (4)$$

where $h_{is\ discharge}$ - specific isentropic discharge enthalpy; $h_{suc/discharge}$ - actual specific enthalpy at compressor suction/discharge.

Volumetric efficiency:

$$\eta_v = \frac{\dot{m}}{V_{dis} \cdot f \cdot \rho_{suc}}, \quad (5)$$

where \dot{m} - actual mass flow; V_{dis} - cylinder displacement; f - compressor speed; ρ_{suc} - gas density at the inlet.

Effective isentropic efficiency and power demand are as follows:

$$\eta_{is\ eff} = \frac{\dot{m}(h_{is\ discharge} - h_{suc})}{P_{shaft}}. \quad (6)$$

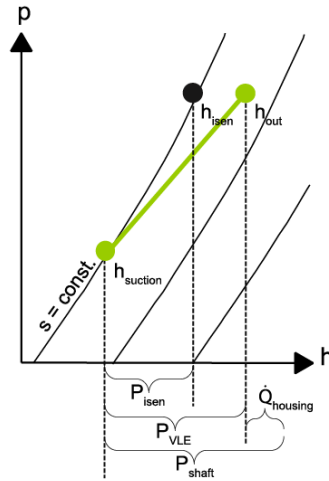
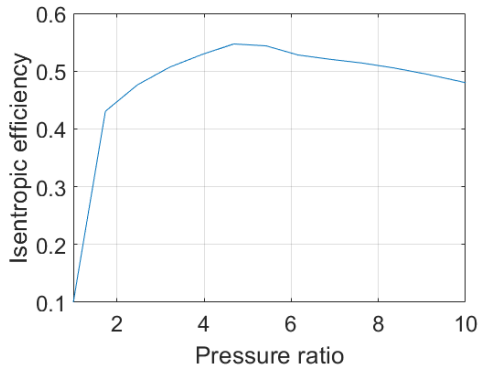


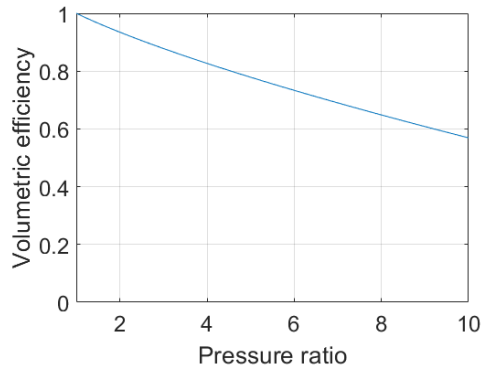
Figure 13: Diagram explaining compressor efficiency in Dymola

Source: TLK-Thermo

In the considered model, no additional losses in the compressor are assumed, and effective and isentropic efficiencies are the same. The compressor model uses a look-up table approach with linear interpolation to obtain compressor efficiency at different operational modes. Developed isentropic and volumetric efficiency curves are provided into the model as tables. The compressor model can also include dependence on compressor speed. Nevertheless, we do not include this in the distribution chain model. Isentropic and volumetric efficiency curves used for compressors in the model are shown in Figure 14a and 14b. Clearance volume, c , is assumed at 10%.



(a) Isentropic efficiency of a compressor



(b) Volumetric efficiency of a compressor

Figure 14: Compressor performance curves

Table 4: Summary of the assumption for a compressor

Type	Piston
Maximum efficiency	55%
Pressure ratio with maximum efficiency	5
Fixed clearance volume	10%

4.4 Thermal modeling of Type IV hydrogen cylinder

Since compressed hydrogen operations may include complex thermodynamics, different thermal effects should be studied. For this purpose several simplified models were created in Dymola to investigate thermal performance of a cylinder model during filling and emptying, at different ambient temperatures.

Figure 15 depicts the model used for temperature studies during cylinder filling. The boundary provides required hydrogen mass flow into the volume at chosen temperature. The mass flow is controlled by PI controller and is set to sustain desired constant pressure ramp rate in the volume. Piping is not modelled nor heat exchange in pipelines. The four heat resistors connected to the volume represent heat transfer from the gas to the wall, heat conduction inside the polymer layer, heat conduction inside carbon layer, and heat transfer to the ambient air. The latter modelled by the thermal boundary at constant temperature. The thermal mass, representing carbon wall, is placed in between the heat resistors. Its initialization temperature is in equilibrium with the ambience.

Table 5 shows the available type IV cylinder data from Hexagon Purus. Outer surface area was calculated as for a cylinder enclosed by two hemispheres:

$$A = \pi(dL + d^2), \quad (7)$$

where d - diameter, L - cylinder length.

Table 5: Type IV cylinder data from Hexagon Purus

Pressure, MPa	D_{out}, mm	Length, mm	Weight, kg	Liquid volume, m^3	A_{out*}, m^2
25	653	5689	342	1.544	13.0
30	509	2342	112	0.35	4.6
31.8	503	2342	94	0.35	4.5
35	509	2342	112	0.35	4.6
50	520	2357	180	0.333	4.7
70	705	2078	272	0.457	6.2

Other than the intermediate storage, all other storage volumes in the chain are assumed to consist of the integer number of type IV cylinders. Thus, geometrical parameters of a storage, i.e. its total area, mass, and volume, are the product of respective parameters of the particular cylinders used and their total number. Without complete cylinder data, outer surface area is used also as the inner one, and the wall thickness is assumed the same. The following table summarizes general assumptions for the hydrogen cylinders such as outer and inner surface convective heat transfer coefficient h , heat conductivity of the materials k , their respective thickness L , and specific heat capacity c .

Table 6: Type IV cylinder general assumptions for modeling of thermal effects

Inner surface	$h_t = 500 \frac{W}{m^2 \cdot K}$	
Polymer layer	$K = 0.5 \frac{W}{m \cdot K}$	$L = 0.005 \text{ m}$
Carbon layer	$K = 0.5 \frac{W}{m \cdot K}$	$L = 0.0316 \text{ m}$
Outer surface	$h_t = 5 \frac{W}{m^2 \cdot K}$	
Composite capacity	$c_t = 1120 \frac{J}{kg \cdot C}$	

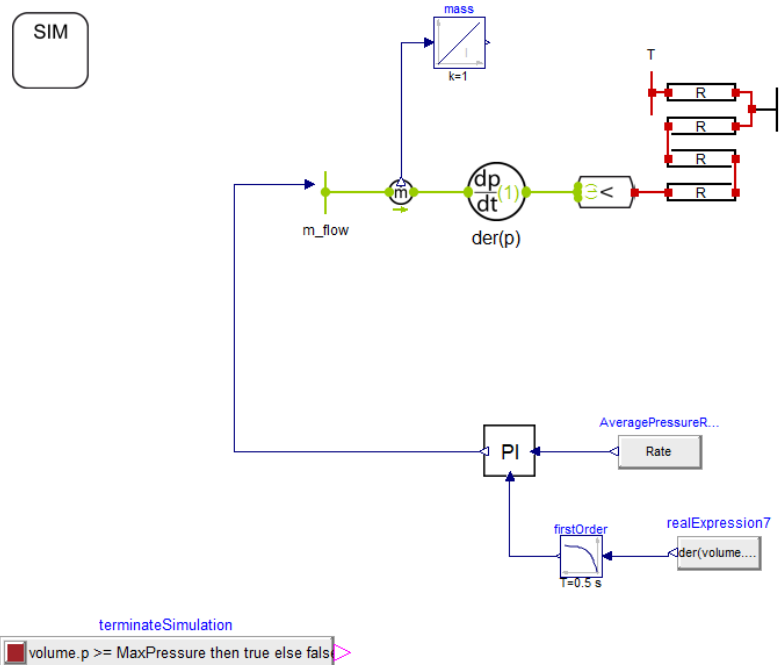


Figure 15: Dymola diagram view of the model for the cylinder filling

To simulate the emptying of a hydrogen tank, a very similar model is used. A second volume (the one that is being filled) is connected to the first volume, both at specified conditions. The PI

controller regulates opening of the throttle valve to provide constant pressure ramp rate at the second cylinder. Simulation ends when either pressure in the first volume drops below specified or specified SOC is achieved in the second volume. The model is presented in Figure 16.

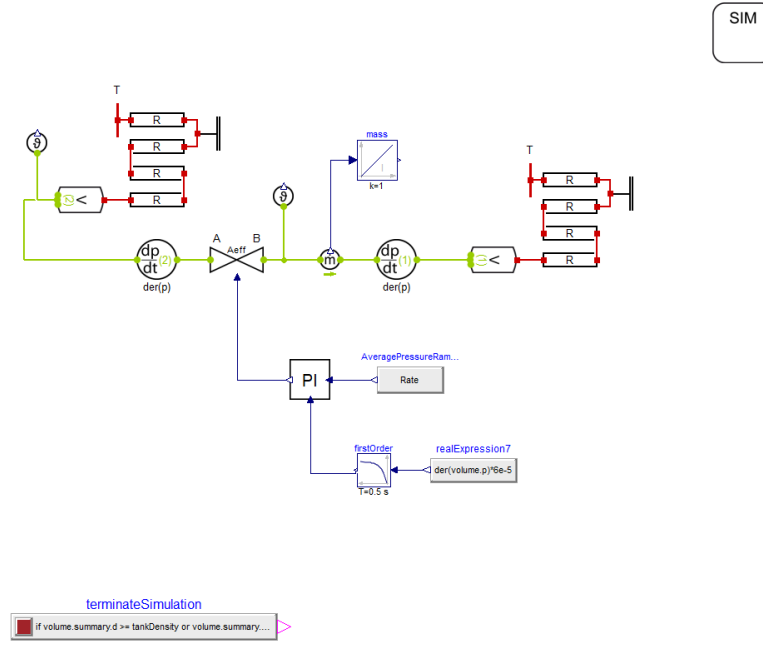


Figure 16: Dymola diagram view of the model for the cylinder emptying

4.5 Compression after electrolyzer

Once hydrogen is produced at atmospheric conditions, it should be compressed. Production is modelled by creating a boundary in Dymola at 1 atm (1.013 bara) pressure and 20 C° . Four table efficiency compressors model multi-stage compression. The existing solutions, for example, from Mehrer compression, include 4-stage piston compressors. The proportional-integral (PI) controller, available from the TIL library, is used to provide constant mass flow of hydrogen at the last stage compressor. Other PI controllers control pressure lift at each stage by adjusting compressor speed. To determine the optimal pressure ratio at each stage for multi-stage compression with intercooling r_p , Eq. 8 is used [24]:

$$r_p = \sqrt[i]{\frac{p_{out}}{p_{in}}} \quad (8)$$

where i - number of stages, p_{out} - output pressure, p_{in} - intake pressure.

After each compressor, hydrogen is cooled down to 30 C° (or more precisely, $T_{amb} + 10$) in inter- or aftercooler which fin-and-tube heat exchanger represents.

The intermediate storage is comprised of steel cylinders and simple heat exchange model is build in Dymola. Length and diameter are arbitrary in this case. The value for volume has been chosen after running several simultaneous simulations with the cascade charging model, to obtain pressure ratios for compressors (the one used to fill intermediate storage and the one to charge cascade system) to be within practical margins.

The three heat resistors represent heat transfer from the gas to the wall, heat conduction inside the wall, and heat transfer to ambient air. The latter modelled by the thermal boundary. The thermal mass representing a steel wall is placed in between the heat resistors. The main parameters used for simulation are presented in Table 7.

The value of stainless steel heat conductance is available through TIL Media library. Wall thickness for a cylinder capped by two hemispheres is calculated by the following equation [23]

$$\frac{d_w}{d_o} = \frac{\Delta p}{2\sigma + \Delta p}, \quad (9)$$

where d_w - wall thickness, m; d_o - outer diameter, m; Δp - pressure difference, MPa; σ - tensile strength, MPa.

Mass of the cylinder is then calculated as

$$m = \rho \left(\frac{\pi}{4} (d_o^2 - d_{in}^2) L + \frac{4}{24} (d_o^3 - d_{in}^3) \right), \quad (10)$$

where ρ - material density; d_{in} - inner diameter; L - cylinder length.

Outer and inner area is calculated by the following equation

$$A = \pi(dL + d^2). \quad (11)$$

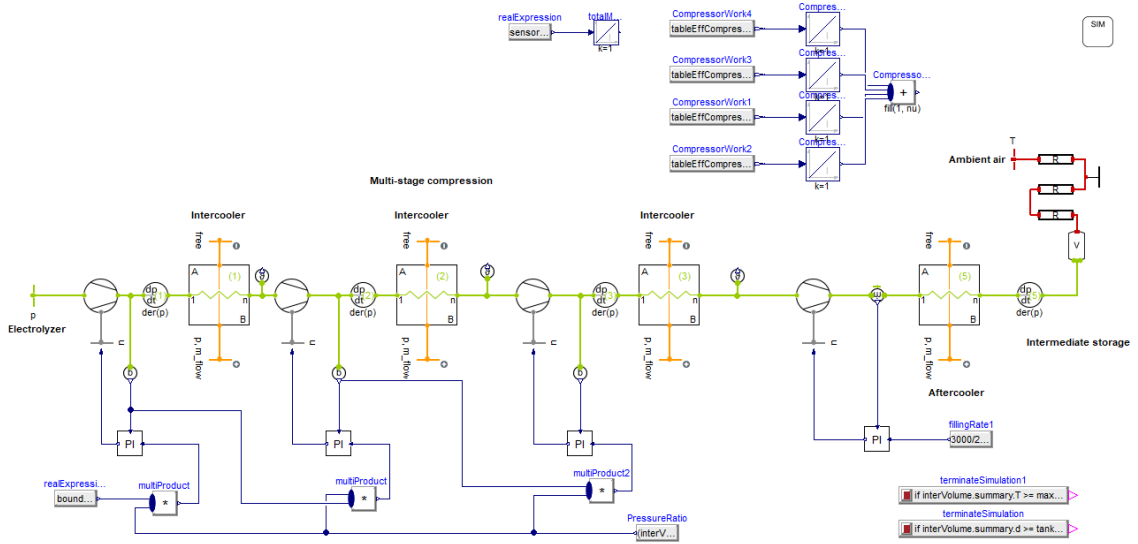


Figure 17: Graphical view of the hydrogen compression after electrolyzer model in Dymola

Here we introduce the main governing equations used in the heat resistor model as provided in TLK library documentation. The equation for heat flow is the following:

$$\dot{Q} = \frac{T_2 - T_1}{R}, \quad (12)$$

where R - thermal resistance.

Thermal resistance is given by equation

$$R_t = \frac{L}{K \cdot A}, \quad (13)$$

where L - length for heat conductance, K - heat conductivity, A - area for heat conductance.

For the modeling of heat transfer between wall and fluid, K is set into the resistor model as the convective heat transfer coefficient and L as 1.

Pressure and initial enthalpy are obtained after running the cascade storage charging model. Temperature in the storage volume can be lower than ambient after that, so the gas is assumed to reach ambient conditions. The new gas state is found using NIST REFPROP and set as the initial values.

Table 7: *Initialization parameters for the compression after the electrolyzer model*

Object	Parameter in Dymola	Value
hydrogen boundary	pressure	1.013 bara
	temperature	20 C°
pressure state 5	pressure	
intermediate storage	fixed volume	500.56 m^3
	initial enthalpy	
heat resistor inner surface	thermal conductivity	500 $\frac{W}{m^2K}$
	distance for heat conductance	1
	cross section for heat conductance	25.6 \times 726 m^2
heat resistor steel wall	thermal conductivity	0.68 $\frac{W}{mK}$
	distance for heat conductance	0.029 m
	cross section for heat conductance	26.37 \times 726 m^2
steel thermal capacity	mass	5412 \times 726 m^2
heat resistor outer surface	thermal conductivity	5 $\frac{W}{m^2K}$
	distance for heat conductance	1
	cross section for heat conductance	27.14 \times 726 m^2
Ambient air thermal boundary	temperature	20 $^\circ C$

Table 8: *Steel cylinder parameters*

	Value
Outer diameter	1.6 m
Length	6 m
Wall	29 mm
Mass	5412 kg
Steel density	7850 $\frac{kg}{m^3}$
Tensile strength	460 Mpa
Reference pressure	200 bar
Reference temperature	15 C°
Max temperature	65 C°

4.6 Cascade storage model. The production site.

The second part at the production site is the cascade storage charging model. After the desired amount of hydrogen is dispensed into trailers, the medium (MP) and high pressure (HP) cascade volumes are filled from the intermediate storage. The table efficiency compressor model is used, and it is set to provide a constant pressure ramp rate in the vessels. The aftercooler is assumed to provide cooling down to 70 C° and does not represent any actual dimensions.

The control algorithm is presented in Figure 19. Firstly, the MP vessel is refilled to the target density with valves 1 and 3 open from the intermediate storage volume. A view of the Dymola model is shown in Figure 20. Then valves 2 and 4 are opened so that the same compressor can refill the HP vessel from the MP vessel. The lower bound of pressure in the MP storage is arbitrary during this operation and equals 180 bar. Should pressure in the MP vessel go below this value,

the vessel will be refilled again. This is realised by using hysteresis block from Modelica standard library. The simulation stops, and the cascade system is ready when both vessels reach complete SOC. Target density is set for each pressure level and is based on the reference operating conditions of the chosen vessels. The initial state of gas at each vessel in the cascade system is assumed at the ambient conditions using the end data from the cascade trailer filling simulation.

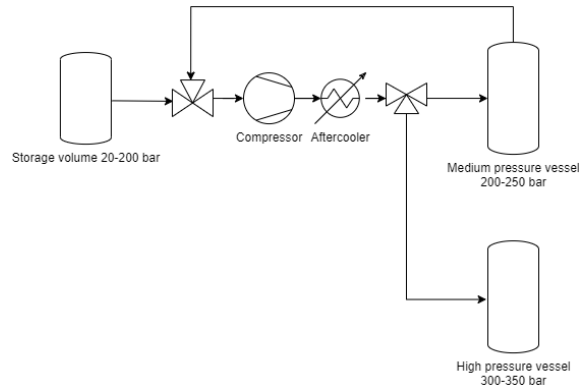


Figure 18: Diagram of the cascade model

Additionally, the simulation is stopped if the gas temperature inside any of the vessels exceeds limits (the specification is given in Table 3). A new gas state is calculated for both pressure levels assuming isochoric cooling to ambient conditions. This cycle is repeated until the target density is reached.

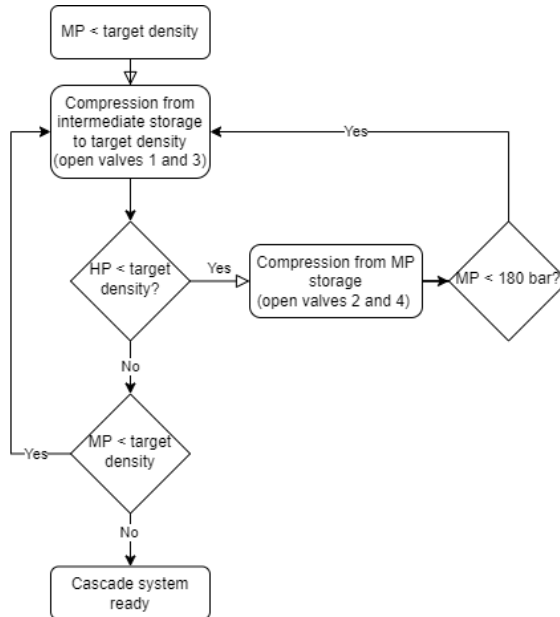


Figure 19: Cascade system charging algorithm

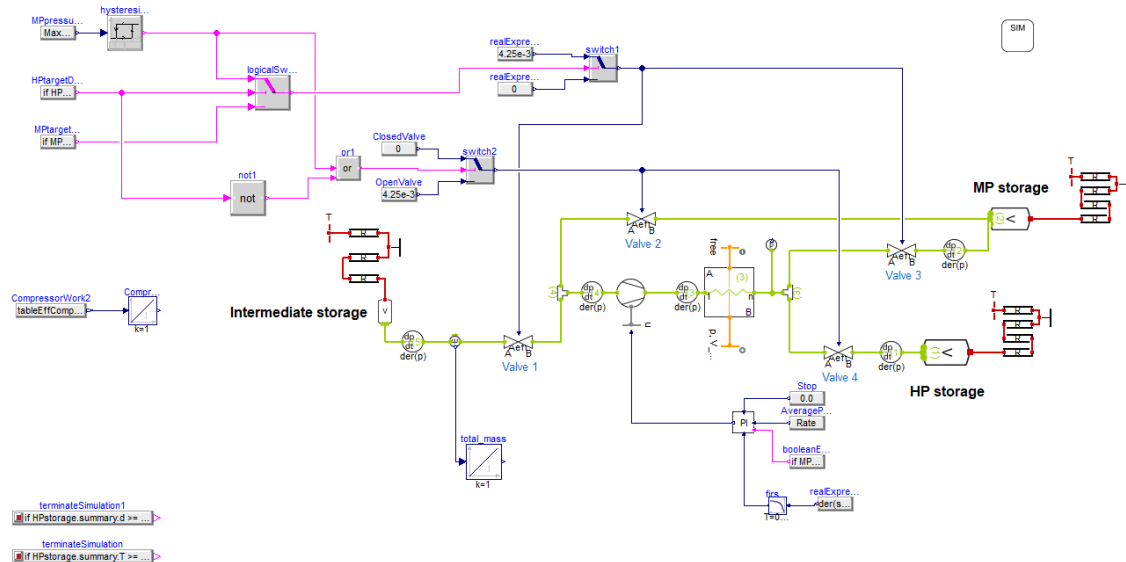


Figure 20: Graphical view of the cascade charging model in Dymola

Table 9 summarizes the main initialization parameters that are set before the simulation. Only several of them are set manually (values are presented), others are obtained from the simulation of the trailer filling model. Parameters for modeling of thermal effects of the cylinders, mass and area, are also set before simulation since they depend on a vessel volume. This, however, is automatized using script in Python. Thermal modeling of the intermediate storage is the same.

The model requires other blocks (objects) to be initialized as well, however, they are not of significance for our simulation purposes. This includes initial enthalpy distribution in heat exchangers and junction elements. Dimension and heat transfer parameters of heat exchanger block are also set to enable complete heat exchange to desired outlet temperatures. They are not indicative of heat exchanger performance at this modeling stage.

Pressure state objects represent pressure values in the elements they are directly connected to. In this case, "pressure state" corresponds to the MP storage, 1 - to the HP storage, and 2 - to the intermediate storage.

The volumes of the intermediate, HP, and MP vessels are chosen after running joint simulations with the trailer filling model.

Table 9: Initialization parameters of the cascade charging model at the production site

Object	Parameter	Values
Intermediate storage	fixed volume	500 m ³
	initial enthalpy	
Pressure state 2	initial pressure	
MP storage	fixed volume	500 m ³
	initial enthalpy	
Pressure state	initial pressure	
HP storage	fixed volume	200 m ³
	initial enthalpy	
Pressure state 1	initial pressure	
	Rate	0.5 MPa/min

4.7 Trailer filling model

The last model at the production site is used to simulate hydrogen cascade filling. Three consecutive trailer filling operations are simulated by running the Dymola model with Python script.

The cascade system consists of two volumes, high pressure and medium pressure, the same as for the previous simulation. Both vessels are filled to the target density and are at ambient temperature at the initial state. The trailers are assumed at the lowest density, which is calculated from the reference parameters presented in the table 3. The model diagram and graphical view in Dymola are presented in Figures 21 and 23.

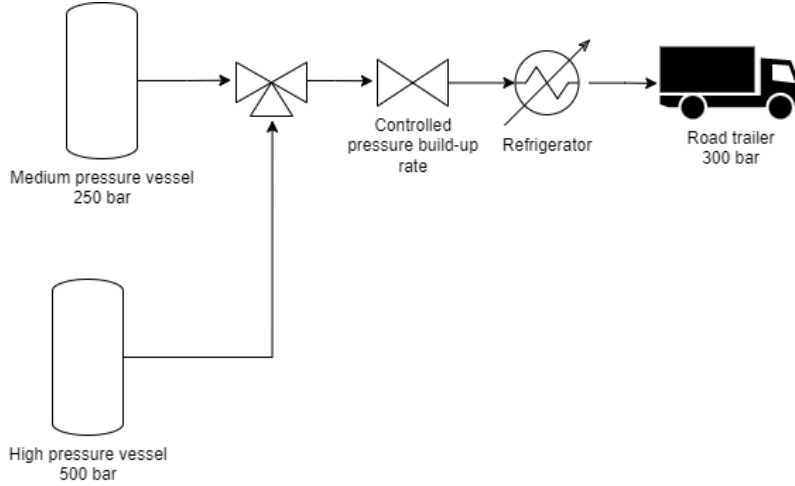


Figure 21: Diagram of the trailer filling model

The filling operation is performed by throttling hydrogen into the trailer with additional refrigeration. Heat exchange is not included in the model since filling operations are assumed to be done in approximately 15 min. In the results section it will be shown that much longer time intervals are needed for heat exchange to cause significant effect. The refrigeration plant and hydrogen heat exchanger only model hydrogen cooling. Energy balance for the heat exchanger has the following form

$$\dot{Q} = \Delta h \cdot \dot{m}, \quad (14)$$

where \dot{Q} - heat flow; Δh - hydrogen specific enthalpy difference at the inlet and outlet of the heat exchanger; \dot{m} - hydrogen mass flow.

Refrigeration power demand is calculated as

$$P = \frac{\dot{Q}}{\text{COP}}, \quad (15)$$

where COP - coefficient of performance.

Coefficient of performance is calculated as ideal Carnot cycle efficiency multiplied by the average refrigerator efficiency of 50%. This yields

$$\text{COP} = \frac{T_C}{T_H - T_C} \cdot 0.5, \quad (16)$$

where T_C - cold temperature, K ; T_H - temperature of heat sink (ambient temperature) K .

As an assumption, the pressure difference of 10 bar is used as a margin to account for pressure losses that inevitably occur in such systems. First, the MP valve is opened if the pressure difference is satisfied. After reaching predefined pressure in the trailer, the HP valve opens. The simulation continues until the target density (SOC=100%) is achieved, or the pressure difference between the HP vessel and the trailer drops below 10 bar. The refilling algorithm is shown in Figure 19.

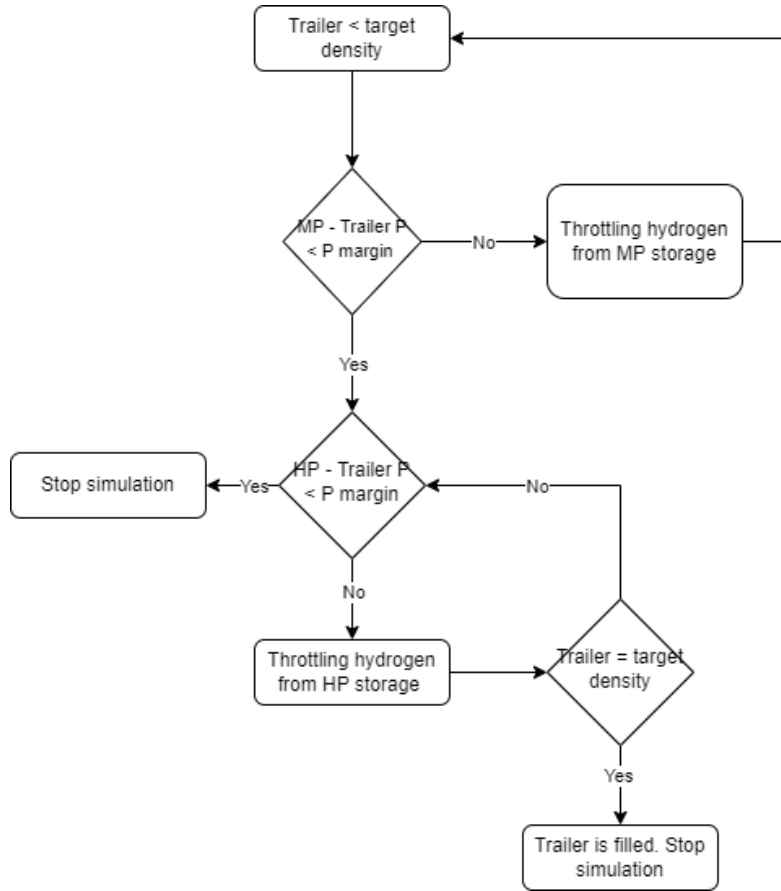


Figure 22: Trailer filling algorithm

The model created in Dymola simulates the filling of only one trailer. Otherwise, modelling three trailers at once would have increased the complexity of the model and made it less versatile. Here, we use FMI compatibility and Python to write a script and automatize the simulation process. Figure 24 shows the algorithm for simulation. Stages of the simulation shown in purple are realized with Python script. At the same time, blue represents the model in the form of an FMU file obtained from Dymola (technically, computation of the FMU is also performed in Python). Transferring end-state parameters of the cascade system, temperature and pressure, as the initialization values for the same model, three consecutive trailer filling operations are simulated.

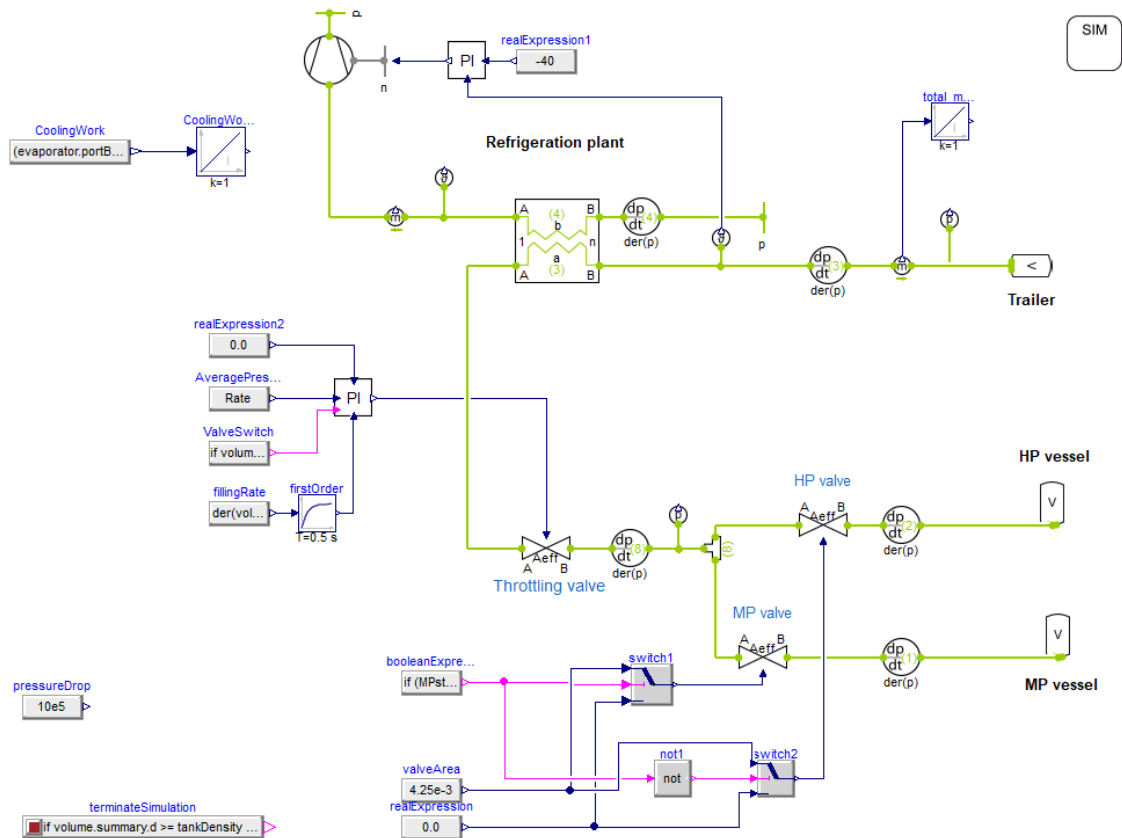


Figure 23: Graphical view of trailer filling model in Dymola

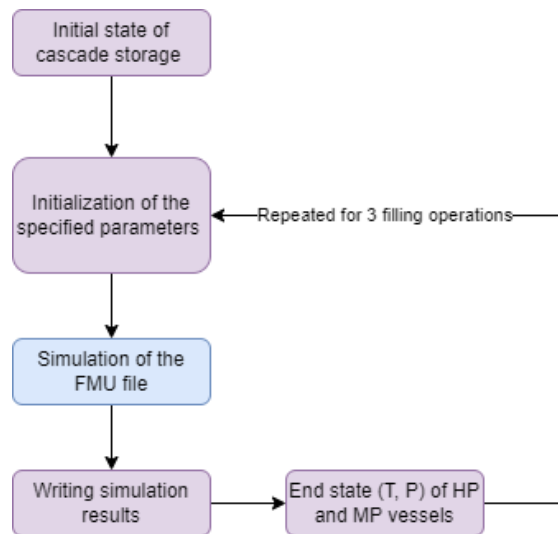


Figure 24: Trailer filling simulation algorithm in Python

4.8 End-user refilling model

End-user refilling model is an extension of the trailer filling model. The principal difference is that all available hydrogen is stored in the cascade system at the refilling site. The goal is to provide refilling of the maximum number of vehicles. For this purpose, HP storage should always be available at the highest pressure to ensure the complete filling of end-users. This leads to the need of additional compression of hydrogen from the MP to HP vessel between (or during) refilling

operations. The model diagram is presented in Figure 25.

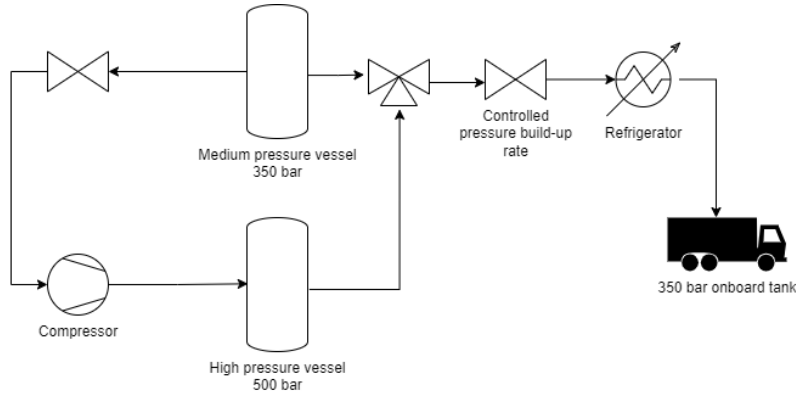


Figure 25: Diagram of the end-user filling model

The control algorithm for the model is shown in Figure 27. The refilling part of the simulation is the same as the trailer filling model. If required conditions are met, first, throttling from the MP vessel is done. Target density in the onboard tank is then obtained by witching the HP vessel. Once the tank is filled, the HP and MP valves are closed, and the refrigeration plant is stopped. The model components can be seen in Figure 26. Refrigeration need is calculated employing previously described principle, according to equations 14, 15, and 16.

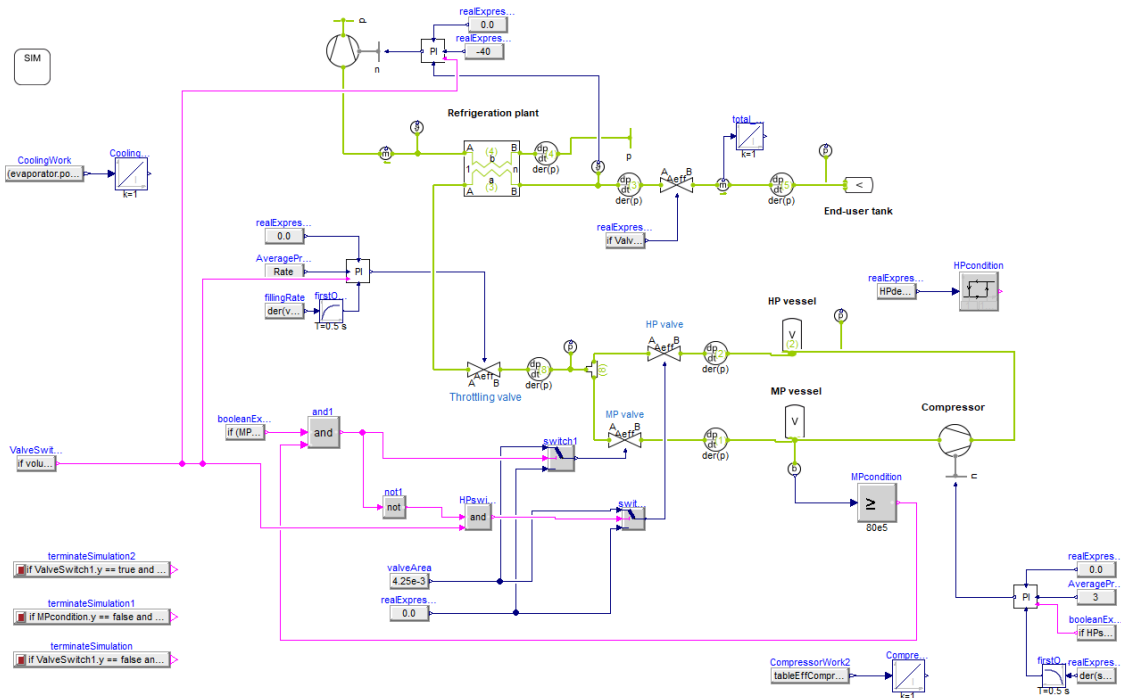


Figure 26: Graphical view of end-user filling model in Dymola

To make the simulation more stable, refilling of the HP storage only starts when the density inside the vessel drops below a specified value. This is realized by using hysteresis block and the condition of $\frac{\rho_{HP} P_{target}}{\rho_{HP}}$. The value is arbitrary, and pressure relation can be used instead. The other condition is that the pressure value in the MP vessel should not go below 80 bar. This is restricted by the compressor used, and in our case, we assume that the compressor should not reach pressure ratios above 10. If both conditions are satisfied, the HP vessel is refilled up to operational (or target)

density or until the MP vessel's pressure drops below 80 bar. Using fixed density instead of fixed pressure always gives the same amount of hydrogen stored and allows precise control of filling operations. Additionally, the simulation is stopped if the temperature inside the onboard tank exceeds 85 °C.

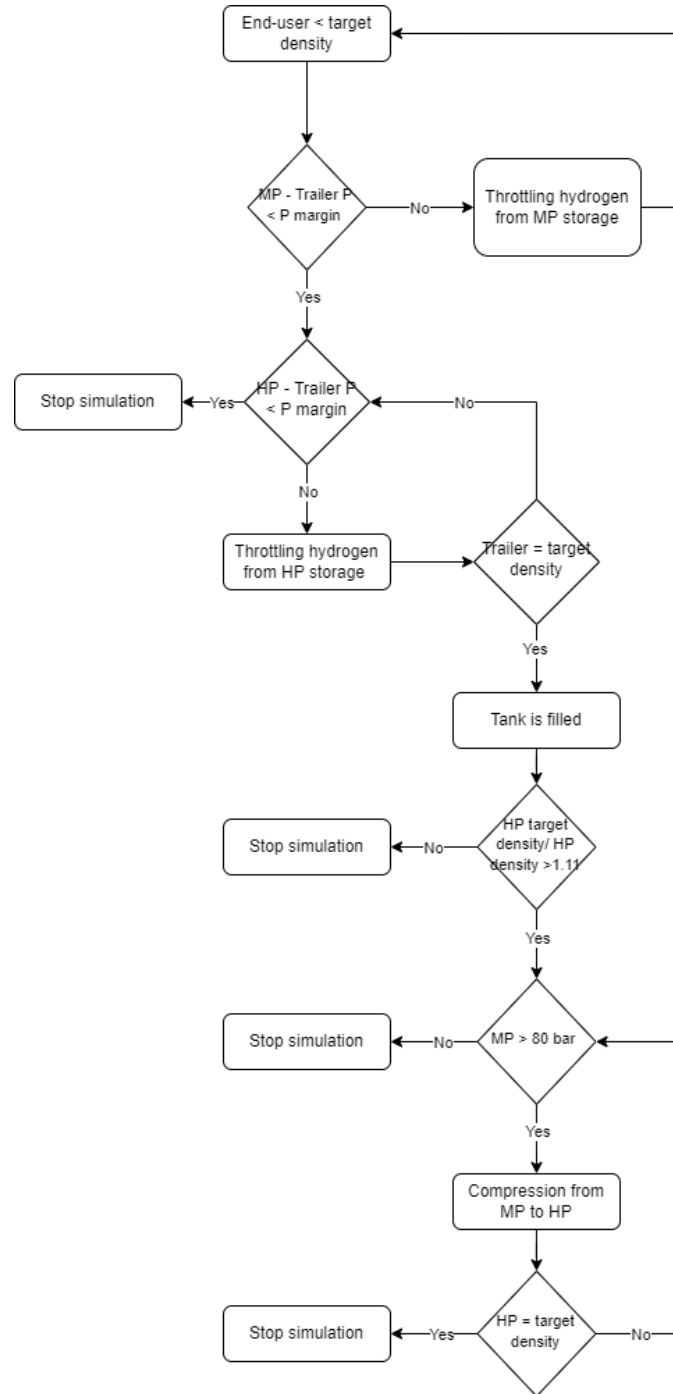


Figure 27: End-user filling algorithm

As with the trailer filling model, the Dymola model only simulates a single refilling operation. However, the number of refilled vehicles is unknown or can be very large. This makes building the model purely in Dymola even more difficult. Thus, the complete process is again simulated using an FMU model file and Python scripting. Figure 28 depicts the simulation algorithm in Python. The “while” loop is run until the end value at the onboard storage is less than the target value.

This would indicate that there is not enough hydrogen in the storage to complete refilling. Since we are interested in complete operations, data from such simulation is not added to the end file.

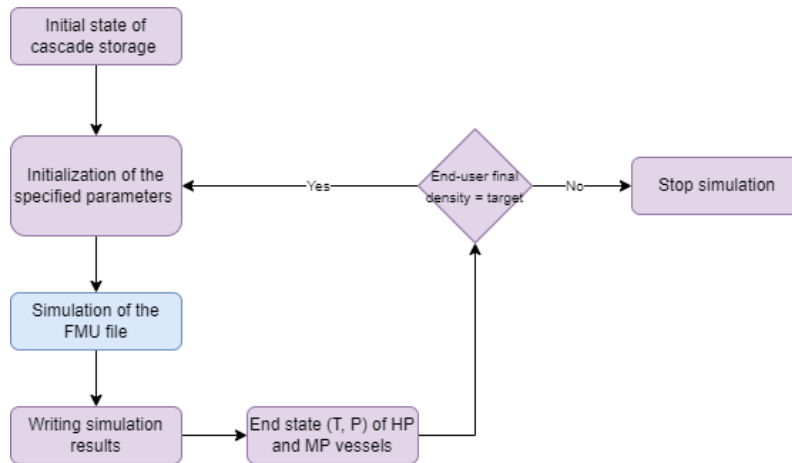


Figure 28: End-user filling simulation algorithm in Python

4.9 Cascade storage charging. End-user site

Cascade storage charging at the refilling site extends the cascade storage refilling model at the production site. Here, a throttling valve is added since the pressure in the MP vessel can drop significantly below the pressure in the trailer. The diagram of the model is presented in Figure 29.

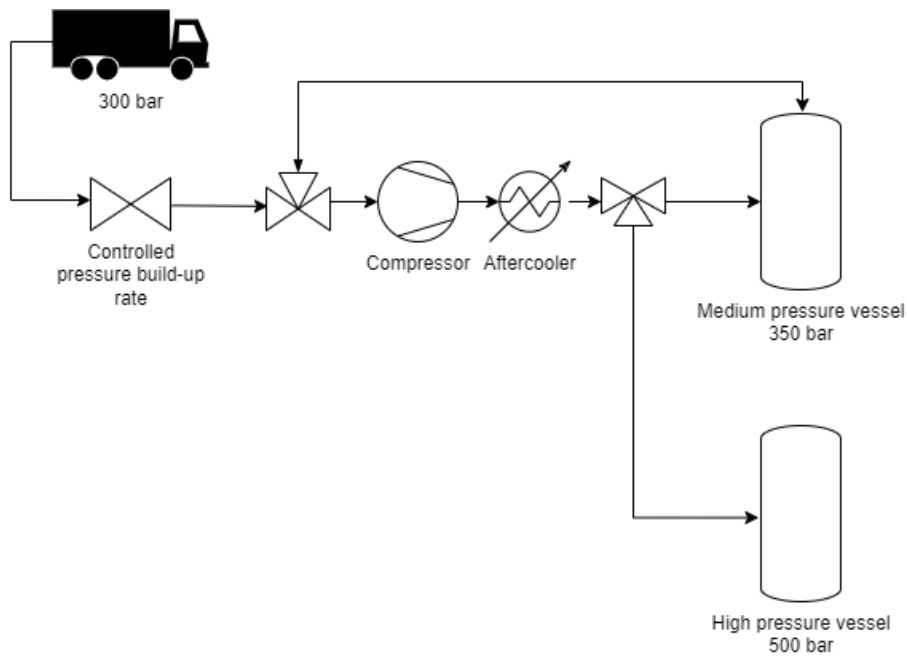


Figure 29: Diagram of the end-user cascade charging model

The initial state of gas inside HP and MP vessels is obtained after running the end-user refilling model. After the simulation is finished, gas is assumed to reach ambient temperature at constant volume. The calculation is done in Python using the REFPROP database.

The control algorithm is different from the cascade refilling at the production site and is shown in Figure 30. The first step is to charge HP storage from the trailer. By doing so, the advantage

of having high pressure in the trailer might be utilized. Hydrogen is compressed from the trailer with valves 1 and 4 opened. Otherwise, throttling into MP vessel with high-pressure difference may cause high exergy losses. However, no investigation on this matter has been done.

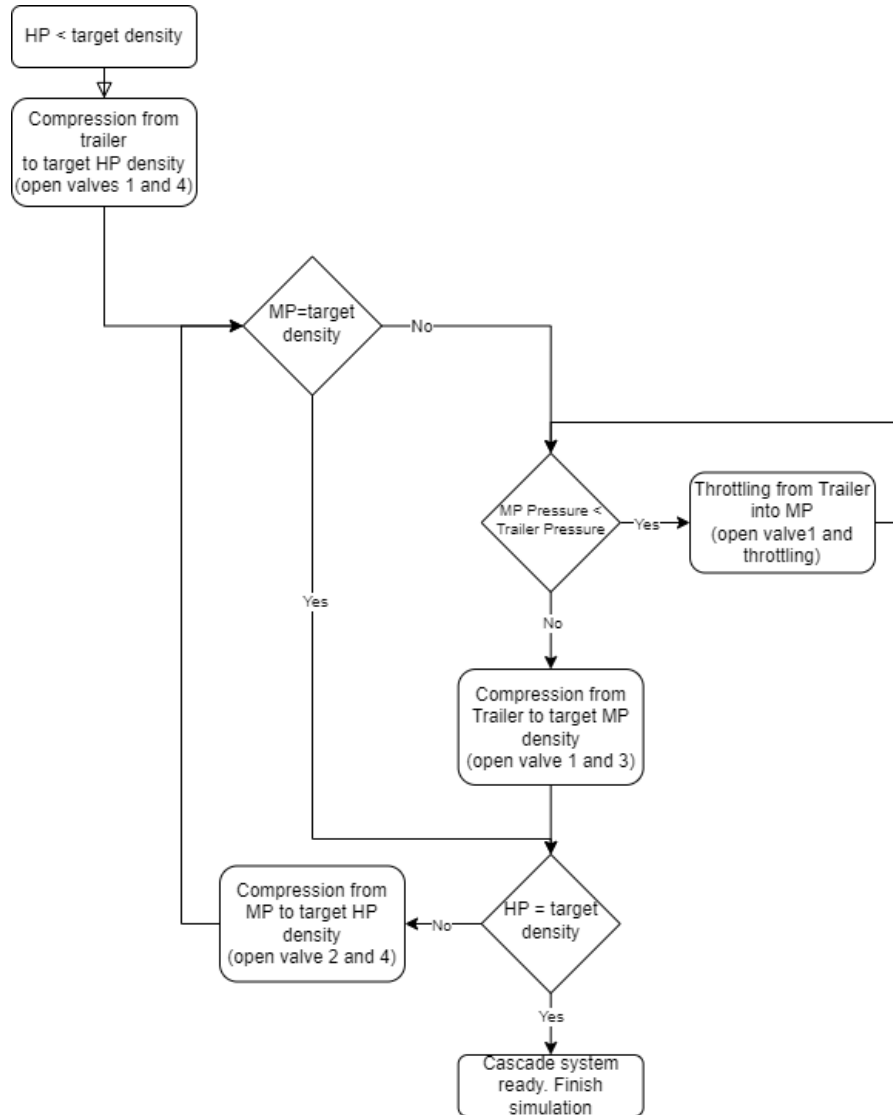


Figure 30: End-user site cascade charging algorithm

Once the target density at the HP vessel is reached, the MP vessel is refilled. If pressure at the trailer is higher than in the MP vessel, the throttling valve is opened, and the pressures are equalized. Then MP storage is filled up to the target density using a compressor with open valves 1 and 3. Additionally, simulation is stopped when any vessel's temperature constraints are breached.

The developed model allows more complex scenarios. However, only the described one is used. Logical blocks that are important for the considered case are marked with blue rectangular shapes and are shown in Figure 31.

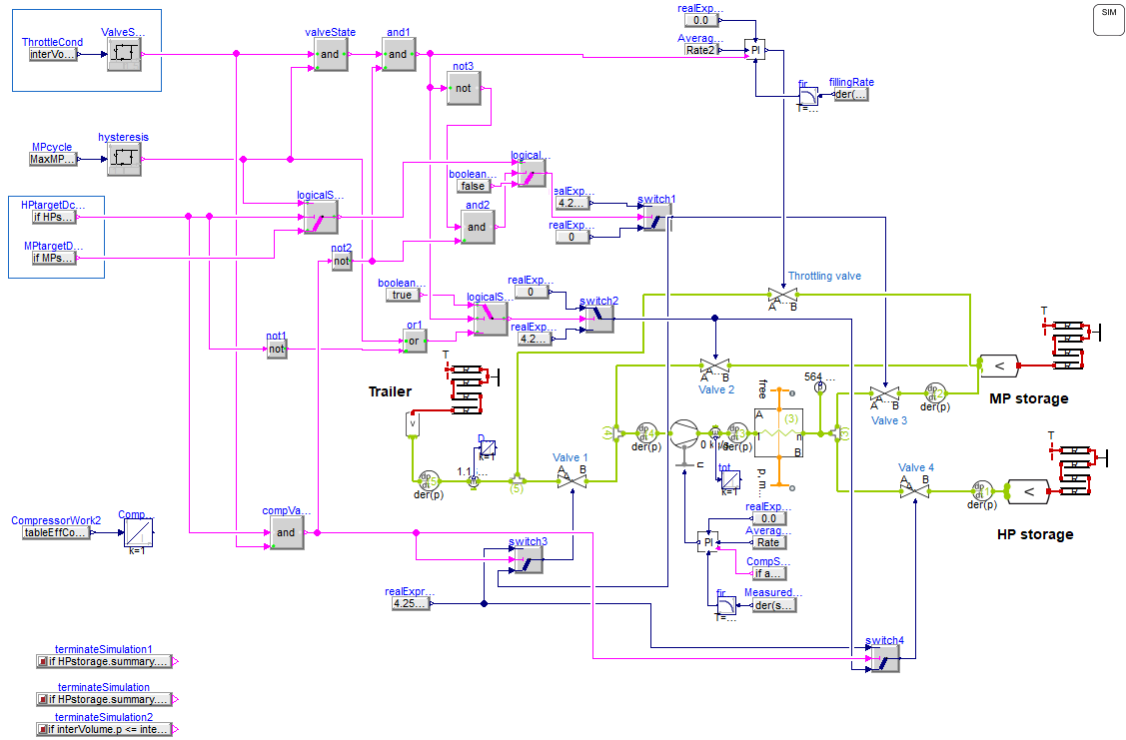


Figure 31: Graphical view of end-user cascade charging in Dymola

5 Results and discussion

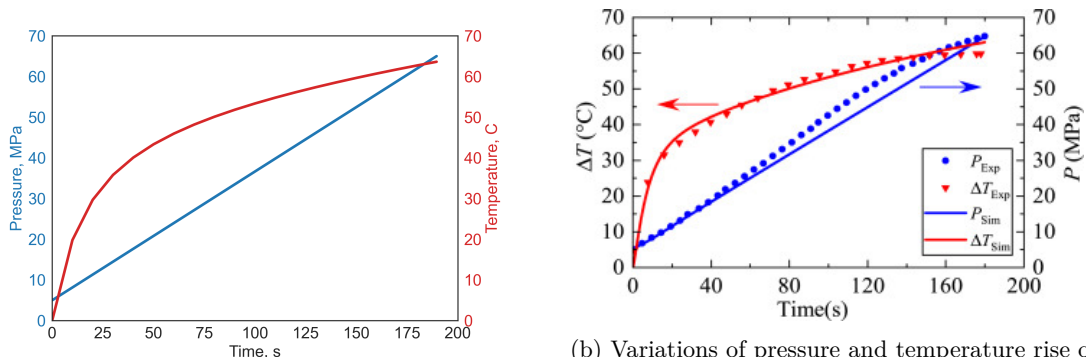
5.1 Thermal simulations results of Type IV hydrogen cylinder

In the article, Lei Xiao et al. [20] provide validation of their thermal model of Type IV vessel, comparing their simulation results with the experiments data for Type III vessel. Specifications for the type IV vessel are very similar to used in the present paper. Parameters marked with an asterisk are obtained from the TLK-Thermo example model of a hydrogen refueling station. The following table summarizes assumptions from the article and the current work.

Table 10: Assumptions for the two models in comparison

Design parameter	Assumption in the article [20]	Present work	Unit
Convective heat transfer coefficient between hydrogen and the inner wall of the liner	400	500*	$\frac{W}{m^2 \cdot K}$
Heat transfer between the outer wall and the ambient air	4.5	5*	$\frac{W}{m \cdot K}$
Thermal conductivity of the plastic liner	0.5	0.5*	$\frac{W}{m \cdot K}$
Thermal conductivity of the composite wrapping	0.5	0.5*	$\frac{W}{m \cdot K}$
Composite wrapping thickness	38.3	31.6*	mm
Plastic liner thickness	5	5*	mm
Tank volume	174	330	L

Figure 32a present simulation result for the filling of a 500 bar cylinder with volume of 0.33 m^3 (cylinder parameters are presented in Table 5). Simulation time is chosen to be the same as in the article. We assume that pre-cooling is done at $-40 \text{ }^\circ\text{C}$. Figure 32b depicts the comparison of the simulation, subscript "sim", and the experiment, subscript "exp".



(a) Result of the simulation of the cylinder thermal model for filling

(b) Variations of pressure and temperature rise of the gas in the vehicle cylinder during the refueling process.

Source: [20]

Figure 32: Model validation

The two figures show good agreement between our model, the model from the article, and the experimental reference data in the considered time range. The overall thermal behaviour is very similar to the adiabatic, and heat exchange does not cause any significant effect. This may explain very similar results considering some differences in cylinder specifications. However, our model might give higher errors for longer processes where heat exchange can play an important role.

Once some validation for the thermal model is obtained, we can run parametric studies on it to better understand the thermal behaviour of storage vessels to set up process parameters later. Figure 33 shows the variation of the final temperature depending on the pressure ramp rate or, in

other words, filling time. The simulation is done for a 300 bar 0.35 m^3 cylinder. We assume the most "aggressive" precooling to -40 C° , and ambient temperature of 20 C° . The highest temperature corresponds to the adiabatic case when no heat exchange occurs inside a vessel. The difference of approximately 10 degrees is obtained for filling rates of $3 \frac{\text{MPa}}{\text{min}}$ and lower. Thus, some operations at constant pressure ramp rate can be modelled as adiabatic to simplify the process.

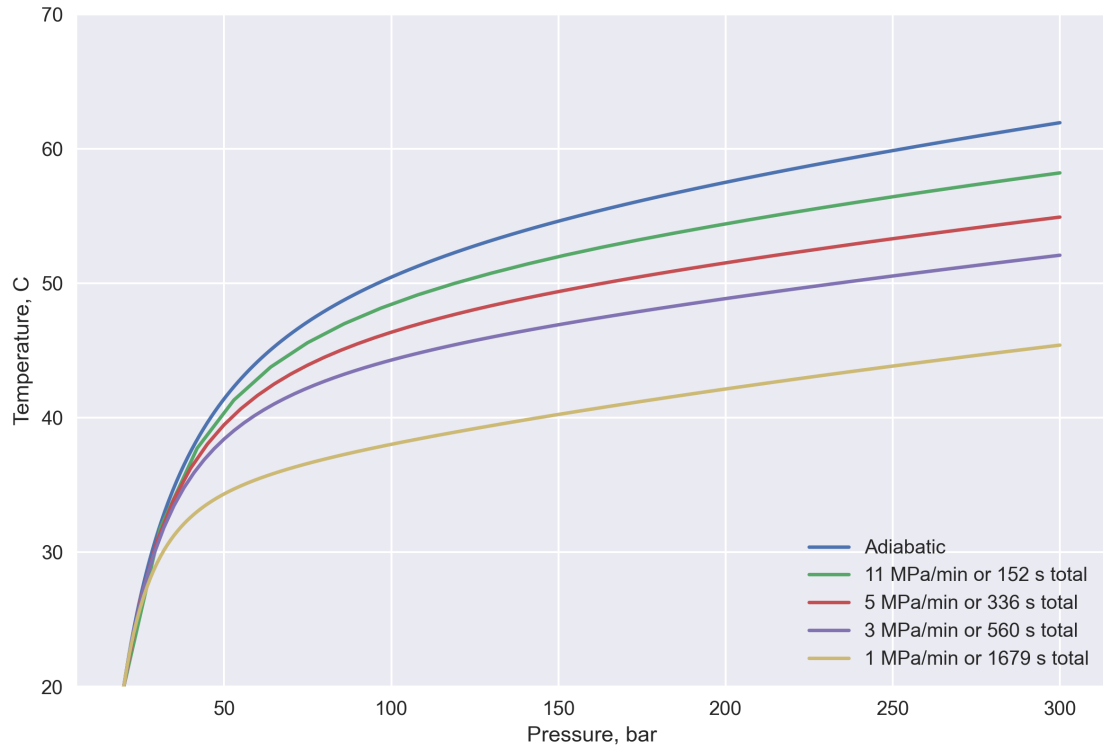


Figure 33: Temperature results with varying pressure ramp rate during filling

Secondly, pre-cooling temperature influence on fast filling operations can be examined. We can assume no heat exchange to simplify modelling since almost adiabatic behaviour might be expected. Adiabatic filling of the cylinder, the same as for the previous simulation, displays that pre-cooling of -40 C° is required to allow safe, fast filling operations of trailers and storage tanks with the upper-temperature constraint of 65 C° at rates of around $3 \text{ MPa}/\text{min}$ and higher. As shown previously, we can exclude heat exchange influence in this time range.

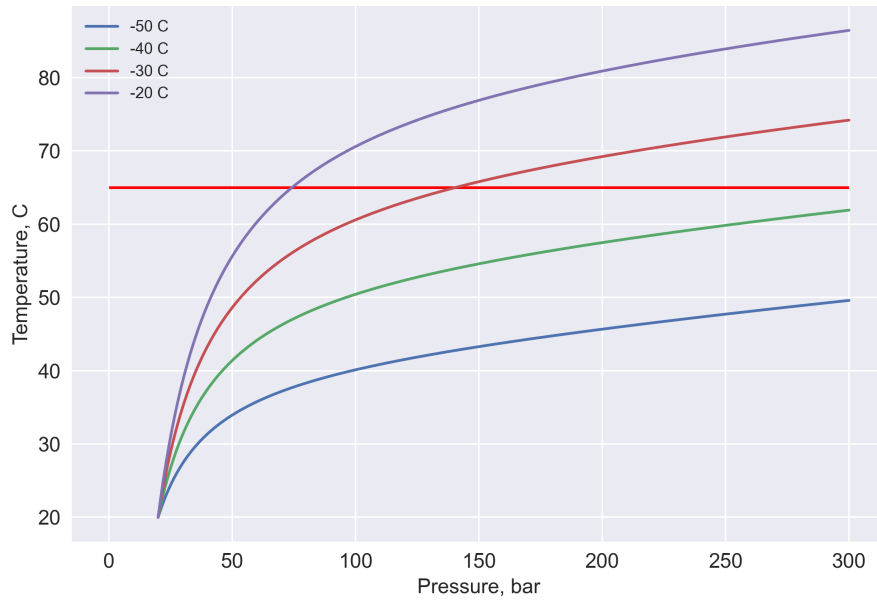


Figure 34: Pre-cooling influence on the final temperature without external heat exchange

Another result from the same simulation that can be useful for understanding filling thermodynamics is the amount of filled hydrogen depending on the final temperature at the same pressure. Figure 35 depicts decline in stored mass in the cylinder at higher temperatures. This is the main reason to use the density value of hydrogen, or SOC, inside a tank to determine the finish of a filling operation and always have the same amount of hydrogen inside a tank.

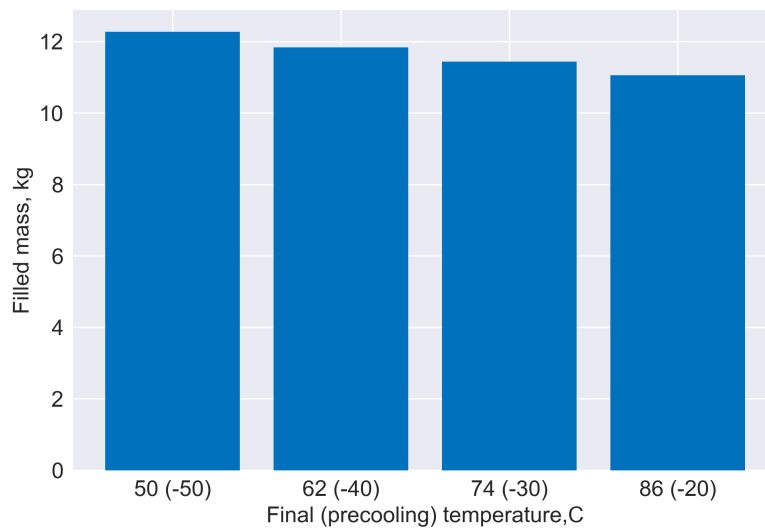


Figure 35: Filled mass results with varying pre-cooling temperature

When the time of operations is long enough, heat exchange and, subsequently, heat exchange with the ambience can play an important role. Figure 36 presents the result of the vessel filling with pre-cooling to $-10\text{ }^{\circ}\text{C}$ at the rate of $1\text{ MPa}/\text{min}$ at different ambient temperatures. The filling time obtained from the simulation is 1680 s or 29 min . Ambient temperatures below $10\text{ }^{\circ}\text{C}$ make it possible for filling operations at such rates with relatively mild pre-cooling. This shows the flexibility of hydrogen filling operations, and that actual filling operations can be set up differently depending on the exact constraints.

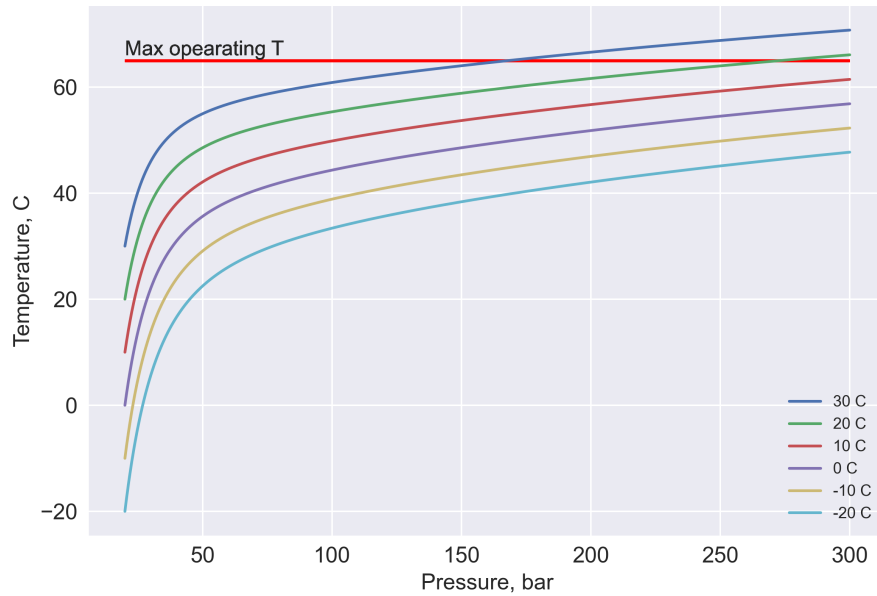


Figure 36: Temperature results for filling at 1 MPa/min and pre-cooling at $-10\text{ }^{\circ}\text{C}$ with varying ambient temperature

The lower temperature limit also restricts the operation of high-pressure vessels. Temperature results during vessel emptying at different rates are demonstrated in Figure 37. Table 11 summarizes simulation data. The lower temperature boundary for all storage vessels in the model is $-40\text{ }^{\circ}\text{C}$, and the results indicate approximate emptying rates for pressure decrease from 300 bar to 80 bar at $20\text{ }^{\circ}\text{C}$ ambient temperature.

The lower pressure limit of Type IV hydrogen pressure vessels is 20 bar at $15\text{ }^{\circ}\text{C}$ (data from Table 5). If emptied to the 80 bar and $-22\text{ }^{\circ}\text{C}$ (the first state outlined in Table 11), in a 45 m^3 300 bar trailer as much as 255 kg of hydrogen still can be unloaded extra until lower operational density limit is reached (it is the same approach as for the highest density calculated from the reference conditions). So a trade-off emerges between hydrogen unloading time and delivery efficiency in the scenario when a trailer should be returned after delivering hydrogen. This can be an argument in favour of detachable containers.

In the proposed hydrogen distribution network, emptying a trailer down to 20 bar requires a multi-stage compressor or several compressors at the end-user refilling site since the lowest storage pressure is 350 bar. Pressure ratio in the end would be very high in the end for one stage compression. Finding an optimum solution would require precise modelling and economic evaluation, which is out of the scope of this work, and there can be many options.

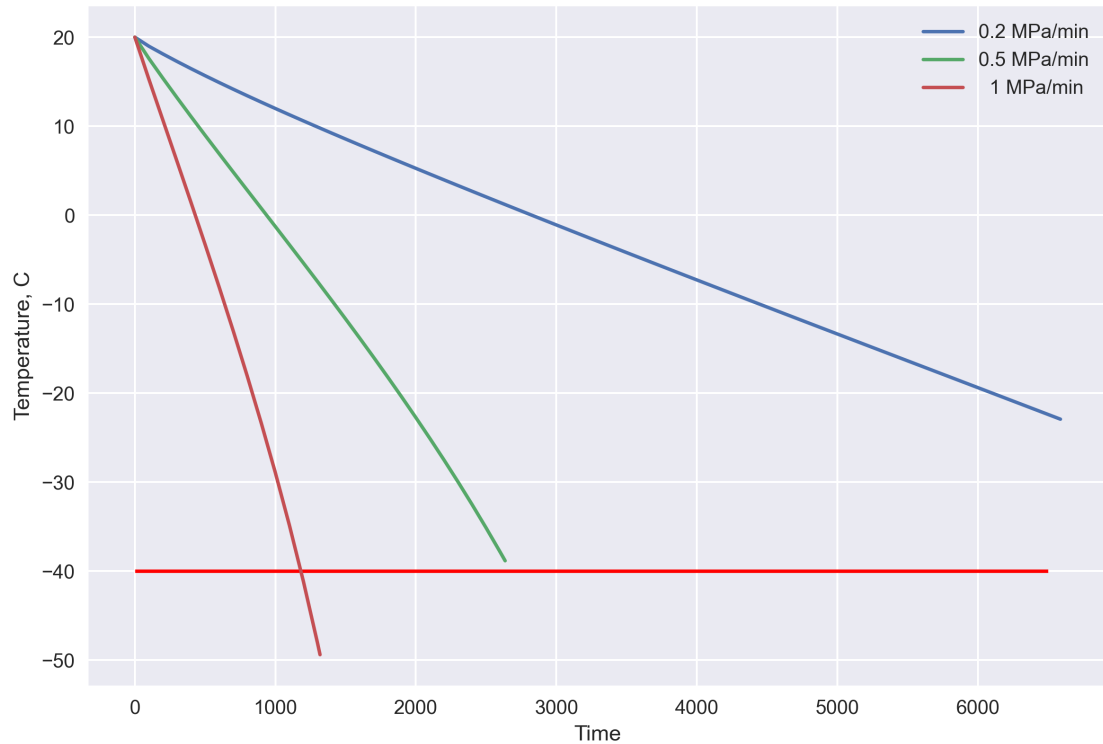


Figure 37: Temperature results with varying rate of vessel emptying

Table 11: *Cylinder emptying simulation parameters and results*

Initial p, bar	End p, bar	Time, s	Time, min	End T, °C
300	80	6588	109	-22
300	80	2635	43	-38
300	80	1318	21	-49

Separately, these results only help establish a general understanding of the thermodynamic behaviour of hydrogen storage vessels. Further on, the development of design solutions may include different combinations of the parameters mentioned earlier, depending on the particular needs and constraints. For example, complying with lower operating temperature may be achieved by lowering operational maximum and minimum pressure ratio. Different storage types may have different heat exchanges and thus be modeled with the adiabatic assumption for different rates. The pre-cooling temperature may vary depending on the filling rate and outside temperature. Furthermore, when compression is done to a specific vessel density, the final temperature may also influence compression power since higher pressures should be achieved for the same density at higher temperatures.

5.2 Chain simulation results

The first simulation in the sequence is trailer refilling at the production site. Figure 38 presents pressure results for three consecutive filling operations of 45.15 m^3 trailers with assumed starting pressure of 80 bar. This number depends on the end-user refilling site design and assumptions and will be discussed further.

Different filling phases from the MP and HP storage are indicated in the figure. The HP and MP storage volumes are 200 and 500 m^3 , respectively. These values were obtained by simulating

with different numbers to ensure the complete filling of 3 trailers. An increase in the HP volume decreases MP volume and vice versa. In the limit, all hydrogen can be stored at high pressure, and no medium pressure will be needed, thus, reducing the overall volume to a minimum. This will become a buffer storage. A small parametric study on this will be presented further.

The trailer is filled at the constant pressure ramp rate of 3 MPa/min, and the process of one complete filling takes 527 s or approximately 9 min. The refilled hydrogen mass for each trailer is 658 kg. It is noticeably less than the specified hydrogen capacity for the trailer of 958 kg because of the assumed starting pressure. It shows that the specified hydrogen capacity of the trailer can be significantly compromised by incomplete emptying.

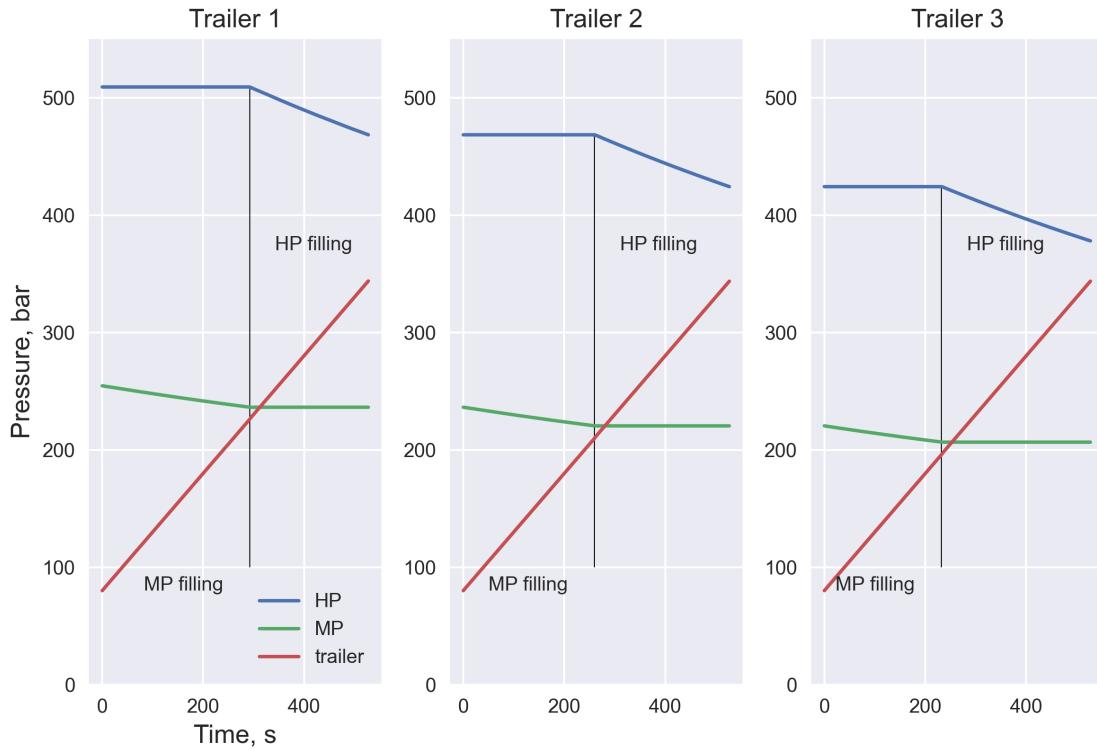


Figure 38: Pressure results of trailer filling simulation

Assumed ambient temperature here and on-wards is 20 °C, and pre-cooling is done at -40 °C. Temperature results of the simulation are given in Figure 39. No heat exchange during and between operations is assumed, and the temperature inside the storage drops as pressure goes down. Each new simulation starts with the same temperature and pressure in the HP and MP vessels. The results indicate that assumed pre-cooling and pressure drop in the storage vessels are adequate to stay well within operational temperature boundaries at assumed conditions even without extra heat inflow from the ambience.

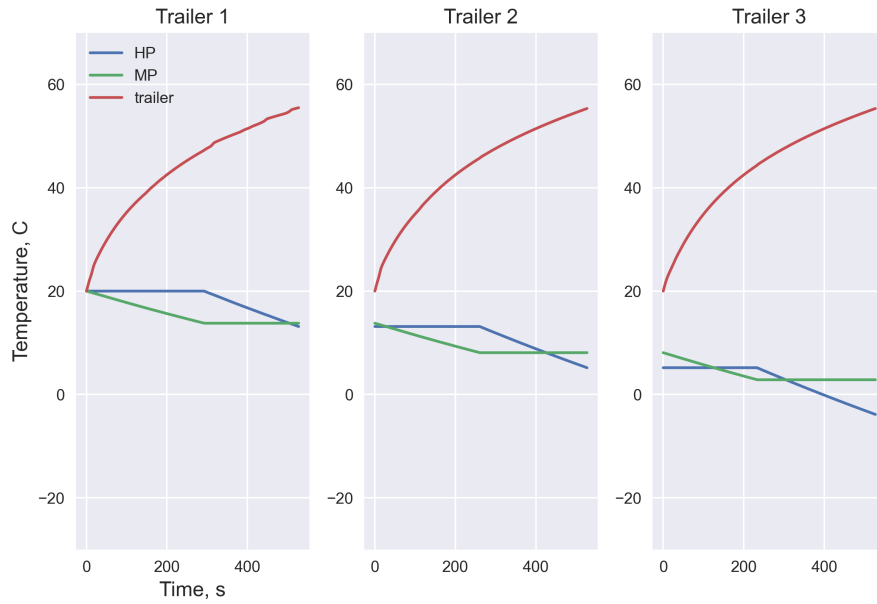


Figure 39: Temperature results of the trailer filling simulation

The only power consumption during this simulation comes from the operation of the refrigerator. Figure 40 indicates specific work for cooling 1 kg of filled hydrogen for each operation. COP for the given conditions is equal to 1.94. The figure demonstrates that power consumption slightly decreases with each filling operation. This corresponds with the pressure decrease in the storage, leading to lower temperatures inside vessels and less heating generated by throttling. The average cooling work is 0.11 kWh/kgH₂.

With the adiabatic filling assumption, the outside temperature will not influence pre-cooling temperatures. However, the refrigerator efficiency will differ and may lead to different power consumption values depending on the region and time of the year.

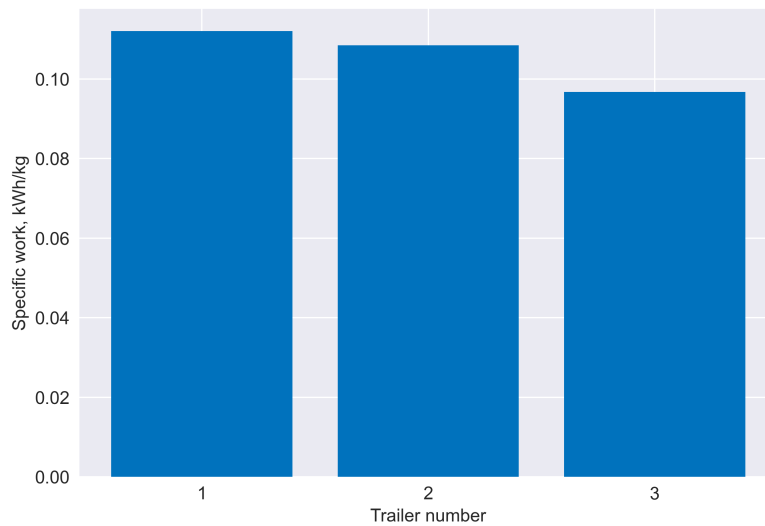


Figure 40: Specific cooling work results of the trailer filling simulation

Table 12 below summarizes storage volumes and end pressure and temperature results. The end temperature and pressure values are obtained from the simulation and used to calculate initial

states at the HP and MP storage for the next simulation of the cascade charging. The initial values are obtained from the NIST REFPROP database, assuming isochoric recovery of hydrogen to equilibrium with ambience.

Table 12: *End and initialization values for the cascade storage simulation*

Section	Volume, m^3	End p, bar	End T, $^{\circ}C$	Initial p, bar	Initial T, $^{\circ}C$
HP storage	200.0	378.0	-4.0	413.0	20
MP storage	500.0	207.0	3.0	220.0	20

Figure 41 presents simulation results of the cascade charging for pressure. The first simulation stage is filling the MP storage up to 250 bar for further compression into HP storage. Under current assumptions, the plot displays that pressure ratios between the intermediate - MP storage and the MP - HP storage are not distributed evenly. However, the results provide a realistic representation of a possible operation and can simplify further optimization and finding optimal design solutions.

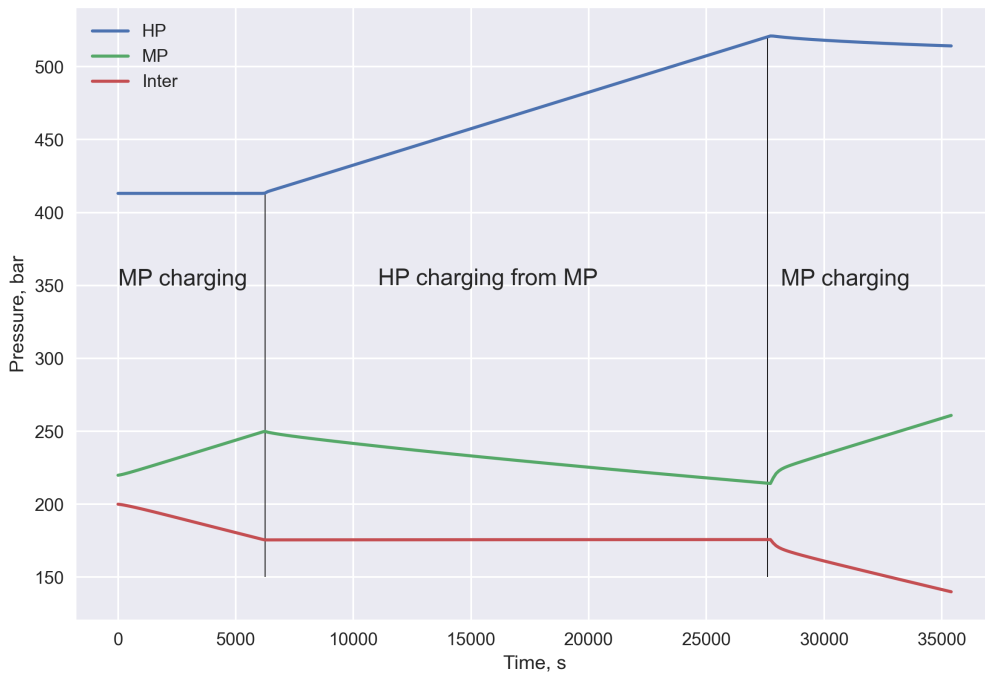


Figure 41: Pressure results of the cascade charging at the production site simulation

Figure 42 depicts temperature results for the simulation. The filling rate is 0.03 MPa/s. For the time range of 35499 s or almost 10 hours, thermal behaviour inside the storage tanks with temperature fluctuations not exceeding 10 degrees might be assumed isothermal. Since the cascade storage is kept under target density, over-compression, in this case, is very low and determined mainly by ambient temperature. This is beneficial in terms of reducing compression power consumption.

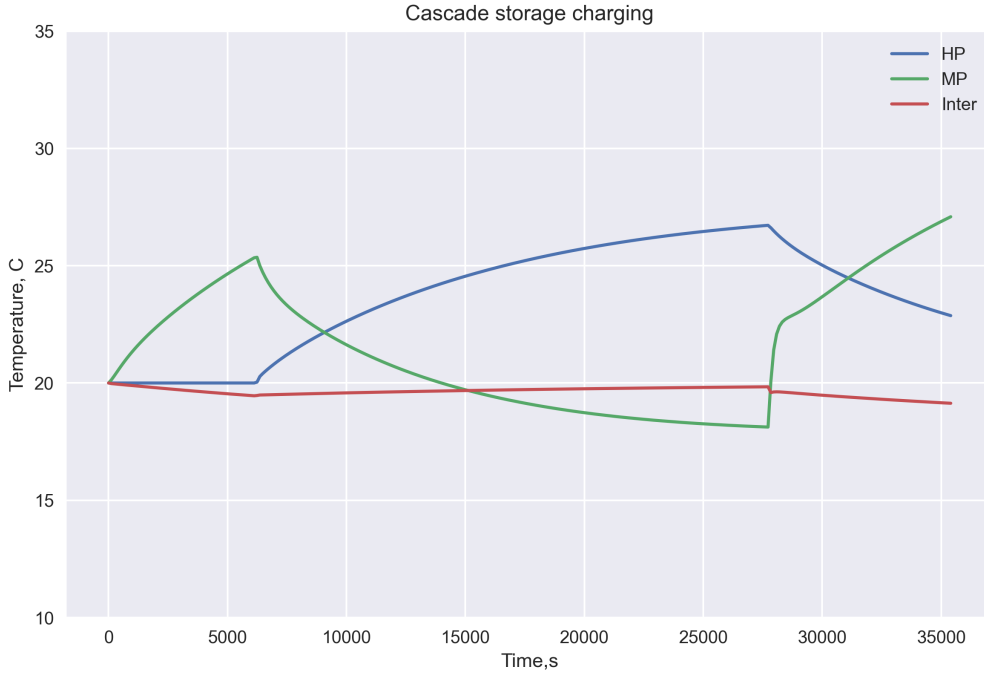


Figure 42: Temperature results of the cascade charging at the production site simulation

Table 13 summarizes main parameters of the compressor during the simulation. Specific power consumption for compression of 1 kg hydrogen is 0.71 kWh/kgH₂. Time average isentropic efficiency of 41 % indicates that with assumed performance characteristics, the compressor is far from the optimal operation range of 55%, and better energy efficiency can be achieved.

Table 13: *The summary of the cascade charging at the production site simulation results for compressor*

Parameter	Value	Unit
Specific compression work	0.71	kWh/kgH ₂
Average pressure ratio	1.80	
Minimum pressure ratio	1.10	
Maximum pressure ratio	2.43	
Average power	143.00	kW
Average massflow	0.082	kg/s
Average isentropic efficiency	41	%

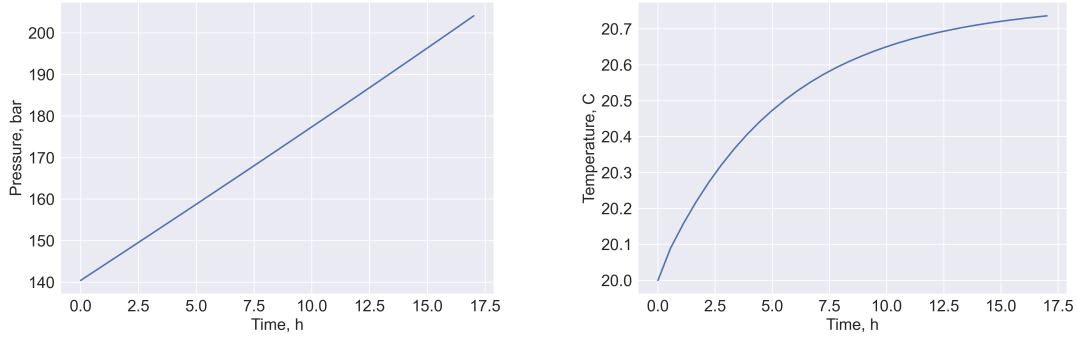
For the further simulation of the intermediate storage filling, end values of pressure and temperature from the cascade charging simulation are used. Again, the temperature is assumed to recover to the ambient temperature before starting the simulation. This is presented in Table 14.

Table 14: *End and initialization parameters for the intermediate storage*

Section	Volume	End p, bar	End T, °C	Initial p, bar	Initial T, °C
Intermediate storage	501.0	139.0	19.0	140.0	20

Figures 43a and 43b demonstrates simulation results for pressure and temperature inside the intermediate storage. Due to better heat conduction of steel storage cylinders and long filling time,

almost isothermal filling is achieved with a temperature difference below 1 degree. The total filling time is 17 hours.



(a) Pressure results for the intermediate storage filling simulation (b) Temperature results for the intermediate storage filling simulation

Figure 43: Pressure and temperature results for the intermediate storage filling simulation

Specific power demand for hydrogen compression, as shown in Table 15, is 4.6 kWh/kgH₂. The average pressure ratio from the simulation is 170.07 and signals that a multistage compression is necessary at this part of the distribution chain.

Table 15: *The summary of the intermediate storage simulation results for compressor*

Parameter	Value	Unit
Specific compression work	4.60	kWh/kgH ₂
Average pressure ratio	170.07	
Minimum pressure ratio	138.58	
Maximum pressure ratio	201.50	
Average power	647.00	kW
Average massflow	0.035	kg/s
Stage average isentropic efficiency	41	%
Temperature behind intercoolers	70	°C

The end-user refilling site simulation gives the total number of 18 heavy vehicle refuellings. Figure 44 presents pressure results for the first two filling operations when the cascade storage is fully charged. The process is the same as for the cascade filling at the production site, Figure 38. The main difference is in the volumetric relation of the cascade storage and the onboard hydrogen tank. Thus, one refilling operation produces a very low-pressure decrease in the cascade.

Final filling operations are more the point of interest since more complex dynamics can be examined. Figure 45 captures pressure behaviour inside the vessels. The refilling time of the onboard tank is 13 minutes. As soon as pressure inside the HP storage drops below the specified value, a compressor restores pressure from the MP storage. This can be seen after the filling of vehicles number 15 and 17. Once the pressure in the MP storage reaches 80 bar, refilling is done only by throttling from high pressure, as seen for vehicle 18. The refilled hydrogen mass for each vehicle is 35.4 kg. It is lower than the tank capacity since it is assumed to contain hydrogen at 20 bar before refilling.

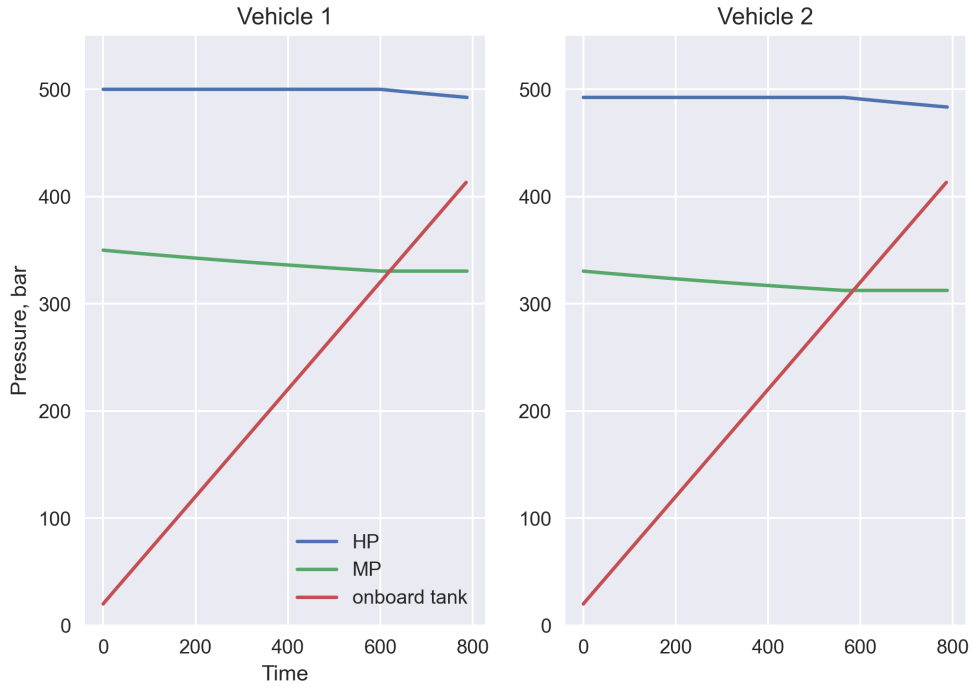


Figure 44: Pressure results of the end-user refilling simulation for the first two vehicles

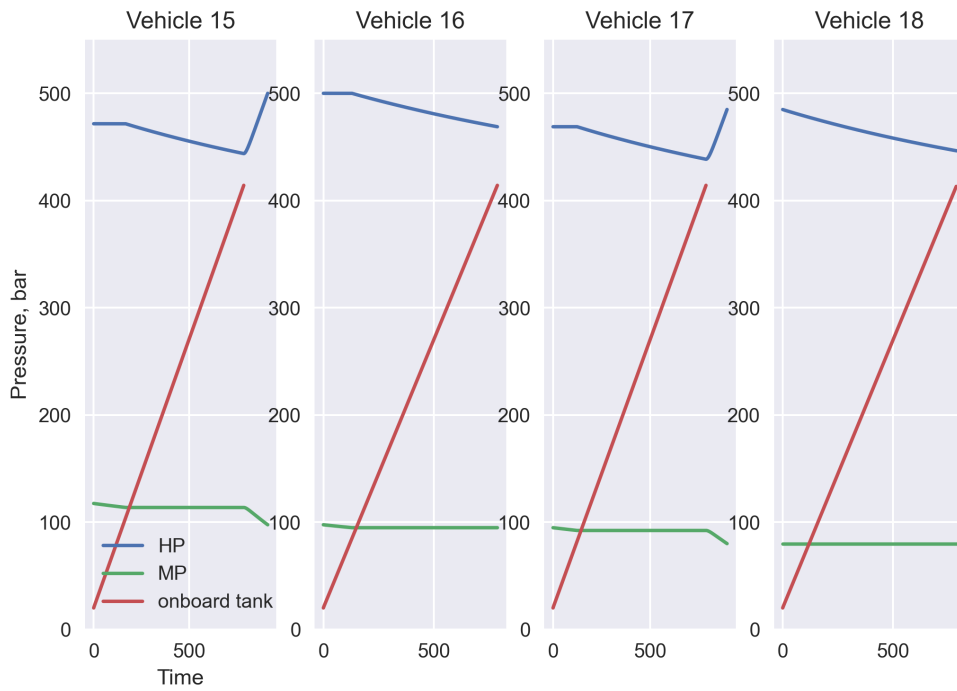


Figure 45: Pressure results of the end-user refilling simulation for the final filling operations

However, temperature results in Figure 46 indicate that adiabatic modelling of the end-user refilling violates lower operational temperature limits of the MP storage, reaching as low as $-84\text{ }^{\circ}\text{C}$. If

consecutive refilling operations are concerned, the resulting combined time of around 3 hours might be enough to stay within temperature limits at 20 °C ambience. Alternatives to overcome this may include the usage of larger MP volume to allow distribution of the same mass with less pressure drop or a more extended operation period. These solutions are very case-specific, and we assume the used model still achieves its goals of estimating the energy usage of such configuration.

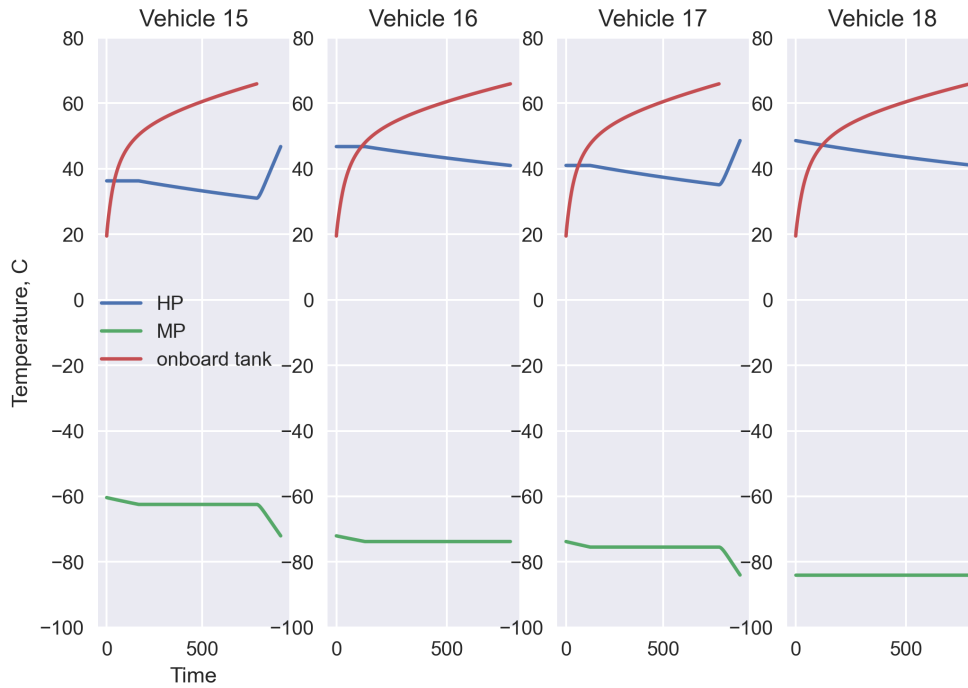


Figure 46: Temperature results of the end-user refilling simulation for the final filling operations

Pressure ratio results for the compressor are presented in Figure 47 with refilling numbers indicated when the compressor was turned on. Together with the resulting efficiency of 48 % provided in Table 16 it indicates that operational conditions are very close to the optimal of the assumed compressor and provide the basis for a better compressor choice.

Specific work for compression and refrigeration, as indicated in Figure 48 is given for each refilling operation. Compression work increases with the MP vessel being more and more depleted. However, according to the operating algorithm, the recompressed amount of hydrogen at the end of operations is not the same. Deviations such as operation number 13 occur. The decrease in refrigeration work up to refilling number 10 is due to reduced temperature and pressure inside the MP vessel. As more and more hydrogen is refilled from the HP vessel, the corresponding increase in the refrigeration work can be seen in the following operations.

The above mentioned might be the point of interest for detailed simulations and modelling of hydrogen refilling stations. For our study, we are interested in averaged values of specific work. The corresponding time-averaged value of specific work is 0.32 kWh/kgH₂ and refrigeration work is 0.13 kWh/kgH₂. This is presented in Table 16.

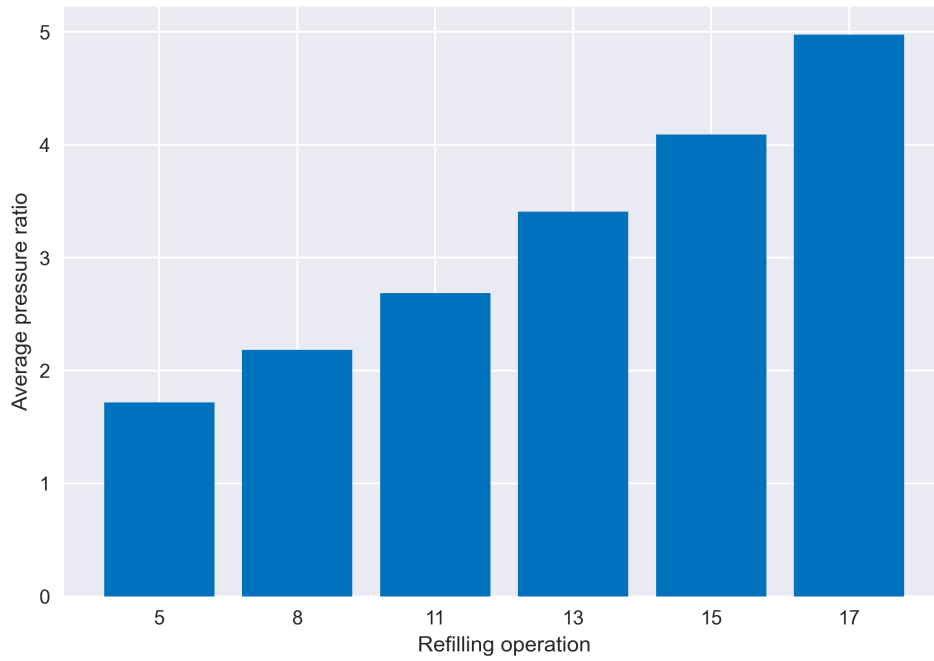


Figure 47: Pressure ratio of the compressor of the end-user refilling simulation

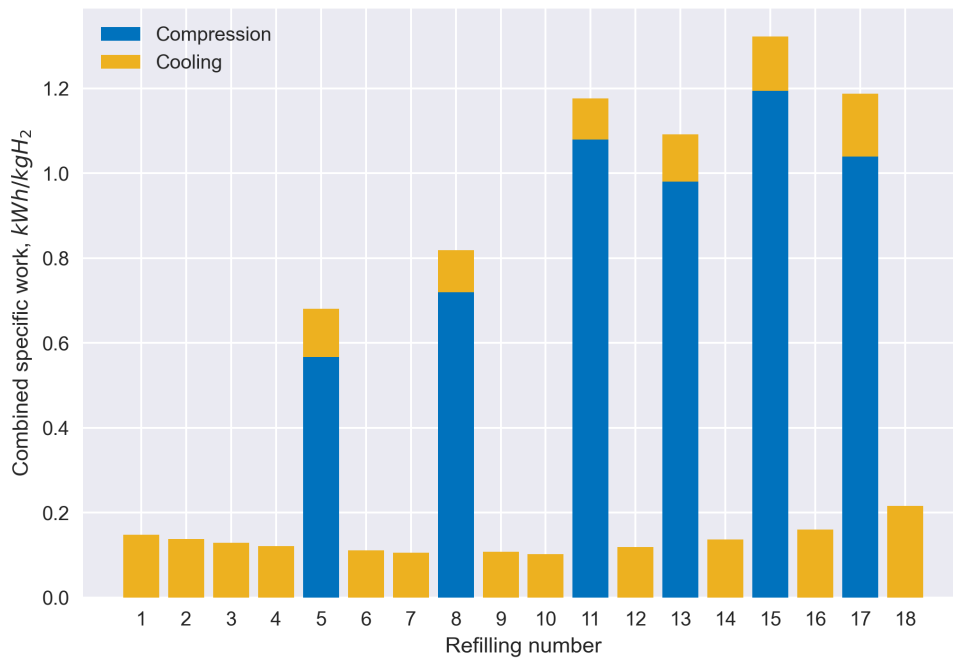


Figure 48: Combined specific energy consumption during each refilling operation

Table 16: *The summary of the end-user filling simulation results*

Parameter	Value	Unit
Specific compression work	0.32	kWh/kgH ₂
Specific refrigeration work	0.13	kWh/kgH ₂
Average compressor pressure ratio	2.96	
Minimum compressor pressure ratio	1.43	
Maximum compressor pressure ratio	6.06	
Average isentropic efficiency	48	%

Before starting the final simulation of the cascade charging at the end-user refilling site, hydrogen at the cascade storage is recalculated for the ambient conditions using the NIST REFPROP database again. The results are presented in Table 17.

Table 17: *End and initialization parameters for the cascade charging at the end-user site*

Section	Volume	End p, bar	End T, °C	Initial p, bar	Initial T, °C
HP storage	30	445.37	40.53	415.17	20
MP storage	40	80	-84	126.07	20

First, the HP storage is filled up to the target density at the end pressure and temperature of 534 bar and 34 °C as can be seen from Figure 49. Since pressure in the MP storage is less than in the hydrogen trailer, throttling is done to equalize pressures before starting the compression. Both compression and throttling are done at the rate of 0.3 MPa/min, and the simulation time is 7257 s or 2 hours. Specific compression work is 0.55 kWh/kgH₂.

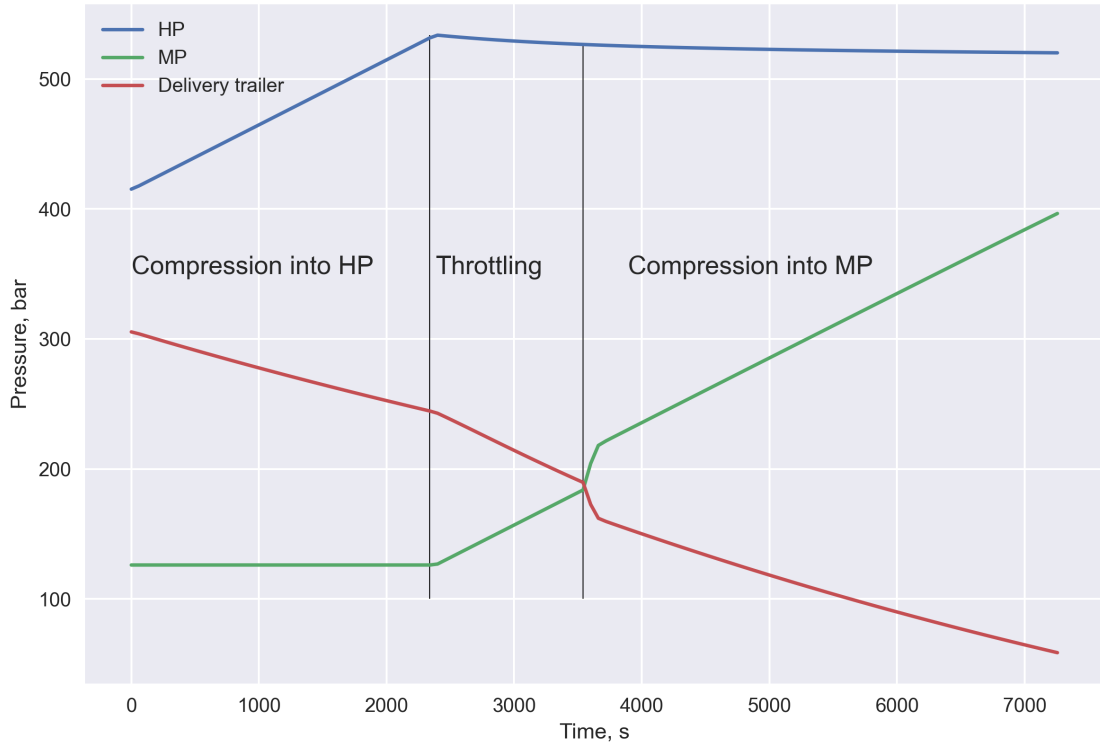


Figure 49: Pressure results of the cascade charging at the end-user site

At the assumed charging rate and ambient temperature, the modelled heat exchange indicates that temperatures stay within operational limits throughout the process. In Figure 50 the temperature dynamics can be seen. End temperature and pressure values are outlined in Table 18. As has been previously shown in section 5.1, ambient temperature may have significant effect on filling or emptying of pressure vessels. Thus, the process might be not suitable for cold or hot environment. An abrupt change at the beginning of compression is due to the model's behaviour at state events and the low amount of plotting points. It, however, should not affect the results.

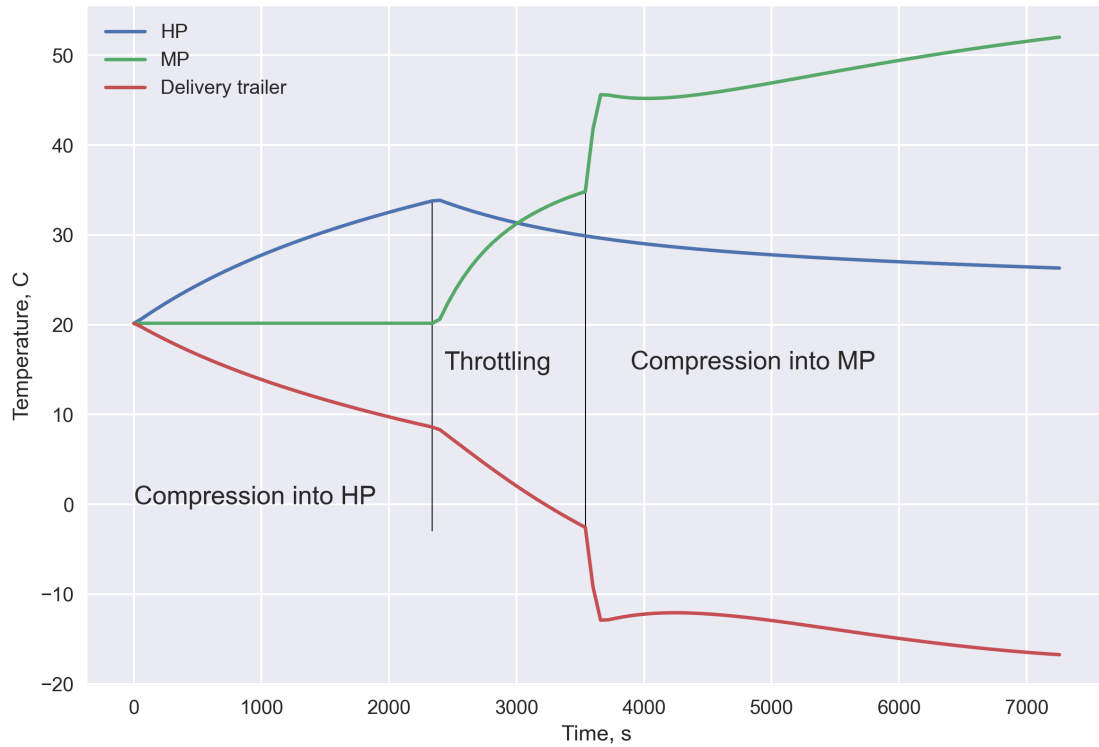


Figure 50: Temperature results of the cascade charging at the end-user site

Table 18: *Pressure and temperature results of the cascade charging at the end-user site*

Section	End pressure, bar	End temperature, °C
HP storage	520.13	26.15
MP storage	396.51	51.85
Trailer	58.63	-16.89

It should be pointed out that when hydrogen inside the trailer returns to the ambient temperature state, using the data from Table 18, the new pressure inside can be found to be 67.22 bar. This value is lower than the 80 bar assumed at the beginning of the chain simulation. This results in a larger mass of unloaded hydrogen than it was initially filled at the production site, 708.13 vs 658.10 kg respectively. A new simulation sequence can be run with the updated initial trailer pressure in the trailer refilling simulation so that quasi-steady state of the chain operation is achieved in a closed loop. Otherwise, the storage volumes can be adjusted in the end-user fuelling model. This, once more, highlights the complexity of the compressed hydrogen distribution chain modelling and design and the relevance of the dynamic modelling approach.

The proposed design uses the same compressor during vehicle refilling operations and the current process. Presented data in Table 19 indicates very similar operation conditions to the previous

simulation of the end-user refilling summarized in Table 16. Suction pressure in this case ranges from 58.63 bar to values slightly above 300 bar. This may be well within capabilities of modern compressors. Even so, a two-compressor set-up might be more relevant approximation in this case (not considering reliability aspects).

Table 19: *The summary of the cascade charging compressor results at the end-user site*

Parameter	Value	Unit
Specific compression work	0.55	kWh/kgH ₂
Average pressure ratio	2.59	
Minimum pressure ratio	1.18	
Maximum pressure ratio	6.77	
Average isentropic efficiency	45	%

5.3 Chain simulation summary

Summarizing the simulation results, values for specific work for hydrogen distribution can be obtained. This includes hydrogen compression after its production at atmospheric conditions, loading into road trailers for transportation at 300 bar, end-user site storage system charging, and final dispensing operations into onboard tanks at 350 bar. In addition, hydrogen refrigeration for quick filling operations is included which in total gives specific energy requirement of 6.41 kWh/kgH₂. Hydrogen lower heating value (LHV) is 33.3 kWh/kg. Thus, the delivery of hydrogen via compressed distribution chain makes 18.53 % of its total energetic value. The results are presented in Figure 51. For comparison, reported hydrogen liquefaction energy requirements are typically from 10 to 13 kWh/kgH₂ [25]. It is difficult to draw particular conclusions without available energy demand for transportation of compressed hydrogen. As long as the combined energy requirement for compressed hydrogen distribution is lower than liquefaction energetic need, compressed transport might be considered. However, many other factors might also influence the final design choice.

Table 20 summarises values of the energy demand for hydrogen compression and cooling in the distribution chain. The cooling need at the production and end-user sites, 0.11 and 0.13 kWh/kgH₂, compares well against the suggested value of 0.15 kWh/kgH₂ for cooling to -40 °C in the DOE report [25]. Worth noting that total power consumption for hydrogen pre-cooling in the chain is relatively low and makes only 3.8 %.

Table 20: *Specific work results for hydrogen distribution throughout the chain*

Section	Compression, kWh/kgH ₂	Cooling, kWh/kgH ₂	Cooling/Comp., %	Total, kWh/kgH ₂
Comp. after electrolyzer	4.60	0.00	0	4.60
Production site	0.71	0.11	14.91	0.82
End user site	0.87	0.13	14.81	1.00
Total	6.17	0.23	3.80	6.41

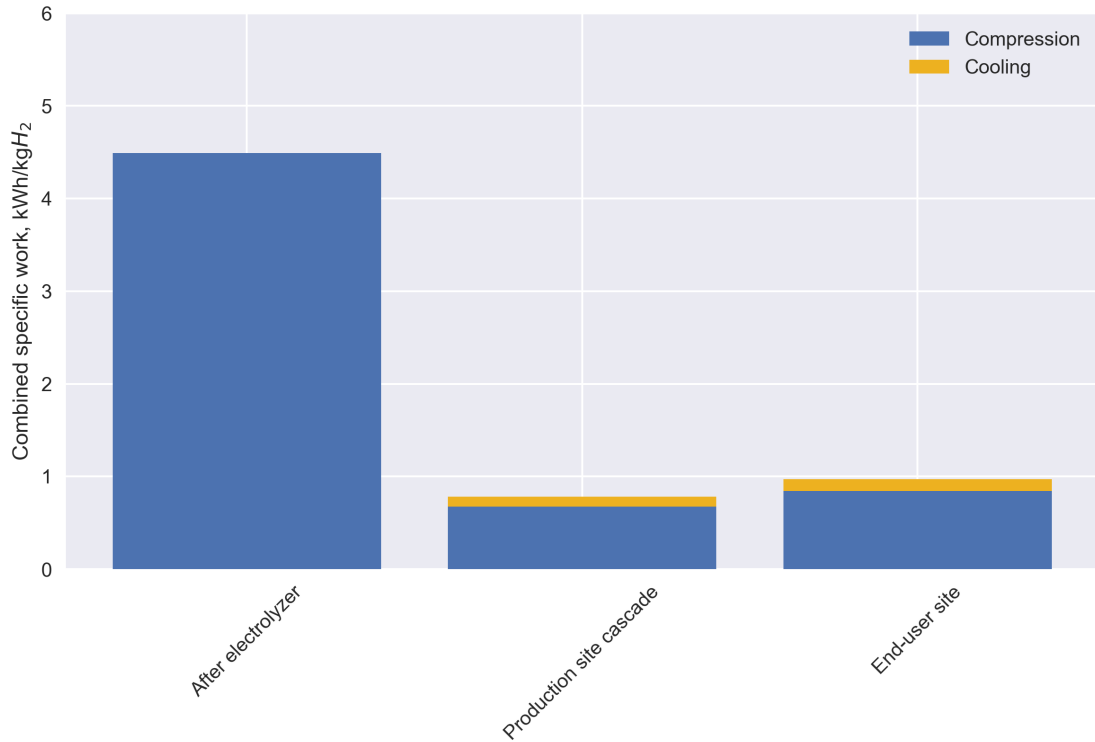


Figure 51: Combined specific work for hydrogen distribution throughout the chain

Hydrogen compression after the electrolyzer is separated from the other production site operations highlights that the most energy demanding part is compressing hydrogen from ambient conditions. With our modelling assumptions and the chain design, it gives 4.6 kWh/kgH₂. For comparison, the ideal isothermal compression of hydrogen from 1 to 300 barg at 20 °C is 1.93 kWh/kgH₂ (from NIST REFPROP database). Another reference is the DOE report on energy requirements for hydrogen compression. It provide numbers ranging from 1.7 to 6.4 kWh/kgH₂ of energy needed for compression after production to refill road vehicles [25]. However, there is no exact data on production and delivery pressure, compressor types or efficiencies. The specific compression work after electrolyzer is more than four times higher than the combined specific work for other operations at the production site.

The difference in compression work for the production site operations and the end-user site is not significantly different. The production site includes combined specific work for trailer filling operations and cascade storage charging, while the end-user site - cascade charging and end-user refilling operations. Even considering the higher pressure level of the MP and HP storage at the end-user site and additional compression to the HP storage, the difference in compression work between the end-user site and the production site is not significant, 0.87 vs 0.71 kWh/kgH₂.

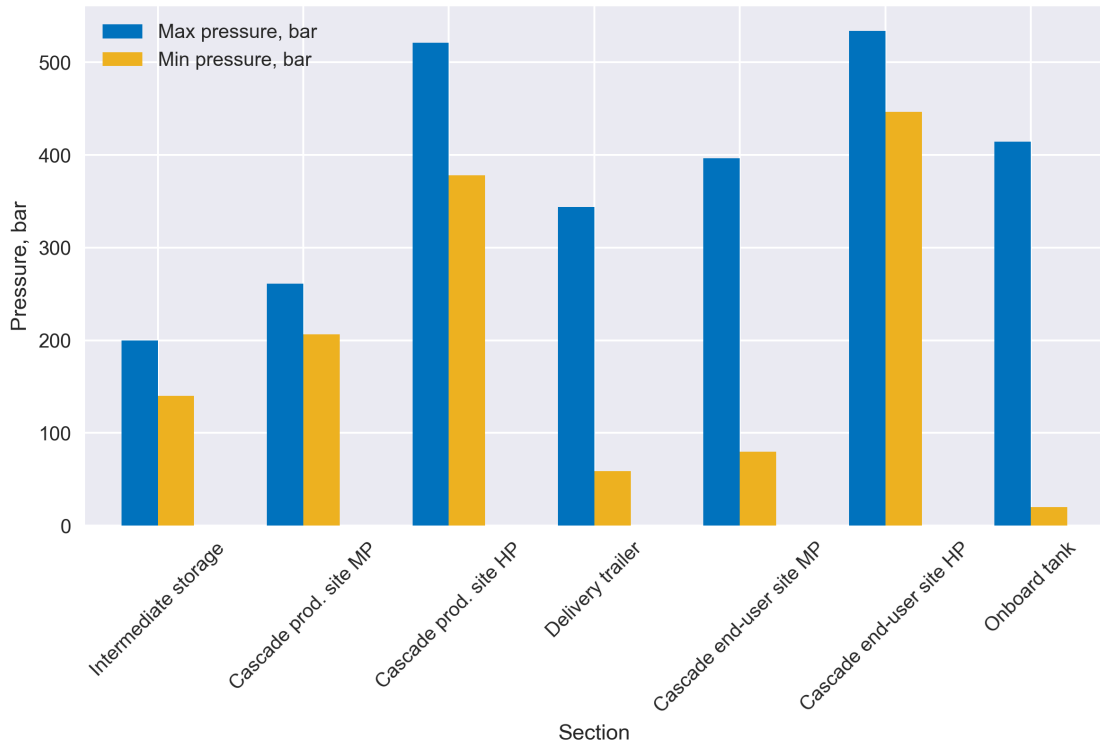


Figure 52: Maximum and minimum pressure levels at different parts of the chain

Figure 52 compares maximum and minimum pressure levels at different hydrogen pressure vessels throughout the chain. This data can be used, for example, to choose a compressor for different parts of the chain. Together with the specific work data and design parameters, it is possible to conclude that operations that involve small pressure difference during filling from higher pressure vessel into another are better in terms of energetic performance (in other words, cascade filling is more efficient as has been discussed previously). However, this can be achieved only by using large storage volumes, which is not always possible. The attempt was made to show this in the operation of the end-user refueling station, where additional compression from the MP to HP storage is used to maximize the amount of distributed hydrogen. As seen from Figure 52, the pressure difference between the empty on-board tank and HP storage is significant (this especially relevant when fueling is done primarily from the HP storage). This resulted in slightly higher specific power than for the production site.

Table 21: *Parameters specified for HDRSAM calculation*

Parameter	Specification
Delivery method	Tube trailer
Refueling method	Cascade dispensing
Fleet number of HDV	18
Onboard storage capacity, kg	38
HDV service pressure, bar	350
Hydrogen trailer pressure, bar	300
Trailer end pressure, bar	60
Isentropic efficiency, %	47

Energy demand at the end-user refueling site can be compared against HDRSAM calculation.

There are many parameters to set, but we are primarily interested in obtaining energetic results. Thus, economic or sizing numbers can be left by default. Table 21 summarizes input parameters. Isentropic efficiency used is an average of simulated compressor efficiency from Table 16 and 18. A general look at the Excel based version of the software with scenario assumptions input is shown in Figure 53.

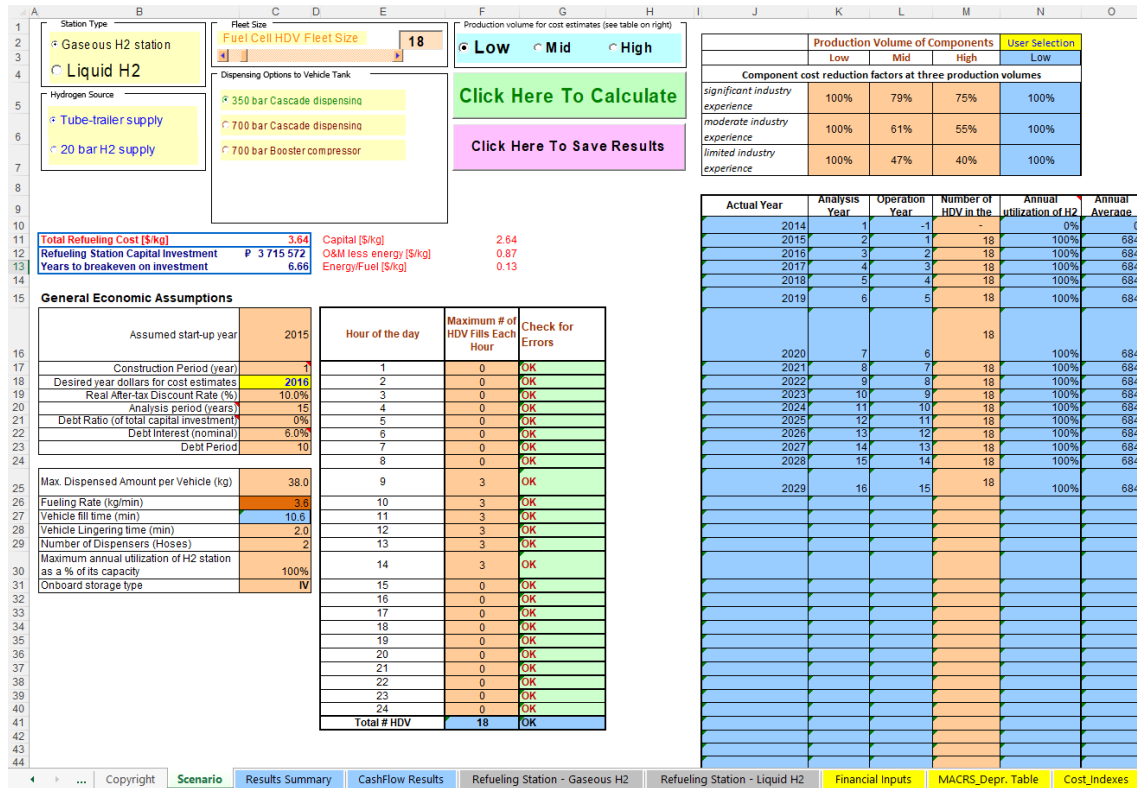


Figure 53: Screenshot from Excel-based version of HDRSAM with scenario parameters

Electrical energy consumption obtained with HDRSAM is 251486 kWh annually or 1.02 kWh/kgH₂ (assuming 365 days in a year). Calculating power consumption over 365 days with the specific power consumption at the end-user site of 1.00 kWh/kgH₂ from our model, we get 249660 kWh. Even though, the details of HDRSAM calculation are not studied, it is possible to say that the built dynamic model gives reasonable values of energy demand. Still, it also provides a good representation of the station dynamic operation and allows wider range of further investigations.

5.4 Parametric studies

As mentioned in the section 4.2, FMI based approach allows for automation of the simulations in Python. In this section, two parametric studies are presented reusing previously built models. A simple extension in Python in the form of "for loop" simulates the trailer filling and cascade charging at the production site models with different cascade storage volumes and ambient temperature values.

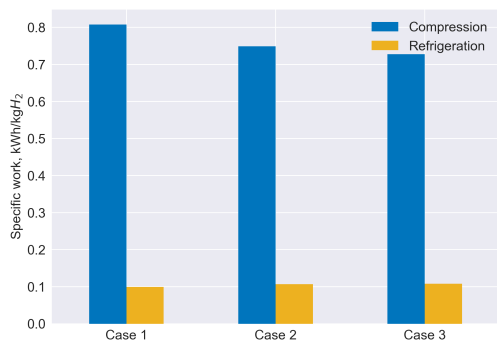
In the first study, we assume three cases with different volumes of high and medium pressure storage tanks as presented in Table 22. Pressure levels stay the same as for the main model, 250 and 500 bar, as well as all other initialization parameters described in section 5.2. The exact amount of hydrogen should be refilled in all the cases, and volume numbers are chosen so that the end pressure in the HP storage is approximately the same. The later assumption maximizes the HP volume usage.

Table 22: Cascade volume data for parametric study

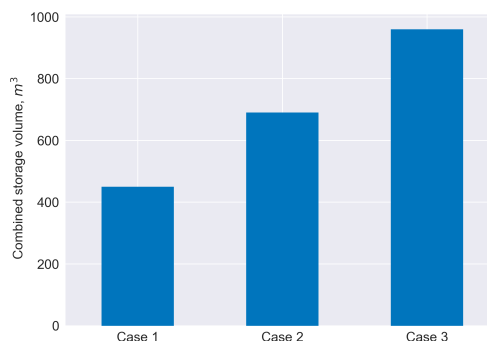
	MP volume, m^3	HP volume, m^3
case 1	200	250
case 2	500	190
case 3	800	160

Figure 54a captures the difference in specific compression and refrigeration work for the three cases. As expected, savings in the storage volume lead to the higher energy demand of the system. The graphics show the correlation between volume change and increased compression work. Almost double the total system volume reduction creates only an 11% rise in the compression work.

A slight change in refrigeration work can also be noticed, but the trend is the opposite and not substantial in our case. A cause is that pressure drop in the HP vessel stays the same for every case, yet the MP storage pressure change is more significant with lower volume. As long as we assume the adiabatic model, resulting temperature decrease inside the vessel helps to reduce the amount of precooling needed while filling hydrogen. Detailed modelling and exact scenarios may show that such behaviour is also influential.



(a) Specific power consumption for different total storage volume cases



(b) Total storage volume of the three cases

Figure 54: Specific work depending on the total storage volume

For the second study, the model is simulated assuming different ambient temperatures: 0, 10, and 20 °C. The cascade storage volume and other model parameters are the same as the main simulation. Figure 55 presents results for the simulation sequence. It highlights the sensitivity of the compressed hydrogen distribution chain to ambient temperatures. The main source of increased compression work is the amount of overpressure needed at higher ambient temperature to achieve the same hydrogen density inside the storage.

The difference in the end pressures after the cascade charging is presented in Table 23, and it is as high as 52 bar for 0 and 30 °C cases. The jump in specific compression work between the two simulations makes 23 %. The most noticeable is the rise in the ratio of refrigeration to compression work: from 8 to 18 %.

Table 23: Specific work, end pressure, and COP data for different ambient temperature simulations

T, °C	Cooling work, kWh/kgH ₂	Comp. work, kWh/kg ₂	Comp./Cooling, %	End HP, bar	End MP, bar	COP
0	0.05	0.65	8	524.77	256.48	2.91
10	0.08	0.7	11	541.2	268.09	2.33
20	0.11	0.75	15	558.91	280.56	1.94
30	0.14	0.8	18	576.61	293.45	1.67

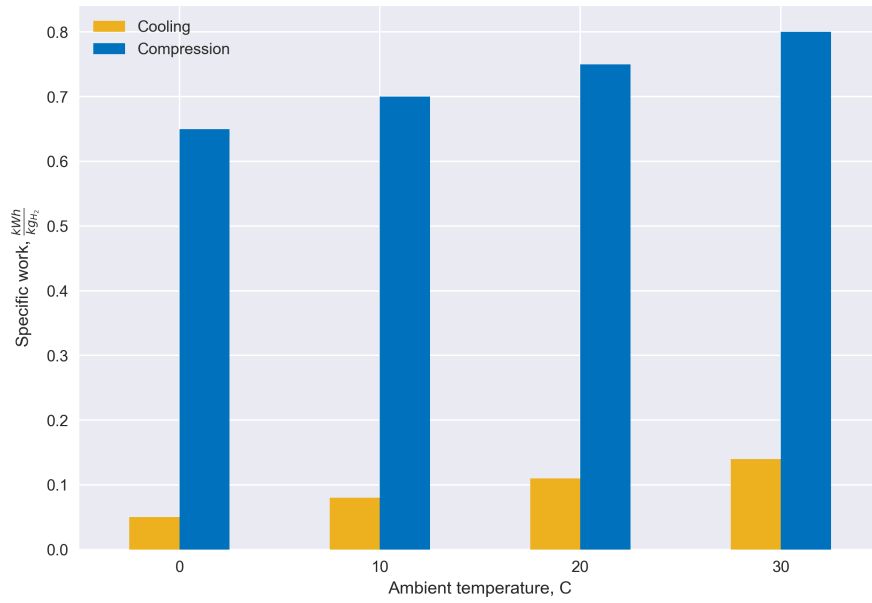


Figure 55: Specific compression and cooling work at different ambient temperature

The refrigeration work is also increased due to higher temperature lift needed and, thus, lower COP value of the refrigeration facility. This constitutes in more than twofold rise in specific refrigeration work from 0.48 to 0.136 kWh/kgH₂. The difference in the COP values is shown in Table 23.

6 Conclusion and further work

The paper investigated power demand in the mid-scale compressed hydrogen distribution chain for heavy-duty vehicles or light maritime passenger transport. A small overview of the current technology, compressors and high-pressure storage was given as part of the work. Obtaining detailed specifications for the equipment is difficult because of the commercial confidentiality of the new technology. Thus, the model is based on openly available information, existing studies, and adequate assumptions. The main regulatory document was SAE J2601.

The initial objective was to build a dynamic model in Dymola software. The process showed that modelling the chain at the desired scale could be substantially simplified and improved with the adoption of FMI-based approach and Python programming language. Dymola and TLK-Thermo libraries were used to create "building blocks" of the distribution chain. Then they were combined by connecting data streams in Python for the complete simulation. In perspective, using FMI approach allows combining different tools for addressing specific needs of the hydrogen distribution network.

First, before modelling the distribution chain, thermal modelling of high-pressure vessels was done. The thermal model was simplified because of insufficient data, yet it still provided some vital understanding of the thermal behaviour. All storage modelling in the chain was done assuming the use of several vessels of the same type without their mutual influence, therefore having a thermal performance as for a single vessel. Assuming that, the thermodynamic simulations were done assuming a single cylinder. Results in section 5.1 show that thermal influence is very low for quick filling operations, so in some cases, modelling can be simplified to adiabatic conditions. It was shown that filling rates above 3 MPa/min have influence no more than 10 °C at 20 °C ambient, and precooling to -40 °C could be needed for fast filling with the upper-temperature constraint of refilled vessel of 65°C (different parameters of compressed hydrogen storage were presented in Table 5).

For operations with slow filling rates, ambient temperature has a significant influence. For example, at 1 MPa/min and ambience below 10 °C, precooling can be reduced to -10 °C for filling from 20 to 300 bar.

One more important observation from these is the constraints on tube trailer emptying operations. The provided data in manufacturers' brochures usually specify hydrogen capacity as the difference between upper and lower storage tank densities. Thermal simulations, however, show that emptying a 45.2 m³ trailer from 300 bar to 80 bar without exceeding the lower temperature limit of -40 °C would require at least 43 min, still leaving approximately 255 kg more hydrogen that could be potentially emptied. This opens up a discussion on optimal hydrogen delivery methods and end-user refueling site design. In the chain simulation all delivered hydrogen is stored inside cascade storage at the end-user site. The layout provided emptying down only to 58 bar and created inefficient utilization of the tube trailer. Ideally, the emptying time, in this case, should be much longer, or the trailer could be left on-site. Tentatively, storage heating technologies might be also considered.

The distribution chain was designed starting from the production site, assuming a hydrogen production rate of 3 tonnes/day. Cascade storage design with two pressure level was chosen as a primary solution for trailer filling and end-user refueling operations. Results for the assumed production site design show, first of all, its operational dynamics. This includes the pressure and temperature change of the storage system, operating conditions of the compressors, and the approximate storage volumes. All this gives a very representative picture for the further investigation and optimization of the current design or its alternatives.

With the modelling of the end-user refuelling site, we tried to take the advantage of the model re-use. A working model was built with some minor changes to the design from the production site,

namely, adding the possibility for additional compression into the HP storage. Nevertheless, its simulation results showed that due to increased pressure drop inside the MP storage temperature exceeded the lower operating limit. Some additional design changes or constraints can be added to the simulation. For example, a restricted number of back-to-back filling operations with resting time afterwards to warm up the storage.

Combined specific energy consumption for compression and cooling in the chain makes 6.41 kWh/kgH₂. Only 3.8 % of that is required for cooling. The main contribution is hydrogen compression from ambient conditions at the production site. It gives 4.6 kWh/kgH₂ for four-stage compression with partial intercooling. Though there is not enough data of energy demand throughout a distribution chain, models for hydrogen refuelling stations exist. HDRSAM by Argonne national laboratory allows to perform comprehensive evaluation of a hydrogen refueling station, including power consumption. Results compare as 1 kWh/kgH₂ for our model and 1.02 kWh/kgH₂ - HDRSAM for the same scenario.

Then two parametric studies on the cascade storage system at the production site were presented. The first one investigates different storage volumes of HP and MP blocks and how the larger amount of hydrogen at high pressure reduces storage volume and increases power consumption in the system. The results show an almost twofold decrease in total storage volume increases specific compression work by 11%.

The second study was done with changing ambient temperature from 0 to 30 °C. Compression and cooling work increases. However, while the increase for the compression work is 23% between two limiting cases, the specific work for cooling more than doubles. This is reflected in the value of relative cooling to compression work, where the rise is from 8 to 18 %.

In general, the simulation highlighted that the assumed compressor efficiency curve results in modest numbers for the presented design, slightly below 50%. It can be accepted for this model since actual numbers are not openly available. However, a case study with different compressor efficiencies can be performed. Results may show the dependence of the overall energy requirement in the chain and compressor efficiency and help determine the chain's components worth primary focus and development.

The model and the described modelling process give a definite and comprehensive basis for further studies. This is especially important, as described previously, in the absence of similar openly available models or studies. The goal was to build a model that could provide data for energy consumption for a mid-scale distribution chain. Still, much effort was also put into creating an efficient workflow approach. As a result, a highly flexible model was completed.

One can study the distribution chain model behaviour with different starting points, since the model blocks can be simulated separately and in different order. In this work we followed the direction from the production site to the end-user. Alternatively, there might be specified number of heavy vehicle fleet, so that the model can be used to investigate needed storage volumes at the end-user refueling site and production capacity. This provides extensive possibilities for model re-use with minimum alterations needed to the code (and not the model blocks).

The mentioned workflow has also some constraints and drawbacks. First, FMUs can only accept data and return a result. This means that a model cannot be accessed during a simulation. Secondly, data handling using FMI workflow is manual or requires creating proper scripts, which can be time consuming. This is valid at least for the PyFMI 2.5 package used.

In this work, only first optimization (from energetic point of view) was made related to the design of hydrogen filling facilities, i.e. the use of cascade storage system. Some design decisions and assumptions proved to be not particularly valid. As the results showed, the assumed compressor

efficiency curve was far from optimum. Delivery scenario do not also provide efficient use of trailer capacity.

It should be noted that no pressure drop modelling has been done (only a constant value assumed for refilling operations). With that, no flow related results were discussed such as mass flow, instant compressor and refrigerator power. SAE J2601 fueling protocol suggests approximate values of pressure drop in dispensing equipment. However, it would require more specific equipment data and modeling in more fine details than the current model provides.

Another point that is missing in the model and might add to energy consumption is transportation energy needs. This, however, might be more relevant with regards to economics or when results from an alternative liquid hydrogen distribution chain are available. Liquid distribution chain was not modelled in the course of this work because of the extensiveness of the compressed hydrogen distribution model and restricted amount of time. However, an attempt was made compare the reported liquefaction energy demand to the results of our simulation in section 5.3.

6.1 Further work

As described above, the model provides a solid ground for further work, but some main directions can be pointed out.

- The model lacks implementation of the actual equipment data. As it stands, difficulties are related to commercial confidentiality. Design and power consumption can be updated if such information is available to investigate the performance of a particular system. Alternatively, the model can be put in better defined operational constraints, which were mostly left out at this stage on purpose.
- Once general dynamic of the system is examined, more specific aspects of the chain can be optimized by running parametric studies. With addition of transportation models and economics, timescales of conducted operations can be set. The cascade storage system volume and pressure levels can be optimized based on the investment costs, energy savings, and land use.
- Model can be expanded to include energy production, electrolysis process, and transportation models. This will allow investigation of large time-scale system dynamics.
- It has been shown that hydrogen pre-cooling may require high investment costs into refrigeration equipment and substantial electricity demand when operating hydrogen filling facilities. A detailed look into hydrogen filling and dispensing scenarios might help finding efficient solutions for such systems.

Bibliography

- [1] International Energy Agency (IEA). *The Future of Hydrogen*. 2019.
- [2] Norwegian Ministry of Petroleum, Norwegian Ministry of Climate Energy and Environment. ‘The Norwegian Government’s hydrogen strategy’. In: (2020).
- [3] *Fueling Protocols for Light Duty Gaseous Hydrogen Surface Vehicles*. Surface vehicle standard. SAE international, May 2020.
- [4] David L Greene, Joan M Ogden and Zhenhong Lin. ‘Challenges in the designing, planning and deployment of hydrogen refueling infrastructure for fuel cell electric vehicles’. In: *eTransportation* (2020), p. 100086.
- [5] Christopher Yang and Joan Ogden. ‘Determining the lowest-cost hydrogen delivery mode’. In: *International Journal of Hydrogen Energy* 32.2 (2007), pp. 268–286.
- [6] Lutz Decker. *Liquid Hydrogen Distribution Technology*. *HYPER Closing Seminar*. Dec. 2019. URL: https://www.sintef.no/globalassets/project/hyper/presentations-day-2/day2_1105_decker_liquid-hydrogen-distribution-technology_linde.pdf.
- [7] A Almansoori and N Shah. ‘Design and operation of a future hydrogen supply chain: multi-period model’. In: *International journal of hydrogen energy* 34.19 (2009), pp. 7883–7897.
- [8] Silviu Nistor et al. ‘Technical and economic analysis of hydrogen refuelling’. In: *Applied Energy* 167 (2016), pp. 211–220.
- [9] Hydrogen and Fuel Cell Technologies Office. *Gaseous Hydrogen Compression*. Nov. 2021. URL: <https://www.energy.gov/eere/fuelcells/gaseous-hydrogen-compression>.
- [10] in Wikipedia. *Ionic liquid piston compressor*. 17th Nov. 2021. URL: https://en.wikipedia.org/w/index.php?title=Ionic_liquid_piston_compressor&oldid=1055691017.
- [11] Linde AG. *Hydrogen technologies. Ionic compressor 50*. Dec. 2021. URL: https://www.linde-engineering.com/en/images/DS_IC_50_tcm19-523715.pdf.
- [12] Terry Johnson et al. *Metal Hydride Compression. Annual progress report*. 2019. URL: https://www.hydrogen.energy.gov/pdfs/progress19/ins_in007_johnson_2019.pdf.
- [13] Burckhardt Compression. *Compressor solutions for hydrogen trailer filling*. Dec. 2021. URL: <https://www.burckhardtcompression.com/solution/industrial-gases/h2-power-to-x-mobility/h2-trailer-filling/>.
- [14] Neumann Esser Compressors. *Hydrogen compressors*. Dec. 2021. URL: <https://www.neumann-esser.de/en/compressors/hydrogen-compressors/>.
- [15] Mehrer Compression GmbH. *Compressors for small fleet hydrogen filling stations*. Dec. 2021. URL: <https://www.mehrer.de/en/applications/hydrogen>.
- [16] Laurens Van Hoecke et al. ‘Challenges in the use of hydrogen for maritime applications’. In: *Energy & Environmental Science* 14.2 (2021), pp. 815–843.
- [17] G Parks et al. *Hydrogen station compression, storage, and dispensing technical status and costs: Systems integration*. Tech. rep. National Renewable Energy Lab.(NREL), Golden, CO (United States), 2014.
- [18] Krishna Reddi Amgad Elgowainy. *Hydrogen Fueling Station Pre-Cooling Analysis*. 2015. URL: https://www.hydrogen.energy.gov/pdfs/review15/pd107_elgowainy_2015_o.pdf.
- [19] Angel Alvarez Pardinas Armin Haffner. ‘CO₂ refrigeration technology: possible innovations’. In: (2019).
- [20] Lei Xiao et al. ‘Effects of pressure levels in three-cascade storage system on the overall energy consumption in the hydrogen refueling station’. In: *International Journal of Hydrogen Energy* 46.61 (2021), pp. 31334–31345.

-
- [21] Hyundai. *XCIENT Fuel Cell*. May 2022. URL: <https://trucknbus.hyundai.com/global/en/products/truck/xcient-fuel-cell>.
- [22] Switch Maritime. *Switch Maritime projects*. May 2022. URL: <https://www.switchmaritime.com/projects>.
- [23] Andreas Züttel. ‘Hydrogen storage methods’. In: *Naturwissenschaften* 91.4 (2004), pp. 157–172.
- [24] Pieter C Koelet and Tom B Gray. *Industrial refrigeration: principles, design and applications*. Macmillan International Higher Education, 2017.
- [25] Monterey Gardiner. *Energy requirements for hydrogen gas compression and liquefaction as related to vehicle storage needs*. 2009. URL: https://www.hydrogen.energy.gov/pdfs/9013_energy_requirements_for_hydrogen_gas_compression.pdf.

Appendix

```
# Import the load function (load_fm)
%matplotlib inline
from pyfmi import load_fm
import pandas as pd
import numpy as np
import matplotlib.pyplot as plt
import seaborn as sns
# Import the main class from the Python library
from ctREFPROP.ctREFPROP import REFPROPFunctionLibrary
import os
#interactive
import ipywidgets as widgets
from ipywidgets import interact, interact_manual

# Now we instantiate the library, and use the environment variable to
# explicitly state which path we want to use. It was decided to make
# the path handling explicit (though more verbose), because explicit
# is almost always better than implicit
RP = REFPROPFunctionLibrary(os.environ['RPPREFIX'])
RP.SETPATHdll(os.environ['RPPREFIX'])
# Get the unit system we want to use (we will revisit this GETENUM function later)
SI_C = RP.GETENUMdll(0, "SI WITH C").iEnum

#Functions
def new_statePH(T,P,T_init):
    """ Calculate new state for a gas at constant density D
        T - temperature in K
        P - pressure in Pa
        T_init - new temperature C
        return J/kg and Pa"""
    r=RP.REFPROPdll("Hydrogen", "TP", "D", SI_C, 0, 0, T-273.15, P*1e-6, [1.0]) #initial density
    H = RP.REFPROPdll("Hydrogen", "TD", "H", SI_C, 0, 0, T_init, r.Output[0], [1.0]) #initial Enthalpy
    P=RP.REFPROPdll("Hydrogen", "TD", "P", SI_C, 0, 0, T_init, r.Output[0], [1.0])
    return H.Output[0]*1e3, P.Output[0]*1e6

def cyl_dat(volume,row):
    #Number of cylinders and their volume (value rounded down)
    number=np.floor(int(volume)/df.loc[row, 'LiquidV'])
    area=df.loc[row, 'InnerA']
    v=number*df.loc[row, 'LiquidV']
    return number,v

#Cylinder parameters
filename = 'CylinderData.xlsx'
df = pd.read_excel(filename)
df

Trailer filling

TrailerStartPressure=80 #bar

#Production site
#pressure state 1 - MP
#Cascades are charged to a target operational density

n=3 #Filling operations
```

```

work_ref_res_1=[] #refrigeration work results
time_1=[]
hp_res_1=[] #pressure in the high pressure storage
mp_res_1=[] #pressure in the medium pressure storage
vp_res_1=[] #pressure in the filled volume (trailer)

hp_temp_res_1=[]
mp_temp_res_1=[]
v_temp_res_1=[]
mass_res_1=[]

p_cas = [25,50] #MPa initial pressure state at the cascade storage
cascade_vol=[200.0,250.0] #Volume of MP and HP storage
T = 20 #degrees C
r = RP.REFPROPdll("Hydrogen","TP","H",SI_C,0,0,T,p_cas[0],[1.0]) #initial Enthalpy in the tanks kJ/kg
r1 = RP.REFPROPdll("Hydrogen","TP","H",SI_C,0,0,T,p_cas[1],[1.0])
r3=RP.REFPROPdll("Hydrogen","TP","H",SI_C,0,0,T,TrailerStartPressure/10,[1.0])

#Target density in the trailer
TrailerReferencePressure=300 # bar
TrailerReferenceT=15 # C
tD_trailer=RP.REFPROPdll("Hydrogen","TP","D",SI_C,0,0,TrailerReferenceT,TrailerReferencePressure/10,[1.0])

val=[45,
      cascade_vol[0], cascade_vol[1],
      new_statePH(15+273.15,p_cas[0]*1e6,T)[1], new_statePH(15+273.15,p_cas[1]*1e6,T)[1],
      TrailerStartPressure*1e5,
      new_statePH(15+273.15,p_cas[0]*1e6,T)[0], new_statePH(15+273.15,p_cas[1]*1e6,T)[0],r3.Output[0]*1e3,
      3,65+273.15,tD_trailer.Output[0]] # Variable values
var_name=['volume.volumeFixed',
          'MPstorage.volumeFixed', 'HPstorage.volumeFixed',
          'pressureState1.pInitial', 'pressureState.pInitial',
          'pressureState2.pInitial',
          'MPstorage.hInitial', 'HPstorage.hInitial', 'volume.hInitial',
          'Rate', 'tankT', 'tankDensity'] # Variable names

for i in range(n):
    model = load_fmu('NewChain/CascadeFillingTargetDensity.fmu')
    model.set(var_name,val)
    res = model.simulate(final_time=1000)
    val[3]=[res['MPstorage.summary.p'][-1]]
    val[4]=[res['HPstorage.summary.p'][-1]]
    val[6]=[res['MPstorage.summary.h'][-1]]
    val[7]=[res['HPstorage.summary.h'][-1]]

#Simulation results
time_1.append(res['time'])

hp_res_1.append(res['HPstorage.p']*1e-5)
mp_res_1.append(res['MPstorage.p']*1e-5)
vp_res_1.append(res['volume.p']*1e-5)
mass_res_1.append(res['total_mass.y'][-1])

```

```

hp_temp_res_1.append(res['HPstorage.summary.T'])
mp_temp_res_1.append(res['MPstorage.summary.T'])
v_temp_res_1.append(res['volume.summary.T'])

work_ref_res_1.append(-res['CoolingWorkTotal.y'][-1]/res['total_mass.y'][-1]/3600/1000)

#Forwarded data
p_mp_end_1=res['MPstorage.summary.p'][-1]
p_hp_end_1=res['HPstorage.summary.p'][-1]
t_mp_end_1=res['MPstorage.summary.T'][-1]
t_hp_end_1=res['HPstorage.summary.T'][-1]

fig1=plt.figure(1)

for i in range(n):
    plt.style.use('seaborn')

    axes=plt.subplot(1,3,1+i)
    axes.plot(time_1[i][:],hp_res_1[i][:], label='HP');
    axes.plot(time_1[i][:],mp_res_1[i][:], label='MP');
    axes.plot(time_1[i][:],vp_res_1[i][:], label='trailer');

    idx = np.argwhere(np.diff(np.sign(mp_res_1[i][:] -vp_res_1[i][:]-10 ))).flatten()
    plt.vlines(time_1[i][idx],100,hp_res_1[i][idx],color='black', linewidth=0.5)
    plt.text(time_1[i][idx]-210, 80, 'MP filling')
    plt.text(time_1[i][idx]+50, 370, 'HP filling')

    axes.set_title('Trailer '+str(i+1));

    plt.ylim(bottom=0,top=550)
    if i==0:
        axes.set_xlabel('Time, s');
        axes.set_ylabel('Pressure, bar');
        axes.legend()

#Save figure 1
fig1.tight_layout()
fig1.savefig('imagesNew/trailer_filling.png', dpi = 300)

fig1_2=plt.figure(2)

c=273.15

for i in range(n):
    plt.style.use('seaborn')

    axes=plt.subplot(1,3,1+i)
    axes.plot(time_1[i][:],hp_temp_res_1[i][:]-c, label='HP');
    axes.plot(time_1[i][:],mp_temp_res_1[i][:]-c, label='MP');
    axes.plot(time_1[i][:],v_temp_res_1[i][:]-c, label='trailer');
    axes.set_title('Trailer '+str(i+1));

    plt.ylim(bottom=-30,top=70)
    if i==0:
        axes.set_xlabel('Time, s');
        axes.set_ylabel('Temperature, C');

```

```

        axes.legend()

#Save figure
fig1_2.tight_layout()
fig1_2.savefig('imagesNew/trailer_filling_temps.png', dpi = 300)

#COP
t_cold=-40
t_ambient=20
COP=(t_cold+273.15)/(t_ambient-t_cold)*0.5

print('COP ', np.round(COP,2))

#Plotting and calculating average specific cooling work

ref_data_1=[]

fig1_3=plt.figure(3)

for i in range(3):
    data1 = work_ref_res_1[i]/COP
    plt.bar(i+1, data1, color='#0072BD')
    ref_data_1.append(data1)

plt.xticks(ticks=[x+1 for x in range(3)], labels=[x+1 for x in range(3)])
plt.ylabel('Specific work, kWh/kg')
plt.xlabel('Trailer number')
#plt.title('Specific refrigeration work for each filling operation')

work_ref_1=np.average(ref_data_1)
print('Average refrigeration work ', np.round(work_ref_1,2))

#Save figure
fig1_3.tight_layout()
fig1_3.savefig('imagesNew/trailer_filling_ref.png', dpi = 300)

mass_res_1

```

Cascade charging

```

# Run intermediate storage calculation first!

#Cascade recharge

time_2=[]
hp_res_2=[] #pressure in the high pressure storage
mp_res_2=[] #pressure in the medium pressure storage
int_p_res_2=[] #pressure in the filled volume (trailer)

hp_temp_res_2=[]
mp_temp_res_2=[]
int_temp_res_2=[]
mass_res_2=[]

work_comp_res_2=[]
comp_pr_2=[]
comp_power_2=[]

```

```

comp_mass_flow_2=[]
comp_isEff_2=[]

HP_d_res=0
MP_d_res=0
count=0

volume_mp_2=cascade_vol[0]
row_mp_2=6
mp_volume_2=cyl_dat(volume_mp_2,row_mp_2)[1]
mp_area_2=df.loc[row_mp_2,'InnerA']*cyl_dat(volume_mp_2,row_mp_2)[0]
mp_mass_2=df.loc[row_mp_2,'Weight']*cyl_dat(volume_mp_2,row_mp_2)[0]

volume_hp_2=cascade_vol[1]
row_hp_2=6
hp_volume_2=cyl_dat(volume_hp_2,row_hp_2)[1]
hp_area_2=cyl_dat(volume_hp_2,row_hp_2)[0]*df.loc[row_hp_2,'InnerA']
hp_mass_2=df.loc[row_hp_2,'Weight']*cyl_dat(volume_hp_2,row_hp_2)[0]

#Density stays the same inside the volume, but temperature and pressure will change
#Temperature is assumed to reach ambient conditions

T_ambient = 20 #degrees C

#Target density
ReferencePressureMP_2=p_cas[0]
ReferenceT_MP_2=15 # C
tD_MP_2=RP.REFPROPdll("Hydrogen","TP","D",SI_C,0,0,ReferenceT_MP_2,ReferencePressureMP_2,[1.0])

ReferencePressureHP_2=p_cas[1]
ReferenceT_HP_2=15 # C
tD_HP_2=RP.REFPROPdll("Hydrogen","TP","D",SI_C,0,0,ReferenceT_HP_2,ReferencePressureHP_2,[1.0])

#inter volume
p_init_2=200 #bar
r = RP.REFPROPdll("Hydrogen","TP","H",SI_C,0,0,T_ambient,p_init_2/10,[1.0])

var_name=['pressureState1.pInitial','pressureState.pInitial',
          'pressureState2.pInitial',
          'MPstorage.hInitial','HPstorage.hInitial',
          'interVolume.hInitial',
          'MPstorage.volumeFixed','HPstorage.volumeFixed',
          'interVolume.volumeFixed','MaxMP','MaxHP','Rate',
          'MPdensity','HPdensity',

          'R_OuterSurface2.crossSection',
          'CompositeCapacity2.solidMass',
          'R_CarbonLayer2.crossSection',
          'R_PolymerLayer2.crossSection',
          'R_InnerSurface2.crossSection',

          'R_OuterSurface1.crossSection',
          'CompositeCapacity1.solidMass',
          'R_CarbonLayer1.crossSection',
          'R_PolymerLayer1.crossSection',

```

```

    'R_InnerSurface1.crossSection',

    'R_InnerSurface.crossSection',
    'R_Steel.sectionLength',
    'R_Steel.crossSection',
    'SteelCapacity.solidMass',
    'R_OuterSurface.crossSection',
    'AmbientT', 'Rate'] #pressureState1 - HP volume

val=[new_statePH(t_hp_end_1,p_hp_end_1,T_ambient)[1],new_statePH(t_mp_end_1,p_mp_end_1,T_ambient)[1],
    p_init_2*1e5,
    new_statePH(t_mp_end_1,p_mp_end_1,T_ambient)[0],new_statePH(t_hp_end_1,p_hp_end_1,T_ambient)[0],
    r.Output[0]*1e3,
    cascade_vol[0],cascade_vol[1],
    volume,p_cas[0]*1e6,p_cas[1]*1e6,0.5,
    tD_MP_2.Output[0],tD_HP_2.Output[0],
    hp_area_2,
    hp_mass_2,
    hp_area_2,
    hp_area_2,
    hp_area_2,

    mp_area_2,
    mp_mass_2,
    mp_area_2,
    mp_area_2,
    mp_area_2,

    area_in*number_inter,
    wall,area_in*number_inter,
    mass_inter*number_inter,
    area_out*number_inter,
    T_ambient+273.15, 0.03] #pressure values from the previous simulation at new gas state

while HP_d_res<tD_HP_2.Output[0] and MP_d_res < tD_MP_2.Output[0]:
    model = load_fm('NewChain/CascadeCharging.fmu')
    model.set(var_name,val)
    res2 = model.simulate(final_time=60000)
    val[4]=new_statePH(res2['HPstorage.summary.T'][-1],res2['HPstorage.summary.p'][-1],T_ambient)[0]
    val[3]=new_statePH(res2['MPstorage.summary.T'][-1],res2['MPstorage.summary.p'][-1],T_ambient)[0]
    val[0]=new_statePH(res2['HPstorage.summary.T'][-1],res2['HPstorage.summary.p'][-1],T_ambient)[1]
    val[1]=new_statePH(res2['MPstorage.summary.T'][-1],res2['MPstorage.summary.p'][-1],T_ambient)[1]
    val[2]=new_statePH(res2['interVolume.summary.T'][-1],res2['interVolume.summary.p'][-1],T_ambient)[1]
    val[5]=new_statePH(res2['interVolume.summary.T'][-1],res2['interVolume.summary.p'][-1],T_ambient)[0]

    #Simulation results
    HP_d_res=res2['HPstorage.summary.d'][-1]
    MP_d_res=res2['MPstorage.summary.d'][-1]

    time_2.append(res2['time'])

    hp_res_2.append(res2['HPstorage.p']*1e-5)
    mp_res_2.append(res2['MPstorage.p']*1e-5)
    int_p_res_2.append(res2['interVolume.p']*1e-5)
    mass_res_2.append(res2['total_mass.y'][-1])

```

```

hp_temp_res_2.append(res2['HPstorage.summary.T'])
mp_temp_res_2.append(res2['MPstorage.summary.T'])
int_temp_res_2.append(res2['interVolume.summary.T'])

comp_power_2.append(res2['tableEffCompressor2.summary.P_vle'])
comp_mass_flow_2.append(res2['tableEffCompressor2.summary.m_flow_A'])

work_comp_res_2.append(res2['CompressorWorkCascade.y'][-1]*1e-3/3600/res2['total_mass.y'][-1])
comp_pr_2.append(res2['tableEffCompressor2.pressureRatio.y'])
comp_isEff_2.append(res2['tableEffCompressor2.isEff'])

count+=1

#Pressure data table
c=273.15
colData3=[[ 'HP storage', cascade_vol[1], np.round(hp_res_1[-1][-1]), np.round(t_hp_end_1-c),
            np.round(new_statePH(t_hp_end_1, p_hp_end_1, T_ambient)[1]*1e-5), T_ambient],
          [ 'MP storage', cascade_vol[0], np.round(mp_res_1[-1][-1]), np.round(t_mp_end_1-c),
            np.round(new_statePH(t_mp_end_1, p_mp_end_1, T_ambient)[1]*1e-5), T_ambient]];
colNames3=['Section', 'Volume', 'End pressure, bar', 'End temperature, C',
           'Initial pressure, bar', 'Initial temperature, C'];

df3 = pd.DataFrame(data = colData3, columns=colNames3)
df3

fig2, axes = plt.subplots(nrows = 1, ncols = 1);
plt.style.use('seaborn')

axes.plot(res2['time'], res2['HPstorage.summary.p']*1e-5, label='HP');
axes.plot(res2['time'], res2['MPstorage.summary.p']*1e-5, label='MP');
axes.plot(res2['time'], res2['interVolume.summary.p']*1e-5, label='Inter');
#axes.set_title('Cascade storage charging');

der=[(res2['HPstorage.summary.p'][x+1]-res2['HPstorage.summary.p'][x])/(res2['time'][x+1]-res2['time'][x])
      for x in range(len(res2['HPstorage.summary.p'][:-1]))]
b =np.argwhere([1 if np.floor(i) else 0 for i in der])
a =np.argwhere([1 if i<0 else 0 for i in der])

plt.vlines(res2['time'][b[1]], 150, res2['HPstorage.summary.p'][b[1]]*1e-5, linewidth=0.5, color='black')
plt.vlines(res2['time'][a[1]-2], 150, res2['HPstorage.summary.p'][a[1]-1]*1e-5, linewidth=0.5, color='black')
plt.text(0, 350, 'MP charging', fontsize=13)
plt.text(res2['time'][a[1]-2]*0.4, 350, 'HP charging from MP', fontsize=13)
plt.text(res2['time'][a[1]-2]*1.02, 350, 'MP charging', fontsize=13)

axes.set_xlabel('Time, s');
axes.set_ylabel('Pressure, bar');
axes.legend()

#Save figure
fig2.tight_layout()
fig2.savefig('imagesNew/cascade_charging_prod.png', dpi = 300)

fig2_3=plt.figure(7)

for i in range(count):
    plt.style.use('seaborn')

```

```

axes=plt.subplot(1,2,1+i)
axes.plot(time_2[i][:],hp_temp_res_2[i][:]-273.15, label='HP');
axes.plot(time_2[i][:],mp_temp_res_2[i][:]-273.15, label='MP');
axes.plot(time_2[i][:],int_temp_res_2[i][:]-273.15, label='intermediate');
axes.set_title('Time interval '+str(i+1));

plt.ylim(bottom=0,top=70)
if i==0:
    axes.set_xlabel('Time');
    axes.set_ylabel('Temperature, C');
    axes.legend()

#Save figure
fig2_3.tight_layout()
fig2_3.savefig('imagesNew/cascade_charging_prod_temp.png', dpi = 300)

fig2_4=plt.figure(8)

for i in range(count):
    plt.style.use('seaborn')

    axes=plt.subplot(1,2,1+i)
    axes.plot(time_2[i][:],hp_res_2[i][:], label='HP');
    axes.plot(time_2[i][:],mp_res_2[i][:], label='MP');
    axes.plot(time_2[i][:],int_p_res_2[i][:], label='intermediate');
    axes.set_title('Time interval '+str(i+1));

    plt.ylim(bottom=0,top=600)
    if i==0:
        axes.set_xlabel('Time');
        axes.set_ylabel('Pressure, bar');
        axes.legend()

#Save figure
fig2_4.tight_layout()
fig2_4.savefig('imagesNew/cascade_charging_prod.png', dpi = 300)

fig2_2, axes = plt.subplots(nrows = 1, ncols = 1);
plt.style.use('seaborn')

axes.plot(res2['time'],res2['HPstorage.summary.T']-273.15,label='HP');
axes.plot(res2['time'],res2['MPstorage.summary.T']-273.15,label='MP');
axes.plot(res2['time'],res2['interVolume.summary.T']-273.15,label='Inter');
axes.set_title('Cascade storage charging');
axes.set_xlabel('Time,s');
axes.set_ylabel('Temperature, C');
axes.set_ylim([10, 35])
axes.legend()

#Save figure
fig2_2.tight_layout()
fig2_2.savefig('imagesNew/cascade_charging_prod_temp.png', dpi = 300)

#compressor data for production site cascade charging operation
a=[]
b=[]
c=[]

```

```

for i in range(count):
    a.append(np.average(comp_pr_2[i],weights=res2['time']))
    b.append(np.max(comp_pr_2[i]))
    c.append(np.min(comp_pr_2[i]))

pr_2=np.average(a)
pr_max_2=np.max(b)
pr_min_2=np.min(c)

print(pr_2,pr_min_2,pr_max_2)

#energy consumption by the compressor
work_comp_2=np.average(work_comp_res_2)
instant_power_2=np.average(comp_power_2)*1e-3
comp_massflow_2=np.average(comp_mass_flow_2)

is_eff_2=np.average(res2['tableEffCompressor2.isEff'], weights=res2['time']) #only for single simulation

print(work_comp_2, instant_power_2, comp_massflow_2)

#Pressure data table
colData4=[['Specific compression work',np.round(work_comp_2,2)],
          ['Average pressure ratio',np.round(pr_2,2)],
          ['Minimum pressure ratio',np.round(pr_min_2,2)],
          ['Maximum pressure ratio',np.round(pr_max_2,2)],
          ['Average power', np.round(instant_power_2)],
          ['Average massflow', np.round(comp_massflow_2,3)],
          ['Average isentropic efficiency', np.round(is_eff_2,2)]];
colNames4=['Parameter', 'Value'];

df4 = pd.DataFrame(data = colData4, columns=colNames4)
df4

mass_res_2=res2['total_mass.y'][-1]
mass_res_2

Intermediate storage

# Steel cylinder parameters
diameter=1.2 # outer m
length=6 # m
volume=500 # m3
ref_pressure=200 #bar
ref_temp=15 # C
rho=7850 #kg/m3 steel density

tD=RP.REFPROPdll("Hydrogen", "TP", "D", SI_C, 0, 0, ref_temp, ref_pressure/10, [1.0])
tP=RP.REFPROPdll("Hydrogen", "TD", "P", SI_C, 0, 0, 60, tD.Output[0], [1.0])

tensile_strength=460 # MPa, steel, ref. article Zuttel2004

wall=diameter*(tP.Output[0]-101325*1e-6)/(2*tensile_strength+(tP.Output[0]-101325*1e-6)) #at 60 degrees
volume_cyl=np.pi*(diameter**2-(diameter-2*wall)**2)*length/4+1/6*(diameter**3-(diameter-2*wall)**3)
number_inter=np.ceil(volume/volume_cyl)
volume_inter=number_inter*volume_cyl

```

```

mass_inter=(np.pi*(diameter**2-(diameter-2*wall)**2)*length/4+1/6*(diameter**3-(diameter-2*wall)**3))*rho

area_in=np.pi*(diameter-2*wall)*length+np.pi*(diameter-2*wall)**2
area_out=np.pi*diameter*length+np.pi*diameter**2
print(wall, volume, mass_inter)
print(area_in, area_out, (area_in+area_out)*0.5, number_inter)

#Intermediate storage simulation
#Forwarding data

#Density stays the same inside the volume, but temperature and pressure will change
#Temperature is assumed to reach ambient conditions

afterT=70

p_inter_end_2=res2['interVolume.summary.p'][-1]

var_name=['pressureState.pInitial',
          'interVolume.hInitial','interVolume.volumeFixed',
          'R_InnerSurface.crossSection',
          'R_Steel.sectionLength','R_Steel.crossSection',
          'SteelCapacity.solidMass',
          'R_OuterSurface.crossSection', 'afterT'] #pressureState
T = 20 #degrees C

val=[new_statePH(res2['interVolume.summary.T'][-1],p_inter_end_2,T)[1],
     new_statePH(res2['interVolume.summary.T'][-1],p_inter_end_2,T)[0],volume_inter,
     area_in*number_inter,
     wall,area_in*number_inter,
     mass_inter*number_inter,
     area_out*number_inter, afterT+273.15] #values from the previous simulation

model = load_fmu('NewChain/CompressionAfterElectrolyzer.fmu')
model.set(var_name,val)
res3 = model.simulate(final_time=1e6)

#Pressure data table
colData5=[['Intermediate storage',np.round(volume_inter),np.round(p_inter_end_2*1e-5),
           np.round(res2['interVolume.summary.T'][-1]-273.15),
           np.round(new_statePH(res2['interVolume.summary.T'][-1],p_inter_end_2,T)[1]*1e-5),T]];
colNames5=['Section', 'Volume','End pressure, bar','End temperature, C',
           'Initial pressure, bar','Initial temperature, C'];

df5 = pd.DataFrame(data = colData5, columns=colNames5)
df5

parameter=1 # 1- temperature, 2 - pressure
if parameter==1:
    fig3, axes = plt.subplots(nrows = 1, ncols = 1);
    plt.style.use('seaborn')
    axes.plot(res3['time']/3600,res3['interVolume.summary.T']-273.15);
    #axes.set_title('Buffer storage filling');
    axes.set_xlabel('Time, h');
    axes.set_ylabel('Temperature, C');
else:
    fig3, axes = plt.subplots(nrows = 1, ncols = 1);

```

```

plt.style.use('seaborn')
axes.plot(res3['time']/3600,res3['interVolume.summary.p']*1e-5);
#axes.set_title('Intermediate storage filling');
axes.set_xlabel('Time, h');
axes.set_ylabel('Pressure, bar');

#Save figure
fig3.tight_layout()
fig3.savefig('imagesNew/buffer_filling_temp.png', dpi = 300)

mass_res_3=res3['totalMass.y'][-1]
mass_res_3

fig3_2, axes = plt.subplots(nrows = 1, ncols = 1);
plt.style.use('seaborn')
axes.plot(res3['time'],res3['tableEffCompressor1.pressureRatio.y']);
axes.set_title('Cascade storage charging');
axes.set_xlabel('Time');
axes.set_ylabel('Pressure ratio');

#energy consumption by the compressor after electrolyzer
work_comp_3=res3['CompressorWork.y'][-1]*1e-3/3600/res3['totalMass.y'][-1]
comp_isEff_3=res3['tableEffCompressor1.isEff'][-1]
print(work_comp_3)

comp_power_3=max(res3['CompressorPower.y'])*1e-3
comp_mass_flow_3=max(res3['tableEffCompressor1.summary.m_flow_A'])
print(comp_power_3,comp_mass_flow_3)

#compressor data
pr_3=np.average(res3['TotalPressureRatio.y'])
pr_max_3=np.max(res3['TotalPressureRatio.y'])
pr_min_3=np.min(res3['TotalPressureRatio.y'])

print(pr_3,pr_min_3,pr_max_3)

#Compressor data table
colData=[['Specific compression work',np.round(work_comp_3,2)],
          ['Average pressure ratio',np.round(pr_3,2)],
          ['Minimum pressure ratio',np.round(pr_min_3,2)],
          ['Maximum pressure ratio',np.round(pr_max_3,2)],
          ['Average power', np.round(comp_power_3)],
          ['Average massflow', np.round(comp_mass_flow_3,3)],
          ['Stage average isentropic efficiency', np.round(is_eff_2,2)]];
colNames=['Parameter','Value'];

df_comp_3 = pd.DataFrame(data = colData, columns=colNames)
df_comp_3

End user refilling

# Onboard tank parameters Hyundai
ref_p_onboard=350 # bar
ref_t_onboard=15 # C
ref_d = RP.REFPROPdll("Hydrogen","TP","D",SI_C,0,0,ref_t_onboard,ref_p_onboard/10,[1.0]) #Target density
ref_mass=38 #kg
onboard_volume=ref_mass/ref_d.Output[0]
print(onboard_volume, ref_d.Output[0])

```

```

colData=[['Reference pressure, bar', 350],
          ['Reference temperature, C', 15],
          ['Hydrogen capacity, kg', 38],
          ['Volume, m3', np.round(onboard_volume,1)]];
colNames=['Parameter', 'Value'];

df_truck = pd.DataFrame(data = colData, columns=colNames)
df_truck

# Refilling site cascade
#pressure state 1 - MP

p = [35,50] #MPa
T = 20 #degrees C
r = RP.REFPROPdll("Hydrogen", "TP", "H", SI_C, 0, 0, T, p[0], [1.0]) #initial Enthalpy
r1 = RP.REFPROPdll("Hydrogen", "TP", "H", SI_C, 0, 0, T, p[1], [1.0])
r2 = RP.REFPROPdll("Hydrogen", "TP", "H", SI_C, 0, 0, T, 0.2, [1.0]) #initial pressure in onboard tank 20 bar

val=[onboard_volume,
      40.0, 30.0,
      p[0]*1e6, p[1]*1e6,
      r.Output[0]*1e3, r1.Output[0]*1e3, r2.Output[0]*1e3,
      ref_d.Output[0], p[1]*1e6]
var_name=['volume.volumeFixed',
          'MPstorage.volumeFixed', 'HPstorage.volumeFixed',
          'pressureState1.pInitial', 'pressureState.pInitial',
          'MPstorage.hInitial', 'HPstorage.hInitial', 'volume.hInitial',
          'tankDensity', 'HPpressure']

fig=plt.figure(1)

time_4=[]
mass_res_4=[]
hp_res_4=[]
mp_res_4=[]
vp_res_4=[]
work_ref_res_4=[]
work_comp_res_4=[]
comp_pr_4=[]
comp_power_4=[]
comp_mass_flow_4=[]
comp_isEff_4=[]

hp_temp_res_4=[]
mp_temp_res_4=[]
v_temp_res_4=[]

truck=0
p=500e5 #Pressure in the HP storage

while p>=430e5: #Assumption to have at least 20 bar overpressure of that in on-board tank
    model = load_fm('NewChain/CascadeFillingEnd.fmu')
    model.set(var_name, val)

```

```

res4 = model.simulate(final_time=1000)
val[3]=[res4['MPstorage.summary.p'][-1]]
val[4]=[res4['HPstorage.summary.p'][-1]]
val[5]=[res4['MPstorage.summary.h'][-1]]
val[6]=[res4['HPstorage.summary.h'][-1]]

p=res4['HPstorage.summary.p'][-1]

if res4['volume.summary.d'][-1]<ref_d.Output[0]:
    break

truck+=1

#simulation results
time_4.append(res4['time'])

hp_res_4.append(res4['HPstorage.p']*1e-5)
mp_res_4.append(res4['MPstorage.p']*1e-5)
vp_res_4.append(res4['volume.p']*1e-5)

hp_temp_res_4.append(res4['HPstorage.summary.T']-273.15)
mp_temp_res_4.append(res4['MPstorage.summary.T']-273.15)
v_temp_res_4.append(res4['volume.summary.T']-273.15)

mass_res_4.append(res4['total_mass.y'][-1])

work_ref_res_4.append(res4['CoolingWorkTotal.y'][-1])
work_comp_res_4.append(res4['CompressorWork.y'][-1])
comp_power_4.append(res4['tableEffCompressor.summary.P_vle'])
comp_mass_flow_4.append(res4['tableEffCompressor.summary.m_flow_A'])
comp_isEff_4.append(res4['tableEffCompressor.isEff'])

comp_pr_4.append(res4['tableEffCompressor.pressureRatio.y'])

print(truck, ' trucks refilled')

print('Amount of hydrogen filled ',mass_res_4[0])

offset=3
n=5
for i in range(n):
    fig4=plt.figure(4)
    plt.style.use('seaborn')

    m=np.argmax(vp_res_4[-offset-n+i][:]) #cutting the excess part of the graph
    axes=plt.subplot(1,n,1+i)
    axes.plot(time_4[-offset-n+i][:],hp_res_4[-offset-n+i][:], label='HP');
    axes.plot(time_4[-offset-n+i][:],mp_res_4[-offset-n+i][:], label='MP');
    axes.plot(time_4[-offset-n+i][:m],vp_res_4[-offset-n+i][:m], label='onboard tank');
    axes.set_title('Vehicle '+str(len(time_4)-offset-n+1+i));

    plt.ylim(bottom=0,top=550)
    if i==0:
        axes.set_xlabel('Time');
        axes.set_ylabel('Pressure, bar');

```

```

        axes.legend()

#Save figure
fig4.savefig('imagesNew/cascade_filling_end.png', dpi = 300)

offset=3
n=4
for i in range(n):
    fig4=plt.figure(4)
    plt.style.use('seaborn')

    m=np.argmax(vp_res_4[-offset-n+i][:]) #cutting the excess part of the graph
    axes=plt.subplot(1,n,1+i)
    axes.plot(time_4[-offset-n+i][:],hp_temp_res_4[-offset-n+i][:], label='HP');
    axes.plot(time_4[-offset-n+i][:],mp_temp_res_4[-offset-n+i][:], label='MP');
    axes.plot(time_4[-offset-n+i][:m],v_temp_res_4[-offset-n+i][:m], label='onboard tank');
    axes.set_title('Vehicle '+str(len(time_4)-offset-n+1+i));

    plt.ylim(bottom=-100,top=80)
    if i==0:
        axes.set_xlabel('Time');
        axes.set_ylabel('Temperature, C');
        axes.legend()

#Save figure
fig4.savefig('imagesNew/cascade_filling_end_temps.png', dpi = 300)

#Plotting and calculating average pressure ratio

n = [idx for idx, val in enumerate(work_comp_res_4) if val != 0] #positions non zero comp work

fig4_3=plt.figure(2)

for i in range(len(n)): #compressor does not work during last refilling
    data1 = np.average(comp_pr_4[n[i]])
    plt.bar(i, data1, color='#0072BD')

plt.xticks(ticks=range(len(n)),labels=[x+1 for x in n])
plt.ylabel('Average pressure ratio')
plt.xlabel('Refilling operation')
#plt.title('Average pressure ratio during compression into HP storage')

#Save figure
fig4_3.savefig('imagesNew/cascade_comp_pr.png', dpi = 300)

#compressor data
a=[]
b=[]
c=[]
d=[]

for i in range(len(comp_pr_4)):
    a.append(np.average(comp_pr_4[i]))
    b.append(np.max(comp_pr_4[i]))
    c.append(np.min(comp_pr_4[i]))
    d.append(np.average(comp_isEff_4[i]))

pr_4=np.average(a)

```

```

is_eff_4=np.average(d)
pr_max_4=np.max(b)
pr_min_4=np.min(c)

instant_power_4=max(map(max, comp_power_4))*1e-3
comp_massflow_4=max(map(max, comp_mass_flow_4))

print(pr_4,pr_min_4,pr_max_4, instant_power_4, comp_massflow_4, is_eff_4)

#COP
t_cold=-40
t_ambient=20
COP=(t_cold+273.15)/(t_ambient-t_cold)*0.5

print('COP ',COP)

mass_distributed=0
ref_data_4=[]
comp_data_4=[]

fig4_2=plt.figure(5)

for i in range(len(mass_res_4)):
    data1 = work_comp_res_4[i]/mass_res_4[i]/3600*1e-3
    data2 = -work_ref_res_4[i]/mass_res_4[i]/3600*1e-3/COP
    plt.bar(i, data1, color='#0072BD')
    plt.bar(i, data2, bottom=data1, color='#EDB120')
    mass_distributed+=mass_res_4[i]
    ref_data_4.append(-work_ref_res_4[i]/mass_res_4[i]/3600*1e-3/COP)
    comp_data_4.append(work_comp_res_4[i]/mass_res_4[i]/3600*1e-3)

plt.xticks(ticks=range(len(mass_res_4)),labels=[x+1 for x in range(len(mass_res_4))])
#plt.title('Combined specific power consumptiong during user refilling operations')
plt.ylabel(r'Combined specific work, $\frac{kWh}{kg_{H_2}}$')
plt.xlabel('Refilling number')
plt.legend(labels=['Compression', 'Cooling'])
print('Total mass ', mass_distributed)

#Save figure
fig4_2.savefig('imagesNew/cascade_energy_end2.png', dpi = 300)

work_ref_4=np.average(ref_data_4)
print('Average cooling demand ', work_ref_4)

work_comp_4=np.average(comp_data_4)
print('Average power demand for compression ', work_comp_4)

#Compressor data table
colData=[['Specific compression work',np.round(work_comp_4,2)],
          ['Specific refrigeration work', np.round(work_ref_4,2)],
          ['Average compressor pressure ratio',np.round(pr_4,2)],
          ['Minimum compressor pressure ratio',np.round(pr_min_4,2)],
          ['Maximum compressor pressure ratio',np.round(pr_max_4,2)],
          ['Average isentropic efficiency', np.round(is_eff_4,2)]];
colNames=['Parameter', 'Value'];

df_comp_4 = pd.DataFrame(data = colData, columns=colNames)

```

df_comp_4

Refilling site cascade charging

p = [35,50] #MPa

#Target density

ReferencePressureMP=p[0]

ReferenceT_MP=15 # C

tD_MP=RP.REFPROPdll("Hydrogen", "TP", "D", SI_C, 0, 0, ReferenceT_MP, ReferencePressureMP, [1.0])

ReferencePressureHP=p[1]

ReferenceT_HP=15 # C

tD_HP=RP.REFPROPdll("Hydrogen", "TP", "D", SI_C, 0, 0, ReferenceT_HP, ReferencePressureHP, [1.0])

#Choose cylinder from data table

volume=45

row=4

trailer_volume=cyl_dat(volume, row) [1]

trailer_area=df.loc[row, 'InnerA']*cyl_dat(volume, row) [0]

trailer_mass=df.loc[row, 'Weight']*cyl_dat(volume, row) [0]

volume_mp=40

row_mp=6

mp_volume=cyl_dat(volume_mp, row_mp) [1]

mp_area=df.loc[row_mp, 'InnerA']*cyl_dat(volume_mp, row_mp) [0]

mp_mass=df.loc[row_mp, 'Weight']*cyl_dat(volume_mp, row_mp) [0]

volume_hp=30

row_hp=8

hp_volume=cyl_dat(volume_hp, row_hp) [1]

hp_area=cyl_dat(volume_hp, row_hp) [0]*df.loc[row_hp, 'InnerA']

hp_mass=df.loc[row_hp, 'Weight']*cyl_dat(volume_hp, row_hp) [0]

p = [mp_res_4[-1] [-1], hp_res_4[-1] [-1]] #bar

T = 20 #degrees C

rH = RP.REFPROPdll("Hydrogen", "TD", "H", SI_C, 0, 0, T, tD_trailer.Output [0], [1.0]) *#Enthalpy in the trailer*

rP = RP.REFPROPdll("Hydrogen", "TD", "P", SI_C, 0, 0, T, tD_trailer.Output [0], [1.0]) *#Pressure in the trailer*

rate=0.3 #MPa/min, filling rate

rate2=0.3

p_init_5=300 #pressure in the trailer

var_name=['MPstorage.volumeFixed', 'HPstorage.volumeFixed', 'interVolume.volumeFixed',
'pressureState.pInitial',
'pressureState1.pInitial',
'MPstorage.hInitial',
'HPstorage.hInitial',

'R_OuterSurface2.crossSection',
'CompositeCapacity2.solidMass',
'R_CarbonLayer2.crossSection',
'R_PolymerLayer2.crossSection',
'R_InnerSurface2.crossSection',

```

'R_OuterSurface1.crossSection',
'CompositeCapacity1.solidMass',
'R_CarbonLayer1.crossSection',
'R_PolymerLayer1.crossSection',
'R_InnerSurface1.crossSection',

'R_OuterSurface.crossSection',
'CompositeCapacity.solidMass',
'R_CarbonLayer.crossSection',
'R_PolymerLayer.crossSection',
'R_InnerSurface.crossSection',
'pressureState2.pInitial',
'interVolume.hInitial',
'CompositeCapacity.TInitial',
'HeatBoundary_Ambient.TFixed',
'Rate','Rate2',
'MPdensity','HPdensity']

val=[mp_volume, hp_volume, trailer_volume,

new_statePH(mp_temp_res_4[-1][-1]+273.15,mp_res_4[-1][-1]*1e5,T)[1],
new_statePH(hp_temp_res_4[-1][-1]+273.15,hp_res_4[-1][-1]*1e5,T)[1],
new_statePH(mp_temp_res_4[-1][-1]+273.15,mp_res_4[-1][-1]*1e5,T)[0],
new_statePH(hp_temp_res_4[-1][-1]+273.15,hp_res_4[-1][-1]*1e5,T)[0],

hp_area,
hp_mass,
hp_area,
hp_area,
hp_area,

mp_area,
mp_mass,
mp_area,
mp_area,
mp_area,
trailer_area,
trailer_mass,
trailer_area,
trailer_area,
trailer_area,
rP.Output[0]*1e6,
rH.Output[0]*1e3,
T+273.15,
T+273.15,
rate,rate2,
tD_MP.Output[0],tD_HP.Output[0]]

model = load_fmu('NewChain/CascadeChargingEnd.fmu')
model.set(var_name,val)
res5 = model.simulate(final_time=30000)

#Pressure data table
colData=[[ 'HP storage',np.round(hp_volume),np.round(hp_res_4[-1][-1]),np.round(hp_temp_res_4[-1][-1]),
```

```

        np.round(new_statePH(hp_temp_res_4[-1][-1]+273.15,hp_res_4[-1][-1]*1e5,T)[1]*1e-5),T],
        ['MP storage',np.round(mp_volume),np.round(mp_res_4[-1][-1]),np.round(mp_temp_res_4[-1][-1]),
        np.round(new_statePH(mp_temp_res_4[-1][-1]+273.15,mp_res_4[-1][-1]*1e5,T)[1]*1e-5),T]];
colNames=['Section', 'Volume','End pressure, bar','End temperature, C','Initial pressure, bar',
        'Initial temperature, C'];

df6 = pd.DataFrame(data = colData, columns=colNames)
df6

#Pressure data table
colData=[['HP storage',np.round(res5['HPstorage.summary.p'][-1]*1e-5,2),
        np.round(res5['HPstorage.summary.T'][-1]-273.15,2)],
        ['MP storage',np.round(res5['MPstorage.summary.p'][-1]*1e-5,2),
        np.round(res5['MPstorage.summary.T'][-1]-273.15,2)],
        ['Trailer',np.round(res5['interVolume.summary.p'][-1]*1e-5,2),
        np.round(res5['interVolume.summary.T'][-1]-273.15,2)]];
colNames=['Section','End pressure, bar','End temperature, C'];

df7 = pd.DataFrame(data = colData, columns=colNames)
df7

new_statePH(res5['interVolume.summary.T'][-1],res5['interVolume.summary.p'][-1],T)[1]*1e-5

fig5, axes = plt.subplots(nrows = 1, ncols = 1);

axes.plot(res5['time'],res5['HPstorage.summary.p']*1e-5,label='HP');
axes.plot(res5['time'],res5['MPstorage.summary.p']*1e-5,label='MP');
axes.plot(res5['time'],res5['interVolume.summary.p']*1e-5,label='Delivery trailer');

der=[(res5['HPstorage.summary.p'][x+1]-res5['HPstorage.summary.p'][x])/(res5['time'][x+1]-res5['time'][x])
        for x in range(len(res5['HPstorage.summary.p'][:-1]))]
a =np.argwhere([1 if i<0 else 0 for i in der])

plt.text(res5['time'][a[1]-2]*1.02, 350, 'Throttling', fontsize=13)
plt.text(0, 350, 'Compression into HP', fontsize=13)

plt.vlines(res5['time'][a[1]-2],100, res5['HPstorage.summary.p'][a[1]-1]*1e-5, linewidth=0.5, color='black')

idx = np.argwhere(np.diff(np.sign((res5['MPstorage.summary.p']...
        -res5['interVolume.summary.p'])*1e-5-10 ))).flatten()
plt.vlines(res5['time'][idx],100,res5['HPstorage.summary.p'][idx]*1e-5,color='black', linewidth=0.5)
plt.text(res5['time'][idx]*1.1, 350, 'Compression into MP',fontsize=13)

#axes.set_title('Refilling site cascade storage charging');
axes.set_xlabel('Time, s');
axes.set_ylabel('Pressure, bar');
axes.legend()
plt.style.use('seaborn')

#Save figure
fig5.tight_layout()
fig5.savefig('imagesNew/cascade_charging_end.png', dpi = 300)

print(res5['HPstorage.summary.T'][a[1]-1]-273.15, res5['HPstorage.summary.p'][a[1]-1]*1e-5)

fig5_1, axes = plt.subplots(nrows = 1, ncols = 1);

axes.plot(res5['time'],res5['HPstorage.summary.T']-273,label='HP');

```

```

axes.plot(res5['time'],res5['MPstorage.summary.T']-273,label='MP');
axes.plot(res5['time'],res5['interVolume.summary.T']-273,label='Delivery trailer');
#axes.set_title('Refilling site cascade storage charging');
axes.set_xlabel('Time, s');
axes.set_ylabel('Temperature, C');
axes.legend()
plt.style.use('seaborn')

plt.text(res5['time'][a[1]-2]*1.04, 15, 'Throttling', fontsize=13)
plt.text(0, 0, 'Compression into HP', fontsize=13)
plt.vlines(res5['time'][a[1]-2],-3, res5['HPstorage.summary.T'][a[1]-1]-273.15,...
           linewidth=0.5, color='black')
plt.vlines(res5['time'][idx],-3,res5['MPstorage.summary.T'][idx]-273.15,color='black', linewidth=0.5)
plt.text(res5['time'][idx]*1.1, 15, 'Compression into MP',fontsize=13)

#Save figure
fig5_1.tight_layout()
fig5_1.savefig('imagesNew/cascade_charging_end_temp.png', dpi = 300)

mass_5=res5['DeliveredMass.y'][-1]
mass_5

fig5_2, axes = plt.subplots(nrows = 1, ncols = 1);
plt.style.use('seaborn')
axes.plot(res5['time'],res5['tableEffCompressor2.pressureRatio.y']);
axes.set_title('Cascade storage charging');
axes.set_xlabel('Time');
axes.set_ylabel('Pressure ratio');

#compressor data
pr_5=np.average(res5['tableEffCompressor2.pressureRatio.y'])
pr_max_5=np.max(res5['tableEffCompressor2.pressureRatio.y'])
pr_min_5=np.min(res5['tableEffCompressor2.pressureRatio.y'])

comp_power_5=max(res5['tableEffCompressor2.summary.P_vle'])*1e-3
comp_mass_flow_5=max(res5['tableEffCompressor2.summary.m_flow_A'])
comp_isEff_5=np.average(res5['tableEffCompressor2.isEff'])

print(pr_5,pr_min_5,pr_max_5,comp_power_5,comp_mass_flow_5)

#energy consumption by the compressor
mass_5=res5['DeliveredMass.y'][-1]
work_comp_5=res5['CompressorWorkCascade.y'][-1]*1e-3/3600/mass_5
print('Power consumption ',work_comp_5)

#Compressor data table end-user simulation
colData=[['Specific compression work',np.round(work_comp_5,2)],
          ['Average pressure ratio',np.round(pr_5,2)],
          ['Minimum pressure ratio',np.round(pr_min_5,2)],
          ['Maximum pressure ratio',np.round(pr_max_5,2)],
          ['Stage average isentropic efficiency', np.round(comp_isEff_5,2)]];
colNames=['Parameter','Value'];

df_comp_5 = pd.DataFrame(data = colData, columns=colNames)
df_comp_5

#Plotting energy demand throughout the chain
fig6=plt.figure(6)

```

```

data1 = [work_comp_3, work_comp_2, work_comp_4+work_comp_5]
data2 = [0, work_ref_1, work_ref_4]
labels=['After electrolyzer', 'Production site', 'End-user site']

plt.bar(range(len(data1)), data1)
plt.bar(range(len(data2)), data2, bottom=data1, color='#EDB120')
plt.ylim(bottom=0, top=6)
plt.xticks(ticks=range(len(data1)), labels=labels)
plt.xticks(rotation=45) #rotate ticks
#plt.title('Specific power consumption throughout the chain')
plt.ylabel(r'Combined specific work, $\frac{kWh}{kg_{H_2}}$')
plt.legend(labels=['Compression', 'Cooling'])

#Save figure
fig6.tight_layout()
fig6.savefig('imagesNew/power_demand_distrib.png', dpi = 300)

np.sum(data1)

#Compressor data table
colData=[['Comp. after electrolyzer',pr_3,pr_min_3,pr_max_3, comp_power_3,
          comp_mass_flow_3, comp_isEff_3],
          ['Cascade prod. site',pr_2,pr_min_2,pr_max_2, instant_power_2,
          comp_massflow_2, max(map(max, comp_isEff_2))],
          ['End user refilling',pr_4,pr_min_4,pr_max_4, instant_power_4,
          comp_massflow_4, max(map(max, comp_isEff_4))],
          ['Refilling site loading',pr_5,pr_min_5,pr_max_5, comp_power_5,
          comp_mass_flow_5, comp_isEff_5]];
colNames=['Section', 'Average pressure ratio', 'Min pressure ratio', 'Max pressure ratio',
          'Max developed power, kW', 'Max mass flow, kg/s', 'Avg isentropic eff'];

df2 = pd.DataFrame(data = colData, columns=colNames)
df2

# Export DataFrame to excel File
df2.to_excel(excel_writer='table_compressors.xlsx',
            index=False)

#Pressure data table
colData=[['Intermediate storage',200,p_inter_end_2*1e-5],
          ['Cascade prod. site MP',max(map(max, mp_res_2)),p_mp_end_1*1e-5],
          ['Cascade prod. site HP',max(map(max, hp_res_2)),p_hp_end_1*1e-5],
          ['Delivery trailer',np.max(vp_res_1),res5['interVolume.summary.p'][-1]*1e-5],
          ['Cascade end-user site MP',max(res5['MPstorage.summary.p']*1e-5),80],
          ['Cascade end-user site HP',max(res5['HPstorage.summary.p']*1e-5),hp_res_4[-1][-1]],
          ['Onboard tank',max(map(max, vp_res_4)),20]];
colNames=['Section', 'Max pressure, bar', 'Min pressure, bar'];

df3 = pd.DataFrame(data = colData, columns=colNames)
df3

# Export DataFrame to excel File
df3.to_excel(excel_writer='table_pressure.xlsx',
            index=False)

ax=df3.plot.bar(x='Section',rot=45,color=['#0072BD', '#EDB120'])
plt.ylabel('Pressure, bar')

```

```
plt.tight_layout()  
plt.savefig('imagesNew/pressure_distrib.png', dpi = 300)
```

